DISSERTATION

submitted to the
Combined Faculty of Mathematics, Engineering and Natural Sciences
of Heidelberg University, Germany
for the degree of
Doctor of Natural Sciences

Put forward by:

JONAS REZACEK
born in: Berlin, Germany
Oral examination: 31st May 2023

RADIATIVE ORIGIN OF MASS SCALES AND COSMIC INFLATION IN SCALE-INVARIANT MODELS

ABSTRACT

In this work we analyze the radiative generation of mass scales in high-energy physics in classically scale-invariant models of particle physics and gravity. Radiative generation in this context is based on the Coleman-Weinberg mechanism which anomalously breaks scale-invariance. This approach is used to dynamically generate the Planck mass, Majorana masses for right-handed neutrinos and the Higgs mass from a common origin, and it also presents a convenient approach for reanalyzing the hierarchy problem. Within this framework, globally scale-invariant quadratic gravity allows to also describe cosmic inflation with a radiatively generated inflaton potential and the computed predictions for inflationary observables are within the strongest experimental constraints. The ensuing discussion with respect to the dynamical generation of the Planck mass and inflation is deepened by the inclusion of radiative effects due to gravitational degrees of freedom into the picture. In particular, we find that the quantum corrections of the massive spin-2 ghost, which is necessarily present in quadratic gravity, plays a decisive role in generating the Planck mass while simultaneously providing inflationary predictions which are consistent with the strongest experimental constraint

ZUSAMMENFASSUNG

In dieser Arbeit analysieren wir die quantenmechanische Erzeugung von Massenskalen in der Hochenergiephysik in Modellen der Teilchenphysik und der Gravitation mit klassischer Skaleninvarianz. Die quantenmechanische Erzeugung basiert in diesem Kontext auf dem Coleman-Weinberg-Mechanismus, der die Skaleninvarianz anomal bricht. Dieser Ansatz wird verwendet, um die Planck-Masse, die Majorana-Massen für rechtshändige Neutrinos und die Higgs-Masse aus einem gemeinsamen Ursprung zu erzeugen. Dieser Ansatz eignet sich insbesondere um das Hierarchieproblem neu zu analysieren. Darüber hinaus erlaubt die Hinzunahme von quadratischer Gravitation mit globaler Skaleninvarianz auch die Beschreibung von kosmologischer Inflation mit einem quantenmechanisch erzeugtem Inflatonpotential. Wir zeigen auch, dass die berechneten Vorhersagen für Observablen, die in Verbindung zu kosmologischer Inflation stehen, im Rahmen der stärksten experimentellen Beschränkungen liegen. Die Untersuchung in Bezug auf die dynamische Erzeugung der Planck-Masse und die der kosmologischer Inflation wird durch die Einbeziehung von Quanteneffekten aufgrund von gravitativen Freiheitsgraden vertieft. Insbesondere stellen wir fest, dass die Quantenkorrekturen des massiven Spin-2-Geistfeldes, der in quadratischer Gravitation zwangsläufig vorhanden ist, eine entscheidende Rolle spielt um gleichzeitig die Planck-Masse zu erzeugen und Vorhersagen in Bezug zur kosmologischen Inflation zu liefern, die konsistent mit den stärksten experimentellen Beschränkungen sind.

Contents

Chapter 1

Introduction

With the steadily increasing number of experimental confirmations and theoretical understandings of Quantum Electrodynamics (QED) over the course of the last century, the merging of special relativity and quantum mechanics was understood to come in the form of quantum field theory (QFT). In that process, it was soon realized that interactions with so-called virtual particles at the quantum level have an effect on observables and should be incorporated in the theoretical predictions for these observables. For example, virtual photons give rise to an anomalous magnetic dipole moment of the electron and this is one of the reasons these effects were dubbed as radiative corrections [1]. In fact, the measurement of the electron's anomalous magnetic dipole is often quoted as the most precise test of QED and the Standard Model (SM) of particle physics. The findings show that theory and experiment agree to 1 part in 10^{12} [2] which demonstrates the remarkable success of the SM and QFT as its foundation. Today, the notion of radiative corrections is defined broader, in the sense that not only photons but any particles take the role of virtual particles in quantum corrections. Radiative corrections are therefore indispensable in our current understanding of particle physics.

More than twenty years after the development of QED, Sidney Coleman and Erick Weinberg [3] showed that radiative corrections may also play a key role in the process of spontaneous symmetry breaking. They realized that theories which show no sign of spontaneous symmetry breaking at the classical level, may do so if radiative corrections to the effective scalar potential are taken into account when computing the vacuum expectation value (VEV) of the theory. In other words, the symmetry is broken by quantum effects and the process is therefore called radiative symmetry breaking (RSB). Adopting this approach, one can pose a fundamental question about the origin of mass scales in particle physics.

In [3] it is shown that theories devoid of explicit mass scales in the Lagrangian at the classical level can generate mass scales dynamically by means of RSB. It is tantalizing to apply this idea to electroweak symmetry breaking in

the SM where this breaking is achieved traditionally by introducing a tree-level mass term for the Higgs boson. This quadratic term in the scalar potential comes with a negative sign in order to trigger the symmetry breaking and is the only dimensionful parameter of the SM. The field content of the SM alone cannot account for triggering RSB as a way to break electroweak symmetry due to the heavy top quark mass [4], however some effort has been made in extending the SM in such way to understand electroweak symmetry breaking along those lines, see e.g. [5–13]. In fact, we know that most of the baryonic matter we observe obtains the majority of its mass through dynamical effects. For example, the mass of the neutron substantially exceeds the sum of the three constituent quark masses and this mass surplus is understood through vacuum condensates of quarks and gluons. This is even the case of quantum chromo-dynamics (QCD) with massless quarks, where in the non-perturbative regime of the theory a finite scale Λ_{QCD} arises giving rise to chiral symmetry breaking and massive bound states. We take this as motivation to apply a similar logic to the origin of the Higgs mass as this might give a theoretically more satisfying answer to the origin of electroweak symmetry breaking rather than through the ad hoc design of the Higgs potential in the SM. If the origin of mass scales is to be explained in this manner, it remains to be understood how to deal with the presence of explicit mass terms in the classical action which do not violate any symmetries of the SM. Already in the fundamental work of RSB [3], theories with no mass scales in the classical action were considered and since the absence of intrinsic mass scales is tantamount to an invariance under rescaling of lengths, the classical action acquires scale-invariance as a symmetry.[1]

Symmetries seem to be the most promising guiding principle in modern physics, may it be internal gauge symmetries, spacetime symmetries or approximate global symmetries. One of the most famous examples is the understanding of the weak and electromagnetic interactions in terms of a locally gauge-invariant theory which culminated in the development of the SM [14–16]. The weak interactions, due to their short range behavior, are expected to be mediated by massive vector bosons. Contrary to the electromagnetic interaction with massless photons, it seemed puzzling at first to formulate the electroweak theory in terms of an exact local non-Abelian gauge-invariant theory i.e. a Yang-Mills theory [17]. The apparent violation of gauge-invariance through the massive vector boson led to theoretical difficulties including non-renormalizability due to the mass terms of vector fields [18]. The Brout-Englert-Higgs-mechanism [19,20] came to the rescue and allowed us to reconcile Yang-Mills gauge theories with massive spin-1 particles as mediators, thereby restoring renormalizability [21, 22]. The introduction of a fundamental scalar, nowadays called the Higgs boson, which non-linearly realizes the electroweak

---

[1]The exact notion of scale-invariance will be defined more carefully in Section 3.5 and the general guiding principle for scale-invariant model building in particle physics and gravity will be laid out.

symmetry by acquiring a finite VEV, allows the W and Z gauge bosons to carry masses while maintaining gauge invariance. One of the lessons learned from this is that the recognition of the symmetry, may it be non-linearly realized, of the theory at hand can be very fruitful when dealing with theoretical inconsistencies. We will adopt this philosophy with classical scale-invariance as a guiding principle in this thesis, and try to apply it to some contemporary puzzles in high-energy physics. In particular, there will be an emphasis on the existence of multiple and largely separated mass scales, their emergence and intertwining.

One of these contemporary puzzles, and a major driving force for physics beyond the SM, is the gauge hierarchy problem of the Higgs mass. The Higgs boson is the only seemingly fundamental scalar we have observed in nature so far and is therefore the only particle which is plagued with a quadratic sensitivity to higher mass scales beyond the SM. The smallness of the Higgs mass with respect to an embedding scale, e.g. the Planck scale, is deemed technically unnatural in the sense introduced by 't Hooft [23]. In this work the notion of naturalness is tightly connected to symmetry arguments in the sense that physical parameter can be small and technically natural if their smallness is protected by an enhancement in symmetry like chiral symmetry protecting small fermion masses, for example. So are also the most popular solutions or alleviations to the hierarchy problem based on symmetry arguments, e.g. low-scale supersymmetry or composite Higgs models. However, an increasing lack of observational evidence from the LHC for new particles at the TeV scale make these approaches challenging and gives a strong impetus to explore alternative ideas. In this thesis, we will adopt scale-invariance as such an alternative. It was argued that scale-invariance, even though it is an anomalous symmetry, i.e. it is not a symmetry of the quantum effective action, can alleviate the hierarchy problem [24]. In this work it was argued that exponentially and radiatively stable separated scales like the electroweak and the Planck scale can emerge through the anomalous breaking of scale-invariance (see Section 3.4 for details). However, one has to keep in mind that there exists evidence for physics beyond the SM like the masses of neutrinos, dark matter, baryogenesis and inflation which are likely to come hand in hand with new mass scales. So having a global picture of mass scales in mind, we want to address the unified emergence of high-energy scales, in particular the Planck scale, inflation scale, Majorana mass scale of right-handed neutrinos and the electroweak scale in scale-invariant models, while simultaneously monitoring the amount of fine-tuning required.

Even if the SM is valid up to very high energies, as it could be up to the Landau pole associated with the hypercharge coupling at around 10^{42} GeV [25], it is expected to be embedded into a theory of gravity at some scale. This is expected to happen at the Planck scale, also interpreted as the scale where quantum gravity effects become important. Aside from the cosmological

constant[2], the Planck mass is the single dimensionful parameter of General Relativity. Following the path of scale-invariance requires a modification to the standard approach of gravity. Since General Relativity is scrutinized by many observational test in astrophysics and cosmology to remarkable precision, it is clear that one must retrieve an effective Einstein-Hilbert term in the action at low energies. As was argued for the electroweak scale, one has to account for a dynamical generation for the Planck scale as has been done e.g. in [26–57]. We will implement this with a scalar field that acquires a finite VEV through the Coleman-Weinberg-mechanism (CW-mechanism) [3] by coupling it non-minimally to the Ricci scalar by two different approaches in Chapter 5 and 6. Furthermore, in globally scale-invariant gravity, the quadratic terms in the curvature invariants must be included in the action meaning that quadratic gravity comes with the advantage of being renormalizable [58], a fact which carries over to scale-invariant versions of gravity [53, 54, 59]. Intuitively this is due to an improved behavior of the graviton propagator which scales with momentum like $1/k^4$ in the ultraviolet (UV). The other side of this coin is the risk of losing unitarity [58] due to presence of higher derivative terms in the action, as these terms also imply the presence of a spin-2 ghost as an additional degree of freedom stemming from the metric. We will review possible solutions to this ghost problem which have been put forward in the literature and show that the radiative corrections of this spin-2 ghost cannot be ignored. In fact, we will show in Chapter 6 it is key to simultaneously generating the Planck scale and a suitable inflaton potential in globally scale-invariant gravity.

The threading of General Relativity into the cosmological context has led to the concordance model of cosmology, the so-called Lambda cold dark matter model (ΛCDM). If the energy density of baryonic matter is complemented with that of dark matter and dark energy, we have a consistent picture from the early universe, starting at big bang nucleosynthesis (BBN), up to the late time evolution of the universe dominated by dark energy. One of the central pillars of cosmology is the observation and understanding of the cosmic microwave background (CMB). The measurement of the CMB by the Planck mission [60] allows for the determination of the cosmological parameters of ΛCDM, e.g. the matter density parameter Ω_m or the Hubble constant H_0. In spite of this success it was realized shortly after the first observation of the CMB that the high degree of isotropy of the CMB is puzzling if to be understood in the framework of the traditional Big Bang theory of Friedmann–Lemaître–Robertson–Walker (FRLW) cosmology. In short, the problem is that within this framework, it is impossible for regions separated by large distances to have been in causal contact, so no causal physics could have made them equilibrate to an isotropic temperature related to the CMB photons. One way to settle this puzzle is simply setting the Big Bang model up with very special initial conditions, but it

---

[2]We will comment only shortly on the related cosmological constant problem in this thesis at a later point.

is desirable to solve this more naturally by some dynamics of the early universe while being insensitive to special initial conditions.

While the possibility of an early accelerated expansion was considered in [61–63], it was Alan Guth who realized that an early inflating phase could resolve the aforementioned problem [64]. The new paradigm of cosmic inflation was then refined in [65,66] which lead to the contemporary consensus that slow-roll inflation should be incorporated into ΛCDM. This necessitates at least one scalar field, the so-called inflaton, which has a flat potential such that the vacuum energy dominates over the kinetic energy while the inflaton slowly roles down the potential. Under these circumstances the universe will inflate until the slow-roll phase ceases and the energy density of the inflaton field has to be transmitted to SM particles. After that, the standard ΛCDM timeline for the evolution of the universe sets in. The slow-roll condition requires a flat scalar potential, and this can be interpreted as a hint towards scale-invariance since flat potentials appear naturally in scale-invariant theories simply due to the lack of mass scales. In this thesis, we will compute the CW-potential in two different models which can give rise to the generation the Planck scale but also serve as inflaton potential. The inflationary period also causes the stretching of primordial quantum fluctuations to cosmological scales which give rise to the anisotropies of the CMB and the large-scale structure of the universe that we observe today. This connection also offers the possibility to analyze the statistical properties of the CMB and learn something about the microscopic theory governing inflation, as we will do also in this thesis. The entailing constraints on inflation [60] show that the power spectrum for scalar perturbations is very close to the scale-invariant limit. One can interpret this again as motivation to consider an underlying scale-invariant model.

Outline

In the next Chapter we will review the derivation of the quantum effective potential to account for radiative corrections. The derivation of the effective potential at the one-loop level will be first presented in a very general way, so that the formulas can also be applied to the gravitational contributions which will be computed in Chapter 6. In Chapter 3 we will review more details on RSB and the CW-mechanism. In this regard, we will also discuss the gauge hierarchy problem in more detail in Section 3.3 and its possible alleviation in scale-invariant models in Section 3.4. Section 3.5 will clarify the terminology of scale-invariance, conformal symmetry and so forth. Chapter 4 serves as a review of the theory of cosmic inflation. After a short recap of ΛCDM and the related Big Bang puzzles, we give a brief overview of slow-roll inflation. We then move on to the study of primordial perturbations generated during inflation with the ultimate goal in mind how to test inflationary models with CMB observations. In Chapter 5 we develop a scale-invariant model which addresses the unified emergence of the Planck scale, an inflaton potential, Ma-

jorana masses for right-handed neutrinos and the electroweak scale. Also, we shortly discuss the process of reheating and a possibility to incorporate a dark matter candidate. To achieve RSB, we base our construction on an additional scalar sector consisting of two real scalars. In Chapter 6 we switch gears and focus more on the additional gravitational degrees of freedom present in globally scale-invariant gravity. After discussing the ghost problem and review possible solutions to it in Section 6.1, we emphasize the effect of the mentioned spin-2 ghost to the effective potential which allows us the reduce the field content we introduce in Chapter 5 in order to generate the Planck mass and the inflaton potential. Chapter 5 and 6 will be complemented with further introductory words extending this introduction.

Conventions

We work in natural units $c = \hbar = 1$ and with metric signature $(+, -, -, -)$. When the Planck mass or Planck scale are mentioned we refer to the reduced Planck mass $M_{\mathrm{Pl}} = 1/\sqrt{8\pi G_N} = 2.435 \times 10^{18}$ GeV.

Chapter 2

The Quantum Effective Action

To take quantum statistical fluctuations into account, the action of classical field theory has to be replaced by the so-called quantum effective action. In particular, we would like to analyze spontaneous symmetry breaking at the quantum level. By taking quantum corrections into account the vacuum expectation value (VEV) of a quantum field can be shifted with respect to its classical value obtained from minimization of the classical potential. Since in this thesis we want to study radiative symmetry breaking (RSB), it is paramount to compute the quantum corrections to the scalar potential. These corrections can be organized in a perturbative manner, i.e. an expansion in couplings. In this chapter, we will show how to account for quantum fluctuations in an manageable manner by constructing the quantum effective action. It is *effective* in the sense that all correlations functions are obtained from functional derivatives of the quantum effective action where we are effectively dealing with classical fields in an effective potential instead of quantum objects. To do so, we will briefly introduce some functional methods following [3,67,68] in order to derive the effective action. This will be illustrated in case of a single scalar field theory. Then, we will specify the results for the effective potential in the one-loop approximation and discuss the generalization to different particle species.

Let us start with specifying the generating functional for n-point correlation functions for a scalar theory defined by the classical action $S[\phi]$ which is given by the partition function

$$Z[J] = \langle 0_{\text{out}} | 0_{\text{in}} \rangle_J = \int \mathcal{D}\phi \exp\left[i\left(S[\phi] + \phi \cdot J\right)\right] , \qquad (2.1)$$

which can be interpreted as the complete vacuum to vacuum amplitude in presence of a classical source J and we introduced the short-hand notation $\phi \cdot J = \int \mathrm{d}^4 x \, \phi(x) J(x)$. By taking functional derivatives with respect to sources one generates the connected and unconnected correlation functions (i.e. Green's functions)

$$G^{(n)}(x_1, \ldots, x_n) = \langle 0 | \, T\phi(x_1) \ldots \phi(x_n) \, | 0 \rangle . \qquad (2.2)$$

To get of rid of irrelevant information on disconnected diagrams, it is useful to define the Schwinger functional by

$$Z[J] = \exp\left(iW[J]\right), \tag{2.3}$$

which generates the connected correlation functions $G_c^{(n)}(x_1, \ldots, x_n)$, i.e. all connected Feynman diagrams with n external lines, by taking functional derivatives of $W[J]$ with respect to the source terms

$$G_c^{(n)}(x_1, \ldots, x_n) = \left. \frac{\delta^n W[J]}{\delta J(x_1) \ldots \delta J(x_n)} \right|_{J=0}. \tag{2.4}$$

The n-point correlation functions obtained by this method are exact, i.e. they are valid in the full interacting theory. The goal is to organize the interacting quantum theory in an expansion of proper vertices which in turn can be computed in a perturbative approach. The purpose of the effective action is therefore to get rid of redundant terms in the Schwinger functional. Since all physical information is encoded in one-particle irreducible (1PI) diagrams, one has to go one step further and formulate a generating functional for 1PI diagrams which is given by the quantum effective action $\Gamma[\varphi]$. This is achieved by the Legendre transform of $W[J]$ where the functional dependence on J will be replaced by the VEV of the field ϕ in presence of the source, i.e.

$$\varphi(x)_J = \frac{\delta W[J]}{\delta J(x)} = \left(\frac{\langle 0|\phi(x)|0\rangle}{\langle 0|0\rangle} \right)_J, \tag{2.5}$$

where $\varphi(x)_J$ is the so-called background field which is a classical field. We will assume that this equation is invertible and define J_φ as the current for which (2.5) is solved by

$$\varphi_J(x) = \varphi(x) \quad \text{if} \quad J(x) = J_\varphi(x). \tag{2.6}$$

The quantum effective action is now defined by the Legendre transformation

$$\Gamma[\varphi] = W[J_\varphi] - \int \mathrm{d}^4x \, \varphi(x) J_\varphi(x). \tag{2.7}$$

Computing the first functional derivative of $\Gamma[\varphi]$ gives

$$\frac{\delta \Gamma[\varphi]}{\delta \varphi(x)} = \int \mathrm{d}^4 x' \left[\left(\frac{\delta W[J]}{\delta J(x')} \right) \bigg|_{J=J_\varphi} \frac{\delta J_\varphi(x')}{\delta \varphi(x)} - \varphi(x') \frac{\delta J_\varphi(x')}{\delta \varphi(x)} \right] - J_\varphi(x)$$
$$= -J_\varphi(x). \tag{2.8}$$

where in the second equality we used (2.5). The above equation can be considered as the quantum equation of motion for φ also called Schwinger-Dyson

equation. In absence of the source we find that the corresponding VEV $v(x) = \varphi(x)_{J=0}$ is determined by a stationary condition of the effective action

$$\left. \frac{\delta\Gamma[\varphi]}{\delta\varphi(x)} \right|_{\varphi=v} = 0\,. \tag{2.9}$$

This nicely illustrates the analogy to classical field theory, where the equation of motions are obtained from the stationary points of the classical action $S[\phi]$. One can state that the VEV of the quantum field ϕ is obtained from the stationary point of the effective action (2.9). Furthermore, it useful to discuss the interpretation of Γ in terms of Feynman diagrams. Expanding the effective action around the field configuration $\varphi = 0$ one obtains the vertex expansion

$$\Gamma[\varphi] = \Gamma[0] + \sum_{n=1}^{\infty} \frac{1}{n!} \int d^4x_1 \ldots d^4x_n\, \Gamma^{(n)}[\varphi_1, \ldots, \varphi_n]\varphi(x_1)\ldots\varphi(x_n)\,, \quad (2.10)$$

where the coefficients

$$\Gamma^{(n)}(x_1, \ldots, x_n) = \frac{\delta^n\Gamma[\varphi]}{\delta\varphi(x_1)\ldots\delta\varphi(x_n)} \tag{2.11}$$

encode the one-particle-irreducible connected correlation functions, also called proper vertices. If we write $\Gamma^{(n)}$ in terms of its Fourier transform $\tilde{\Gamma}^{(n)}$ and then expand $\tilde{\Gamma}^{(n)}$ around zero momentum, the effective action takes the form

$$\Gamma[\varphi] = \sum_{n=1}^{\infty} \frac{1}{n!} \int d^4x\, \tilde{\Gamma}^{(n)}(0, \ldots, 0)\varphi(x)^n + \frac{1}{2} \int d^4x\, Z(\varphi)\partial_\mu\varphi\partial^\mu\varphi + \ldots\,, \tag{2.12}$$

where the dots stand for higher orders of derivatives. We are usually interested in vacuum configurations with are invariant under translations, i.e. for $\varphi(x) = \varphi_c$ constant in space-time. In this case, the description with the functional $\Gamma[\varphi]$ can be replaced by

$$\Gamma[\varphi_c] = \sum_{n=1}^{\infty} \frac{1}{n!} \int d^4x\, \tilde{\Gamma}^{(n)}(0, \ldots, 0)\varphi_c^n = -V_{\text{eff}}(\varphi_c) \int d^4x\,, \tag{2.13}$$

where we are dealing now with an ordinary function V_{eff} called the effective potential. The functional stationary condition (2.9) is then replaced by a stationary point of the effective potential

$$\left. \frac{\partial V_{\text{eff}}}{\partial\varphi} \right|_{\varphi=v} = 0. \tag{2.14}$$

Eq. (2.13) offers an interpretation in terms of Feynman diagrams. The expansion is organized in the so-called proper vertices $\tilde{\Gamma}^{(n)}(0, \ldots, 0)$. After the

desired loop order is specified, one can compute $\tilde{\Gamma}^{(n)}(0, \ldots, 0)$ for arbitrary n in a diagrammatic approach and then performing the summation in (2.13) will yield the effective potential as is reviewed e.g. in [69]. In contrast to this, we will derive a more general formula for the one-loop corrections in the following section, since it will turn out useful in Chapter 6 to compute gravitational contributions.

2.1   The One-loop Effective Potential

We derive a general formula for the one-loop effective potential, i.e. to order $\mathcal{O}(\hbar)$, by following [68]. The classical action is expanded around the field configuration ϕ_0 which solves the classical equations of motion in presence of a source, i.e.

$$\left.\frac{\delta S}{\delta \phi}\right|_{\phi=\phi_0} = -J(x)\,. \tag{2.15}$$

Then we expand the action around this field configuration

$$
\begin{aligned}
S[\phi + \phi_0] =&\, S[\phi_0] + \int \mathrm{d}^4 x \left.\frac{\delta S}{\delta \phi(x)}\right|_{\phi=\phi_0} \phi(x) \\
&+ \frac{1}{2} \int \mathrm{d}^4 x \int \mathrm{d}^4 x' \phi(x) \left.\frac{\delta^2 S}{\delta \phi(x)\delta \phi(x')}\right|_{\phi=\phi_0} \phi(x') + I(\phi_0, \phi)\,,
\end{aligned}
\tag{2.16}
$$

where the last term collects the higher order interaction terms in this background. One can define the inverse propagator of the classical theory in a constant background by

$$iD^{-1}(\phi_0; x, x') = \left.\frac{\delta^2 S}{\delta \phi(x)\delta \phi(x')}\right|_{\phi=\phi_0}\,. \tag{2.17}$$

Taking also (2.15) into account, (2.16) is written in the compact form

$$S[\phi + \phi_0] = S[\phi_0] - J \cdot \phi + \frac{1}{2}\phi \cdot \left(iD^{-1}(\phi_0)\right) \cdot \phi + I(\phi_0, \phi)\,. \tag{2.18}$$

The generating functional (2.1) for the shifted theory after taking (2.16) and (2.15) into account reads

$$Z[J] = \exp\{i(S[\phi_0] + \phi_0 \cdot J)\} \int \mathcal{D}\phi \exp\left\{i\left(\phi \cdot (iD^{-1}(\phi_0)) \cdot \phi + I(\phi_0, \phi)\right)\right\}\,, \tag{2.19}$$

where the last term will lead to terms of order $\mathcal{O}(\hbar^2)$. The Schwinger functional (2.3) for the connected n-point functions is therefore at the one-loop level

$$W[J] = S[\phi_0] + \phi_0 \cdot J + \frac{i}{2}\ln \mathrm{Det}(iD^{-1}(\phi_0)) + \mathcal{O}(\hbar^2)\,, \tag{2.20}$$

where we have used the Gaussian path integral

$$\int \mathcal{D}\phi \exp\left\{\frac{i}{2}\phi \cdot M \cdot \phi\right\} = (\mathrm{Det}M)^{-1/2}. \tag{2.21}$$

To obtain the effective potential (2.7) we need to perform a Legendre transformation and the functional dependence on J in (2.20) is traded for dependence on the background field φ. Plugging (2.20) into the definition (2.7) we obtain

$$\Gamma[\varphi] = S[\phi_0] + (\phi_0 - \varphi) \cdot J(\phi_0) + \frac{i}{2}\ln\mathrm{Det}(iD^{-1}(\phi_0)) + \mathcal{O}(\hbar^2), \tag{2.22}$$

where $J(\phi_0)$ indicates that J is to be taken as a functional of ϕ_0 in light of (2.15). Expanding the ϕ_0 dependent terms in (2.22) around φ and noting that $\phi_0 - \varphi \sim \mathcal{O}(\hbar)$, one can expand the effective action up to one-loop order (see [68] for a detailed derivation). One obtains the final result at one-loop[1]

$$\Gamma[\varphi] = S[\varphi] + \frac{i}{2}\ln\mathrm{Det}(iD^{-1}(\varphi)) + \mathcal{O}(\hbar^2), \tag{2.23}$$

which shows that the one-loop contribution to the effective potential is given by the functional determinant of the inverse propagator iD^{-1} in presence of a background φ. For practical calculations one often uses the relation $\ln\mathrm{Det}\,iD^{-1} = \mathrm{Tr}\,\mathrm{Ln}\,iD^{-1}$ and then evaluates the trace in momentum space, since it is diagonal for $\varphi = \mathrm{const}$, as shown in the next section. The remaining (infinite) integral one has to solve can then be regularized and renormalized with well-known methods.

2.1.1 Effective Potential for Scalar Fields

Let us illustrate the effective potential computation for a simple scale-invariant model of a single real scalar field with the classical action

$$S[\phi] = \int \mathrm{d}^4 x \left(\frac{1}{2}\partial_\mu\phi\partial^\mu\phi - \frac{\lambda}{4}\phi^4\right). \tag{2.24}$$

As mentioned, the inverse propagator for a translational-invariant background $\varphi = \mathrm{const}$ in momentum space is diagonal

$$iD^{-1}(\varphi, p, q) = \left[p^2 - m(\varphi)^2\right]\delta^4(p - q), \tag{2.25}$$

where we have introduced the field-dependent mass $m(\varphi)^2 = 3\lambda\varphi^2$ of the scalar field. The one-loop contribution of (2.23) is computed by

$$\Gamma^{(1)}[\varphi] = \frac{i}{2}\ln\mathrm{Det}(iD^{-1}(\varphi)) = \frac{i}{2}\mathrm{Tr}\,\mathrm{Ln}\left(iD^{-1}(\varphi)\right), \tag{2.26}$$

---

[1]The capitalized operations Det(...) and Ln(...) are understood to be taken in the functional sense.

and since the inverse propagator (2.25) is diagonal in momentum space, we can evaluate the functional trace

$$\Gamma^{(1)}[\varphi] = \frac{i}{2} \operatorname{Tr} \delta^4(p-q) \ln \left[k^2 - m(\varphi)^2\right]$$
$$= \frac{i}{2} \int \frac{\mathrm{d}^4 k}{(2\pi)^4} \ln \left[p^2 - m(\varphi)^2\right] \int \mathrm{d}^4 x \,. \tag{2.27}$$

The extra volume term to the right is removed in the effective potential contribution (cf. (2.13)) so we are left with

$$V_{\mathrm{eff}}^{(1)}(\varphi) = -\frac{i}{2} \int \frac{\mathrm{d}^4 k}{(2\pi)^4} \ln\left(k^2 - 3\lambda\varphi^2\right). \tag{2.28}$$

The effective potential $V_{\mathrm{eff}}^{(1)}(\varphi)$ for this example can be also interpreted in Feynman diagrams by

where the dotted propagator on the left hand side is understood as the propagator (2.25) with field-dependent mass $m(\varphi)$ in a constant background. The propagators on the right hand side are considered massless and one has to sum over the infinite insertion of external legs which contribute the factors φ^{2n} of the background field .

The integral in (2.28) is UV-divergent and should be regularized with e.g. dimensional regularization. The finite part when the minimal subtraction scheme ($\overline{\mathrm{MS}}$) is employed gives the standard result

$$V_{\mathrm{eff}}^{(1)}(\varphi) = \frac{m(\varphi)^4}{64\pi^2} \left[\ln\left(\frac{m(\varphi)^2}{\mu^2}\right) - \frac{3}{2}\right], \tag{2.29}$$

where the divergent terms have been absorbed into the renormalized λ. In the process the renormalization scale μ was introduced.

The nice feature of the functional form derived in (2.23) is that it can be easily generalized to more complicated theories. For example, considering a theory consisting of N scalar fields φ_i with inverse free propagator given by

$$iD^{-1}(\varphi, p, q) = \left[p^2 \delta_{ab} - M_{ab}(\varphi_i)^2\right] \delta^4(p-q), \tag{2.30}$$

where the mass matrix is obtained from the tree-level potential

$$M_{ab}^2(\varphi_i) = \frac{\partial^2 V^{(0)}}{\partial \varphi_i \partial \varphi_j}. \tag{2.31}$$

The derivation of the one-loop effective potential is analogous to the $N = 1$ case, but with the trace operation acting now also over the mass matrix of the scalar fields. The finite part in $\overline{\text{MS}}$-scheme is

$$V_{\text{eff}}^{(1)}(\varphi_i) = \text{tr}\left(\frac{M(\varphi_i)^4}{64\pi^2} \left[\ln\left(\frac{M^2(\varphi_i)}{\mu^2} \right) - \frac{3}{2} \right] \right). \tag{2.32}$$

If the mass matrix is diagonalized, it is easy to see that the trace will account for the N scalar degrees of freedom.

2.1.2 Effective Potential for General Field Content

The result can be further generalized to different particles species, always taking into account that the trace operation in (2.23) has to be taken over spin and other internal degrees of freedom. Following this approach, one can write down the general formula for the one-loop contributions in $\overline{\text{MS}}$-scheme as [69]

$$V^{(1)}(\varphi) = \frac{1}{64\pi^2} \sum_i N_i m_i^4(\varphi) \left[\ln\left(\frac{m_i^2(\varphi_i)}{\mu^2} \right) - c_i \right], \tag{2.33}$$

where the sum runs over the particles with respective field-dependent masses $m_i(\varphi)$ and the remaining constants are given respectively by

$$N_i = \begin{cases} 1 & \text{for real scalars} \\ 3 & \text{for vector bosons} \\ -2 & \text{for Weyl fermions}, \end{cases} \tag{2.34}$$

$$c_i = \begin{cases} \frac{3}{2} & \text{for scalars and fermions} \\ \frac{5}{6} & \text{for vector bosons}. \end{cases} \tag{2.35}$$

Chapter 3

Radiative Symmetry Breaking and Scale-invariance

The methods laid out in the previous section are very useful to study spontaneous symmetry breaking at the quantum level. The radiative corrections are taken into account perturbatively by a n-loop expansion [3] to the scalar potential. As the scalar potential is crucial for the study of symmetry breaking, this begs the question whether an analysis at the tree-level compared to the one-loop level give the same result. In the SM the breaking of electroweak symmetry is based on the Higgs mechanism which relies on the tree-level potential with inclusion of a mass term with negative sign to induce the so-called "Mexican hat" potential

$$V_{\mathrm{SM}}^{(0)}(h) = -\frac{m^2}{2}h^2 + \frac{\lambda_H}{4}h^4 \,, \tag{3.1}$$

where h is the neutral component of the Higgs doublet H. The minimzation of the tree-level potential shows that the scalar condensate $v_{\mathrm{EW}} = \langle h \rangle \neq 0$ is formed which breaks electroweak symmetry spontaneously. Consequently, the SM fermions become massive through their Yukawa coupling to the Higgs doublet and all scales of the SM are generated.[1] The general formula for one-loop corrections (2.33) allows to take into account the one-loop radiative corrections $V_{\mathrm{SM}}^{(1)}$ to the tree-level potential of the SM. In the resulting SM effective potential $V_{\mathrm{SM}}^{\mathrm{eff}}$ it is sufficient to sum only particles with masses close to the electroweak scale, i.e. the electroweak gauge bosons, the Higgs boson and the top quark. This effective potential then also allows to compute the Higgs mass at one-loop through

$$m_H^2 = \left.\frac{\partial^2 V_{\mathrm{SM}}^{\mathrm{eff}}}{\partial h^2}\right|_{h=v_{\mathrm{EW}}} \,, \tag{3.2}$$

---

[1]Note however, that the QCD condensation scale Λ_{QCD} can arise independently with massless quarks due to its asymptotically free nature.

where

$$V_{\text{SM}}^{\text{eff}}(h) = V_{\text{SM}}^{(0)}(h) + V_{\text{SM}}^{(1)}(h) \,. \tag{3.3}$$

Irrespective whether the tree-level potential (3.1) or the one-loop effective potential (3.3) are utilized, the qualitative result is the same: Electroweak symmetry breaking is successful within the SM which means that the pole mass of the Higgs and the electroweak scale are given by the measured values

$$m_H = 125 \text{ GeV}\,, \quad v_{\text{EW}} = 246 \text{ GeV}\,. \tag{3.4}$$

Quantitatively, the inclusion of higher orders alters the fundamental renormalized SM parameters in order to fix the SM observables (3.4).[2]

The question we want to address now is whether electroweak symmetry breaking is possible in a scale-invariant version of the SM, i.e. when the Higgs mass parameter of (3.1) is set to $m = 0$, also called conformal SM (cSM). Thus, working with a scale-invariant tree-level potential in the effective potential

$$V_{\text{cSM}}^{\text{eff}}(h) = \frac{\lambda_H}{4}h^4 + V_{\text{SM}}^{(1)}(h)\,, \tag{3.5}$$

one finds a qualitatively different result. It is well known that the heavy mass of the top quark dominates the potential (3.5) in such a way that it is not possible to obtain the correct values for the Higgs mass and electroweak scale shown in (3.4), which renders the scale-invariant SM phenomenologically not viable. For this reason, one has to complement the particle content of the cSM with additional bosonic degrees of freedom in order to dynamically generate the electroweak scale and Higgs mass consistent with (3.4). The viability and concrete realizations of this approach are studied e.g. in [5–11,13,72]. Furthermore, such studies come often hand in hand with incorporation of BSM topics like dark matter, neutrino masses, baryogenesis and cosmological first-order phase transitions [73–99]. Parallel approaches haven been developed in [12, 100–106] which are not based on the CW-mechanism but on non-perturbative mechanisms which give rise a confinement scale, analogous to the situation in QCD. In this thesis, we will base the dynamic generation of scales on the perturbative methods by Coleman and Weinberg [3], which we introduce in the following section with scalar QED as an easy example at hand.

3.1   Coleman-Weinberg Mechanism

The CW-mechanism can be studied within the context of perturbation theory as outlined in Chapter 2. As the simplest scenario one can address the

---

[2]The process of electroweak symmetry breaking is often studied, e.g. in [25, 70, 71], by the parametrization $V_{\text{eff}}(h) = -m^2(\mu)h^2 + \lambda(\mu)h^4/4$ of the effective potential where one uses the running couplings in the $\overline{\text{MS}}$-scheme to include orders beyond tree-level. Electroweak symmetry is then achieved at the scales μ where $m^2(\mu) > 0$ and $\lambda(\mu) > 0$.

scale-invariant theory of one scalar field discussed in Section 2.1.1. To answer the question, whether this model can lead to RSB, let us collect the effective potential up to one-loop order (cf. (2.24) and (2.29))

$$V_{\text{eff}}(\varphi) = \frac{\lambda}{4}\varphi^4 + \frac{m(\varphi)^4}{64\pi^2}\left[\ln\left(\frac{m(\varphi)^2}{\mu^2}\right) - \frac{3}{2}\right] . \tag{3.6}$$

It is obvious that the tree-level term proportional to λ alone can not lead to spontaneous symmetry breaking, but can the addition of the one-loop term with its logarithmic form induce a non-trivial minimum? The stationary condition

$$\left.\frac{V_{\text{eff}}(\varphi)}{\partial\varphi}\right|_{\varphi=v} = 0 \tag{3.7}$$

at one-loop order for this theory can be rewritten as

$$\lambda\left[\ln\left(\frac{3\lambda v^2}{\mu^2}\right) - 1\right] = -\frac{16\pi^2}{9} . \tag{3.8}$$

For a minimum to occur at finite v, this equation shows that the logarithm $L = \lambda\ln\left(3\lambda v^2/\mu^2\right)$ must be large, i.e. $|L| \gg 1$ [3]. On the other hand, higher orders in perturbation theory will bring additional terms containing higher powers of L and this shows that for $|L| \gg 1$, the one-loop approximation cannot be trusted since the higher orders would be dominant. Therefore, one cannot trust the outlined analysis of radiative symmetry breaking (RSB) for a single scalar. In fact, [3] showed that the perturbative approach can be improved with the help of renormalization group (RG) methods which effectively resum certain terms containing powers of L up to infinite loop order. Nevertheless, this analysis confirms that the minimum obtained by (3.8) is phony and one can conclude that a single scalar theory cannot induce RSB by itself in the perturbative regime.

We turn now to the arguable simplest model of massless scalar QED which can achieve successful RSB within the range of validity of perturbation theory, where we again follow [3]. Massless scalar QED with the classical action

$$S_{\text{sQED}} = \int \mathrm{d}^4x \left(-\frac{1}{4}F_{\mu\nu}F^{\mu\nu} + \frac{1}{2}(D_\mu\Phi)^*(D^\mu\Phi) - \lambda(\Phi^*\Phi)^2\right) \tag{3.9}$$

is classically scale-invariant and consists of a complex scalar $\Phi = (\phi_1 + i\phi_2)/\sqrt{2}$ charged under an $U(1)$ gauge field A_μ with field strength $F_{\mu\nu}$ and gauge coupling g. The effective potential up to one-loop order is (cf. (2.33))

$$V_{\text{eff}}(\varphi) = \frac{\lambda}{4}\varphi^4 + \frac{3\,m_A(\varphi)^4}{64\pi^2}\left[\ln\left(\frac{m_A(\varphi)^2}{\mu^2}\right) - \frac{5}{6}\right] , \tag{3.10}$$

with field-dependent vector mass $m_A^2(\varphi) = g^2\varphi^2$ and the effective potential can only depend on the gauge invariant combination $\varphi^2 = \varphi_1^2 + \varphi_2^2$ of the

background fields for the two real scalars ϕ_1 and ϕ_2. In (3.10) we have omitted the one-loop contribution coming from the scalar itself since it is subdominant in the perturbative regime as we have seen in the above example. This can be underpinned with the simple following estimate. The tree-level potential is $\mathcal{O}(\lambda)$ and the one-loop correction due to the scalar is $\mathcal{O}(\lambda^2)$. For a radiatively induced minimum the one-loop part of the effective potential needs to compete with the tree-level part, i.e. a scaling like $\mathcal{O}(\lambda) = \mathcal{O}(\lambda^2)$ is needed which violates perturbativity. The situation changes in the effective potential for scalar QED (3.10), where the one-loop contribution from the gauge field A_μ scales as $\mathcal{O}(g^4)$. There is nothing wrong with a scaling of the parameters like $\mathcal{O}(\lambda) = \mathcal{O}(g^4)$ and so the one-loop term can substantially modify the tree-level potential. The stationary condition (2.14) derived from (3.10) with the self-consistent choice $\mu = v = \langle\varphi\rangle$ for $v \neq 0$ reads

$$\lambda = -\frac{3g^4}{16\pi^2}\left[\ln(g^2) - \frac{1}{3}\right].\qquad(3.11)$$

This equation can be satisfied within the validity of perturbation theory, i.e. for small λ. One can conclude, that a finite VEV v is generated. This process is also called dimensional transmutation in [3], since the λ-dependence of the effective potential can be replaced through (3.11). Effectively, the dependence on two dimensionless parameters λ and g is then replaced by g and the scale of the VEV v. In the broken phase the scalar and the gauge boson acquire the masses

$$m_\phi^2 = \left.\frac{\partial^2 V_{\text{eff}}}{\partial \varphi^2}\right|_{\varphi=v} = \frac{3g^4}{8\pi^2}v^2,\qquad m_A^2 = g^2 v^2,\qquad(3.12)$$

where the would-be Goldstone boson is absorbed into the massive vector boson. As this mechanism was presented, (3.11) might read as a restriction between the coupling constants λ and g in order to achieve RSB. However, in the RG language, the coupling constant should be considered as running coupling constants $\lambda(\mu)$ and $g(\mu)$ depending on the renormalization scale μ. As discussed in [3], if some perturbative boundary values for $\lambda(\mu_0)$ and $g(\mu_0)$ are defined at some scale μ_0 with no sign for RSB, the RG running will always lead to a lower scale μ^* at which (3.11) is satisfied. So the classical scale-invariance of scalar QED will be necessarily broken through the RG-running for arbitrary but perturbative values of λ and g. It seems like the charging of the scalar field under some gauge group is necessary for the CW-mechanism to work, but as we show in the nextion section it can be achieved in a similar fashion for multi-scalar models.

3.2   Gildener-Weinberg Approach

A few years after the CW-mechanism was proposed [3], E. Gildener and S. Weinberg (GW) [107] formulated an approach to study RSB by applying the

CW-mechanism to multi-scalar models. This approach is widely used in the literature for dynamical generation of the electroweak scale when the SM is extended with additional scalars. The advantage of the GW-approach is that it allows to approximate the effective potential with multi-field dependence effectively by a one-field description of the effective potential. The most minimal setup to achieve RSB within the GW-approach is a two scalar theory, without the necessity for additional gauge fields, a setup we will utilize in chapter 5.

First, we briefly review the GW-approach in the general case of a tree-level potential with quartic interactions for N scalar fields

$$V^{(0)}(\mathbf{\Phi}) = \lambda_{ijkl}\Phi_i\Phi_j\Phi_k\Phi_l \,, \tag{3.13}$$

where $\mathbf{\Phi}^T = (\Phi_1, \ldots, \Phi_N)$. The underlying assumption is that at high energies the theory is in the symmetric phase, i.e. the global minimum is located at $V^{(0)}(0) = 0$, but at lower energies the potential develops a flat direction. The latter, is stated by a condition on the set of couplings $\lambda_{ijkl}(\mu)$ which become RG-running quantities when quantum effects are taken into account.[3] We refer to the scale at which this condition is fulfilled as the GW scale μ_{GW} in dimensional regularization. The flat direction of the tree-level potential (see also Fig. 3.1) can be thought of as a ray in field space parametrized by the vector

$$\mathbf{\Phi}_0 = \boldsymbol{n}\varphi \,, \tag{3.14}$$

where $\boldsymbol{n}$ is a unit vector and φ is the radial field value along the flat direction. The tree-level potential vanishes along this ray, i.e.

$$V^{(0)}(\mathbf{\Phi}_0) = 0 \,, \tag{3.15}$$

and this gives an infinite set of degenerate non-trivial minima. Including now the one-loop corrections will give some curvature to the potential along the flat direction and thereby picks out a non-degenerate minimum at $v_\varphi = \langle\varphi\rangle \neq 0$. The nice feature of the GW approach is that the effective potential, which in general depends on N scalar fields, can be parameterized solely with the radial field φ in (3.14). Doing that and keeping in mind that the tree-level part vanishes by construction (3.15), we can write down the following parametrization of the effective potential along the flat direction at the GW scale

$$V_{\mathrm{eff}}(\mathbf{\Phi}_0) = V_{\mathrm{eff}}(\boldsymbol{n}\varphi) = A\varphi^4 + B\varphi^4\ln\left(\frac{\varphi^2}{\mu_{\mathrm{GW}}^2}\right). \tag{3.16}$$

One should be aware that this in approximation and that the one-loop corrections might change the shape of the tree-level potential substantially by shifting the flat direction or removing it completely. In particular, the addition of gauge fields or fermions which couple not uniformly to the scalar fields Φ_i

---

[3]See e.g. [76, 107] for details on the GW condition.

might change this analysis. In such cases, one should therefore carefully check with the full effective potential $V_{\text{eff}}(\Phi_1, \ldots, \Phi_N)$, keeping the dependence on all fields, if this is the case. We take these matters aside in the rest of this work, and refer to [13] for a more detailed discussion. The non-trivial stationary point of (3.16) can now be easily obtained by

$$\ln\left(\frac{v_\varphi^2}{\mu_{\text{GW}}^2}\right) = -\frac{1}{2} - \frac{A}{B} \tag{3.17}$$

and determines the VEV v_φ and can be related to VEVs of the Φ_i-fields with (3.14). The dimensionless functions A and B are obtained by the general one-loop formula for the effective potential (2.33) depending on the field content of the model. They explicitly read

$$A = \frac{1}{64\pi^2 v_\varphi^4} \sum_i N_i m_i^4(\boldsymbol{n}v_\varphi)\left[\ln\left(\frac{m_i^2(\boldsymbol{n}v_\varphi)}{v_\varphi^2}\right) - c_i\right], \tag{3.18}$$

$$B = \frac{1}{64\pi^2 v_\varphi^4} \sum_i N_i m_i^4(\boldsymbol{n}v_\varphi), \tag{3.19}$$

where the masses of the scalars, vectors and fermions in the model are evaluated on the flat direction (3.14). The second derivative of the effective potential evaluated at the minimum

$$m_\varphi^2 := \left.\frac{\partial^2 V_{\text{eff}}(\boldsymbol{n}\varphi)}{\partial\varphi^2}\right|_{\varphi=v_\varphi} = 8Bv_\varphi^2 \tag{3.20}$$

confirms that the stationary point is indeed a minimum if the field content is such that $B > 0$ is satisfied (cf.(3.19)). The scalar excitation φ with mass m_φ is often interpreted as the pseudo-Goldstone boson related to the breaking of scale-invariance. It is also called scalon in [107] and obtains its mass at the one-loop level through the anomalous breaking of scale-invariance.

Even if the model contains only scalars, RSB can be achieved in this approach as we show next with a two scalar field example. We assume the following scale-invariant tree-level potential

$$V^{(0)}(\varphi_1, \varphi_2) = \frac{1}{4}\left(\lambda_1\varphi_1^4 + \lambda_{12}\varphi_1^2\varphi_2^2 + \lambda_2\varphi_2^4\right). \tag{3.21}$$

and the two tree-level stationary conditions with respect to φ_1 and φ_2 can be rewritten as

$$4\lambda_1\lambda_2 - \lambda_{12}^2 = 0, \tag{3.22}$$

$$\frac{v_1^2}{v_2^2} = -\frac{\lambda_2}{2\lambda_{12}}, \tag{3.23}$$

where we have assumed that $v_1 = \langle\varphi_1\rangle \neq 0$, $v_2 = \langle\varphi_2\rangle \neq 0$ and $\lambda_{12} < 0$. The above equations can be understood as the GW-condition for a flat direction
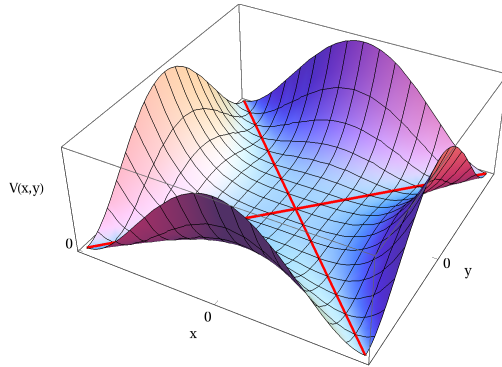
Figure 3.1: Example of a 2-dimensional scalar potential with the red lines indicating the flat directions.

which should be satisfied at the scale μ_{GW}. Using polar coordinates for the VEVs $v_1 = v_\rho \cos(\theta_0)$ and $v_2 = v_\rho \sin(\theta_0)$, one can determine from (3.23) that the angle θ_0 of the flat direction is determined by

$$\tan \theta_0 = \sqrt{-\frac{2\lambda_1}{\lambda_{12}}}\,, \tag{3.24}$$

which can be used to adjust the desired flat direction by tuning the quartic couplings. The one-loop corrections coming from the scalar degrees have to be included along the flat direction to obtain the value of the radial VEV v_ρ. The other case $\lambda_{12} > 0$ has the GW-conditions

$$\lambda_1 = 0\,, \tag{3.25}$$

$$\sin(\theta_0) = 0\,, \tag{3.26}$$

such that only one field $v_1 = \langle \varphi_1 \rangle$ develops a VEV. This be will the case for our construction in Section 5.2.

3.3 The Gauge Hierarchy Problem

It is generally accepted that the SM is not complete. One the one hand due to its shortcomings to account for certain phenomenology we observe like dark matter, neutrino masses and baryogenesis. On the other hand, there are theoretical motivations to extend the SM to account for example for the grand unification of the gauge couplings or to solve the strong CP-problem. It is therefore not far-fetched to expect related higher mass scales beyond the electroweak scale. Even if this does not apply, we know that the SM needs to be embedded in gravity which gives rise to the Planck scale. The fact that the Higgs boson is interpreted as the only elementary scalar in coexistence with higher energy scales, may it be the Planck scale, beyond the SM introduces the infamous

gauge hierarchy problem of the Higgs mass within the SM. The hierarchy problem is connected to the bare Higgs mass m^2 in the tree-level potential (3.1) and the appearance of quadratic divergences when one-loop corrections to this parameter are computed. The presentation of the problem is often stated by regularization with a hard momentum cutoff Λ_{UV}. The Higgs mass corrections are then quoted to be proportional to $\delta m^2 \propto g_i^2 \, \Lambda_{\text{UV}}^2$, where g_i stands for some SM coupling. The sole intention of this argument is to expose the quadratic sensitivity of the Higgs mass to some potential UV scale of new physics, but one should add two comments to not misinterpret this. First, of course the cutoff Λ_{UV} is purely technical and any physical result should be independent of it. Therefore, it should be only seen as a placeholder of a high-energy scale with physical interpretation. Considering theoretically the SM by itself, meaning if it is not embedded in some larger theory in the UV like quantum gravity, does not have a hierarchy problem. To make these subtle points clear-cut, we find it best to understand the hierarchy problem in the effective field theory (EFT) picture as for example done in [108]. In this picture, one defines a matching scale, usually taken to be the heavy mass scale, at which the heavy degrees of freedom are integrated out and matched to the EFT which is valid at lower energies, meanwhile computing the induced threshold corrections on the parameters of the EFT. To clarify the latter comment on the SM in isolation, one can consider a simple scalar theory. The model consists of a single scale so the application of EFT methods might seem superfluous, but this treatment nevertheless shows that a single scale EFT is well behaved at all scales when RG improved methods are used [108]. Similar arguments apply to the SM in isolation since it has no heavy scales it can talk to. For example, the Higgs mass obtains a one-loop correction from itself running in the loop with finite part given by

$$\delta m^2 = m^2 \frac{\lambda_h^2}{32\pi^2} \left[\ln\left(\frac{\mu^2}{m^2}\right) + 1 \right] , \qquad (3.27)$$

which is not too large, as for any other particle of the SM running in the loop. To understand the root of the hierarchy problem, one should consider the EFT picture for a model consisting of two separated mass scales which will depict the lack of decoupling of IR physics from UV physics for masses of elementary scalars. As a toy model, we consider a light scalar ϕ of mass m (resembling the Higgs boson) coupled to a heavy scalar Φ with mass M (placeholder for UV scales) with the Lagrangian of the full theory

$$\mathcal{L} = \frac{1}{2}\partial_\mu \phi \partial^\mu \phi - \frac{m^2}{2}\phi^2 + \frac{1}{2}\partial_\mu \Phi \partial^\mu \Phi - \frac{M^2}{2}\Phi^2 - \lambda_{12}\Phi^2\phi^2 , \qquad (3.28)$$

where we have omitted other quartic couplings for the sake of the simplicity of the argument to be made. Note that the role of Φ could be replaced by a heavy Dirac fermion for the sake of this argument. We integrate out the heavy scalar

at the matching scale $\mu_M \simeq M$ and match it onto the EFT consisting solely of the light scalar ϕ as propagating degree of freedom. The threshold corrections at the matching scale μ after renormalization induce the matching condition for the mass parameter [108]

$$\delta m_{\text{EFT}}^2 = m^2 - \frac{\lambda_{12}}{32\pi^2} M^2 \left[\ln\left(\frac{\mu_M^2}{M^2}\right) + 1 \right] , \qquad (3.29)$$

where the m and M are the mass terms in the full theory (3.28) and m_{EFT} is the mass of the light scalar in the EFT. We see that for $m \ll M$ the threshold corrections $\delta m^2 \propto M^2$ dominate which shows clearly the quadratic sensitivity to the heavy scale. This mismatch can be absorbed by fine-tuning the bare m^2 term in the full theory order by order in perturbation theory but this is deemed technically unnatural [23]. This in contrast to a light fermion with mass m_F coupled to a heavy scale M since it is protected by chiral symmetry in the limit $m_F \to 0$ which manifests itself by threshold corrections which scale as $\delta m_F \propto m_F$ and thus show no dangerous sensitivity to the heavy scale.

We can conclude that if the SM is embedded into an UV theory at the scale Λ_{UV}, the Higgs mass parameter would obtain large corrections of order Λ_{UV} in light of the EFT matching condition (3.29) with $M \simeq \Lambda_{\text{UV}}$ and this would require extreme fine tuning of the Higgs mass parameter to account for viable electroweak symmetry breaking.

3.4 Anomalous Breaking of Scale-invariance

We turn now to the interpretation of the hierarchy problem in scale-invariant theories. In Section 3.1 we have seen that when tree-level mass terms are set to zero, masses can be generated dynamically with the CW-mechanism. Since scalar mass terms are central to the discussion of the hierarchy problem, as shown in the previous section, this is a fair question to ask. At first sight, it might seem convincing that scale-invariance is the symmetry which would make a small Higgs mass technically natural [23] because the SM is scale-invariant in the limit $m \to 0$. It is important to note that this is only a symmetry at the classical level which is not preserved when quantum corrections are taken into account since they necessarily introduce a dependence on the energy scale through the process of renormalization for any regularization method used [109, 110].[4] In other words, the quantum effective action derived in (2.23) does not respect the scale-invariance of the classical action. Contrary to spontaneous symmetry breaking where only the ground state but not the effective action break the symmetry, this process is called anomalous breaking. The so-called conformal anomaly is quantified by the anomalous Ward identity of conformal

---

[4]Other approaches where scale-invariance is preserved at the quantum level and scale-invariance can be broken spontaneously haven been proposed but come at the price of non-renormalizable interactions [111]. We will not follow this approach in this thesis.

symmetry, which encapsulates how the symmetry is broken. This is encoded in the non-conservation of the dilatation current J_μ, or equivalently the trace of the improved energy-momentum tensor $T_{\mu\nu}$ [112]. In general, for a classically scale-invariant theory it can be written as

$$\partial^\mu J_\mu = T^\mu_{\ \mu} = \sum_i \beta_i \cdot \hat{O}_i + \mathcal{C}\,, \qquad (3.30)$$

where β_j are the one-loop beta functions to the corresponding local dimension four operators $\hat{O}_i$ [109]. The second term $\mathcal{C}$, also called Weyl anomaly [113], arises in curved backgrounds and contains curvature-dependent terms (see also [114–116]). We will focus now on the first term in (3.5) because it encapsulates the anomalous breaking of scale-invariance in flat space at the quantum level through the scale-dependence induced by the RG-running of the couplings which arise when $\beta_i \neq 0$. It has been argued in [24] that this anomalous breaking can solve the hierarchy problem, or at least offer a new perspective on it. Assuming that the conformal anomaly is the only source of breaking, (3.5) reveals that IR physics are only logarithmically sensitive to UV physics, because the β-functions do not know about quadratic divergences and only encode the logarithmic running of the coupling constants [7, 24]. From this fact it is deduced in [24] that two scales, i.e. a radiatively generated scale (for example with the CW-mechanism) and some embedding scale can be exponentially separated and remain radiatively stable. This argument is only valid if there are no other intermediate scales between the breaking scale and the embedding scale. One should therefore also account for the absence of Landau poles or instabilities in the potential up to the embedding scale to ensure that the model is viable in that range [6, 7]. In this approach, the embedding scale is interpreted differently as a standard physical threshold scale in the QFT picture. Rather than seeing it as some physical scale where EFT matching as in (3.29) is to be performed, it has been advocated in [7, 117] to rather interpret it as scale-invariant boundary condition at the embedding scale on the RGE of the couplings. The hypothesis is therefore that the embedding scale, usually identified with the Planck scale above which concepts beyond QFT might apply, is therefore not interpreted in the Wilsonian picture of EFTs [6–8].

Under these working assumptions, it seems plausible to dynamically generate a mass scale which is radiatively stable and exponentially smaller than the Planck scale and can be applied to a scale-invariant extension of the SM as has been done e.g. in [5–13, 72–106]. If the model under consideration consists of multiple scalar fields which are supposed to have widely separated VEV scales, the hierarchy problem is reformulated in the fine-tuning of the respective portal terms, as λ_{12} in (3.28), because they can transmit one VEV scale from one sector to another. In the introduction we have motivated to generate widely separated mass scales by one common radiative origin, so this will be an issue of our studies and calls for further explanation. We return to the issue of small portal couplings and their stability under RG-running in Section 5.4 and 5.5,

while the answer might still be far from ultimate and satisfactory, we demonstrate how to soften this huge hierarchy and hope to offer a new perspective on the hierarchy of dynamically generated mass scales.

3.5 Scale-invariance, Conformal Symmetry and Weyl Symmetry

We conclude this chapter by clarifying the notion of scale-invariance used in this thesis and comment on the related concepts of conformal symmetry and Weyl symmetry. Scale transformations or dilatations have one parameter λ and rescale the coordinates according to

$$x^\mu \to \lambda\, x^\mu\,. \tag{3.31}$$

It useful to define the transformation rule in field theories for scalars, fermions and vector boson according to their scaling dimension

$$\phi(x) \to \lambda^{-1}\phi(\lambda x)\,, \quad \psi(x) \to \lambda^{-3/2}\psi(\lambda x)\,, \quad A_\mu(x) \to \lambda^{-1}A_\mu(\lambda x)\,. \tag{3.32}$$

We refer to a classical Lagrangian invariant under (3.31) and (3.32) as scale-invariant since it conserves the dilatation current at the classical level. From this follows, that in $d = 4$ space-time dimension the general building blocks of a scale-invariant theory consisting of real scalars ϕ_i, Weyl fermions ψ_a and vector gauge bosons Z_μ^A can be written in general in flat space as

$$S = \int \mathrm{d}^4x \left(-\frac{1}{4}F_{\mu\nu}^A F^{A,\mu\nu} + \frac{1}{2}D_\mu\phi_i D^\mu\phi_i - \lambda^{ijkl}\phi_i\phi_j\phi_k\phi_l \right.$$
$$\left. +\frac{i}{2}\overline{\psi_a}\slashed{D}\psi_a - (y_i^{ab}\phi^i\overline{\psi_a}\psi_b + \mathrm{h.c.})\right), \tag{3.33}$$

where D is the gauge-covariant derivative acting on scalar and fermions, respectively. We will base the scale-invariant models discussed in Chapter 5 and 6 on this construction.

Conformal symmetry, on the other hand, is obtained if dilatations (3.31) are complemented with special conformal transformations which transform coordinates according to

$$x^\mu \to x'^\mu = \frac{x^\mu + v^\mu x^2}{1 + 2v \cdot x + v^2 x^2}\,, \tag{3.34}$$

and belong to the four parameter group of special conformal transformations. Invariance under (3.31) and (3.34) is defined as conformal symmetry. The corresponding conformal group consists of, next to the ten Poincaré generators, of the dilatation generator and the four generators of special conformal transformation. Combining only the dilatation generator and the Poincare group

one obtains a closed algebra which is therefore just a subgroup of the full conformal algebra [115]. Mathematically speaking, scale-invariance and conformal symmetry should therefore in general be distinguished. It is also obvious that conformal symmetry implies scale-invariance, but not vice versa. However, if the emphasis is put on well-behaved field theories which are of interest in physics this view is softened and scale-invariance implies also conformal invariance [118]. More generally speaking, this is conjectured for QFTs in $d = 4$ on quite general assumptions (unitarity, Poincaré invariance, discrete spectrum in scaling dimensions, existence of scale current and unbroken scale invariance) which is discussed in detail in [115].

The previous consideration where made in the absence of gravity. The generalization to curved space-time where the metric is considered as a dynamical field, leads to the further distinction between conformal symmetry and Weyl symmetry. In this setting, the conformal transformations are coordinate transformation which transform the metric locally according to [119–121]

$$g_{\mu\nu}(x) \to g'_{\mu\nu}(x') = \frac{\partial x^\lambda}{\partial x'^\mu}\frac{\partial x^\sigma}{\partial x'^\nu}g_{\lambda\sigma}(x) = \hat{\Omega}^2(x')g_{\mu\nu}(x')\,, \qquad (3.35)$$

which can be read as a coordinate transformation which leaves the metric invariant up to the conformal factor $\hat{\Omega}^2$. This places restrictions on the rescaling function $\hat{\Omega}^2$. On the other hand, Weyl transformations are not defined by acting on the coordinates but transform the metric and fields pointwise [119–121]

$$g_{\mu\nu}(x) \to g'_{\mu\nu}(x) = \Omega^2(x)g_{\mu\nu}(x)\,, \quad \Phi(x) \to \Phi'(x) = \Omega^{-d_\Phi}(x)\Phi(x)\,, \quad (3.36)$$

where d_Φ denotes the scaling dimension of the field Φ and $\Omega(x)$ is an arbitrary but non-vanishing function. From these considerations one can deduce that a diffeomorphism invariant theory with Weyl invariance in a general background implies conformal invariance in flat space-time but not necessarily vice versa [119, 120]. In [119] however, it is argued that conformal invariance in flat space-time implies Weyl invariance for a general background for all local unitary QFTs with $d \leq 10$. One can furthermore define a global version of the Weyl transformation, i.e. (3.36) with $\Omega(x) = \Omega = \text{const}$, which leads to the notion of global scale-invariance. When we are dealing with gravitational theories in Chapter 5 and 6 we will assume global scale-invariance. Under the condition of global scale-invariance, the building blocks (3.33) are extended to the gravitational sector by

$$S = \int \mathrm{d}^4x\,\sqrt{-g}\left(c_1 R_{\mu\nu\lambda\sigma}R^{\mu\nu\lambda\sigma} + c_2 R_{\mu\nu}R^{\mu\nu} + c_3 R^2 + \frac{\beta_{ij}}{2}\phi_i\phi_j R\right)\,, \quad (3.37)$$

where we included the square of the Riemann tensor $R_{\mu\nu\lambda\sigma}$ and its contractions, as well as the non-minimal couplings of the scalar fields to the Ricci scalar R. In the rest of this thesis, we will not further distinguish these subtle matters and instead use the notion of scale-invariance, more precisely global scale-invariance when gravity is included in the picture.

Chapter 4

Cosmic Inflation

In this chapter we review the theory of cosmic inflation which sets the theoretical foundation for our further studies presented in Chapter 5 and 6. To do that, we will follow the lectures notes [122, 123] and the text books [124–127].

Our understand of the universe is well established and corroborated by observations for temperatures below the MeV scale.[1] Certainly the most important observational pillar of cosmology is the cosmic microwave background (CMB). It was released at temperatures $T \sim 0.1$ eV when protons and electrons recombined to form neutral hydrogen. Subsequently, photons could free stream for the first time and they do so (approximately) until today where we observe them on the sky as the blackbody radiation known as CMB. The CMB thereby offers the oldest snapshot of the universe from the so-called last scattering surface. The observed CMB anisotropies indicate the existence of density perturbations which grew through gravitational instabilities to the large-scale structure of the universe we observe today. Collecting this evidence and more, our understanding of the universe has culminated in a model called Lambda cold dark matter (ΛCDM) which explains the evolution of the universe under the laws of General Relativity where the total energy density consists of dark energy (Λ), cold dark matter (CDM) and baryonic matter. For example, ΛCDM offers an understanding of the angular power spectrum of the CMB, the power spectrum of large-scale structure, the formation and precise abundance of the light nuclei by BBN and the accelerated expansion of the universe at late times.

The ΛCDM model is based on the Friedmann-Lemaitre-Robertson-Walker (FLRW) ansatz for the metric

$$\mathrm{d}s^2 = \mathrm{d}t^2 - a^2(t) \left(\frac{\mathrm{d}r^2}{1 - kr^2} + r^2 \left(\mathrm{d}\theta^2 + \sin^2\theta \mathrm{d}\phi^2 \right) \right) , \qquad (4.1)$$

where the scale factor $a(t)$ depends only on the time coordinate and k is the

---

[1]The process of Big Bang nucleonsynthesis (BBN) is taking place at temperatures $T \sim$ 1 MeV.

spatial curvature parameter. The FLRW ansatz (4.1) is obtained from the cosmological principle, which states the homogeneity and isotropy of the universe when smoothed out on large enough scales. The time evolution of $a(t)$ is dictated by Einstein's Equations and for (4.1) they reduce to two differential equations called Friedmann equations

$$H^2 := \left(\frac{\dot{a}}{a}\right)^2 = \frac{\rho}{3M_{\text{Pl}}^2} - \frac{k}{a^2} \,, \tag{4.2}$$

$$\frac{\ddot{a}}{a} = -\frac{1}{6M_{\text{Pl}}^2}\left(\rho + 3p\right) \,, \tag{4.3}$$

where ρ is the energy density and p the isotropic pressure of the energy-momentum tensor for a perfect fluid which contributed to the Einstein's Equations. If this energy-momentum tensor is specified as being the sum of the energy density of matter ρ_m, radiation ρ_r and dark energy ρ_Λ, the first Friedmann equation (4.2) reads

$$\frac{H^2}{H_0^2} = \frac{\Omega_r}{a^4} + \frac{\Omega_m}{a^3} + \frac{\Omega_k}{a^2} + \Omega_\Lambda \,, \tag{4.4}$$

where the dimensionless density parameters Ω_i are defined by

$$\Omega_i = \frac{\rho_i}{\rho_{\text{crit}}} \,, \quad \rho_{\text{crit}} = 3H_0 M_{\text{Pl}}^2 \,, \tag{4.5}$$

except $\Omega_k = -k/a_0^2 H_0^2$. Furthermore, we have introduced the Hubble constant H_0 which is the Hubble parameter evaluated at the present time $H_0 = H(a_0)$ where $a_0 = a(t_0)$ is the present scale factor.

If the time evolution of the universe is solely understood by (4.4) at all times, one obtains the so called hot Big Bang model of FLRW cosmology. It has an initial singularity at $a(t = 0) = 0$ and starts with an era of radiation domination, i.e. when the first term in (4.4) dominates the evolution. If the structure we observe in the CMB is tried to be understood fundamentally in the Bing Bang model, one is confronted with the so-called Big Bang puzzles such as the flatness and horizon problem.

4.1   Big Bang Puzzles

The Big Bang puzzles could be resolved by setting up the Big Bang model with special and fine-tuned initial conditions. Of course, one can accept this fate, but as physicists, we would like to find a more *natural* explanation.

The flatness problem is related the small curvature energy density $|\Omega_k| < 1$ we observe today. The combination of CMB and baryonic acoustic oscillations (BAO) data is consistent with a flat universe $\Omega_k = 0.001 \pm 0.002$ [60]. This is hard to understand with the evolution of the Big Bang model because tracing

the energy density of curvature $\Omega_k(a) = -k/(aH)^2$ back in time shows that it must have been constantly increasing through radiation and matter domination [124]. Therefore, $\Omega_k(a)$ must have been even smaller at earlier times, for example one finds that $\Omega_k(a_{\text{BBN}}) \sim 10^{-16}$ at the time of BBN [122, 124]. The flatness problem can be avoided if the comoving Hubble radius $(aH)^{-1}$ (also called Hubble horizon) is decreasing at early times but this is not the case during radiation or matter domination. So postulating an early phase, where $(aH)^{-1}$ is decreasing with time, the problem is solved because $\Omega_k(a) \propto (aH)^{-2}$ is then also decreasing. So no matter what the initial value of $\Omega_k(a)$ at some primordial time was, it is driven to flatness $\Omega_k \approx 0$ during this period.

The second well-known problem related to the Big Bang picture is the horizon problem. The CMB is very well fitted by a blackbody spectrum of temperature $T_0 \simeq 2.7$ K and the statistical anisotropy is very small and is quantified by

$$\frac{\Delta T}{T_0} \sim 10^{-5} \,, \tag{4.6}$$

where ΔT is the average deviation from the monopole temperature T_0 of the CMB. One can conclude that the universe was homogeneous and isotropic to a high degree at the moment of recombination, which is in accordance with the cosmological principle. The high degree isotropy of the CMB poses however a problem when it is tried to be understood within the Big Bang picture. In this cosmological model, the regions we observe in the CMB at different patches of the sky could have not been in causal contact. To understand this point better, it is useful to define the comoving particle horizon

$$d_H = \int_0^t \frac{\mathrm{d}t'}{a(t')} = \int_0^a \frac{\mathrm{d}a'}{a'} \frac{1}{a'H(a')} \,, \tag{4.7}$$

which measures the maximal distance light can travel between some initial time $t = 0$ and time t, and thus serves as an indicator for causal structure in cosmology. In the last equality we have rewritten the integral in terms of the comoving Hubble radius. The time evolution for the comoving Hubble horizon is governed by (4.4) and specifically reads

$$\frac{1}{aH} = \frac{1}{H_0} \begin{cases} a^{1/2} & (\text{MD}) \\ a & (\text{RD}) \,, \end{cases} \tag{4.8}$$

for a purely matter dominated (MD) and radiation dominated universe (RD), respectively. This establishes that the comoving Hubble horizon is growing monotonically in the Big Bang model and therefore the integral over the past in (4.7) shows that the particle horizon is increasing in time according to

$$d_H \propto \begin{cases} a^{1/2} & (\text{MD}) \\ a & (\text{RD}) \,, \end{cases} \tag{4.9}$$

and must have been smaller in the past compared to today. This entails that regions which are widely separated during last scattering haven not been necessarily in causal contact in light of (4.9). In fact, the particle horizon at the time of recombination subtends an angle of only 1.6° if observed in the sky today [124], but we do observe isotropy on larger scales. As for the flatness problem, this can be solved by a phase with decreasing comoving Hubble radius prior to radiation domination. Then, the integral in (4.7) will be modified due to this additional period in the far past and if that period lasts long enough it can causally connect all the regions which we observe at different patches of the CMB today. In other words, the particle horizons of each point in the CMB are then overlapping such that the appearance of an isotropic CMB poses no problem.

The two puzzles we discussed here can be resolved by an early phase during which the comoving Hubble horizon is shrinking monotonically, as first noted in [64]. Such an early phase can be realized by an early accelerated expansion of the universe which is called (cosmic) inflation. Inflation was previously considered in [61–63] without application to the Big Bang puzzles.

4.2   Slow-roll Inflation

The condition on the shrinking Hubble horizon $\mathrm{d}(aH)^{-1}/\mathrm{d}t < 0$ can be reformulated to

$$\frac{\ddot{a}}{a} = H^2(1 - \epsilon) > 0\,, \tag{4.10}$$

which indicates an accelerated expansion and we introduced the slow-roll parameter

$$\epsilon = -\frac{\dot{H}}{H^2}\,. \tag{4.11}$$

Using the second Friedmann equation (4.3) we can rewrite (4.10) to a condition on the energy density ρ and pressure p of a perfect fluid

$$\frac{\ddot{a}}{a} = -\frac{1}{6M_{\mathrm{Pl}}^2}(\rho + 3p) > 0 \quad \text{or} \quad w < -\frac{1}{3}\,, \tag{4.12}$$

where $w = p/\rho$ is the equation of state. The situation with $(\rho + 3p) < 0$ is reminiscent of dark energy which is needed for accelerated expansion in the late universe. However, the difference is that primordial inflation needs to end at some point and the vacuum energy during inflation needs to be transferred to the SM particles such that the conventional Bing Bang timeline can set in. This transition process is called reheating.

The first ideas in that direction go nowadays under the name of "old inflation" [64]. In that case the inflationary dynamics are realized by a first-order

phase transition. A scalar field is trapped in the false vacuum and the universe expands due to the vacuum energy domination. This dominance is ended when the field tunnels to the true vacuum and consequently the accelerated expansion would stop. The old inflation idea suffers under the "graceful exit" problem. Due to the nature of first-order phase transitions, the transition proceeds via nucleation of true vacuum bubbles in sea of the false vacuum. The idea that these bubbles coalesce at some point to fill the entire universe with the true vacuum is problematic. By construction the regions in the false vacuum get inflated exponentially such that in this background the true vacuum bubbles have trouble merging and filling the universe. This situation would evolve into an inhomogeneous universe with most regions trapped in the false vacuum.

A little later the idea of "new inflation" was born which led to the modern picture of so-called slow-roll inflation [65, 66] where a scalar field called the "inflaton" is slowly rolling down a potential hill such that accelerated expansion can be achieved. We will explain this more quantitatively by a scalar field coupled minimally to gravity

$$S = S_\phi - \frac{M_{\mathrm{Pl}}^2}{2} \int \mathrm{d}^4x \, \sqrt{-g} \, R \,, \tag{4.13}$$

$$S_\phi = \int \mathrm{d}^4x \, \sqrt{-g} \left(-\frac{1}{2} g^{\mu\nu} \partial_\mu \phi \partial_\mu \phi - V(\phi) \right) \,, \tag{4.14}$$

by following [122, 123]. The related energy-momentum tensor of the scalar ϕ is as usual derived by

$$T_{\mu\nu}^{(\phi)} = -\frac{2}{\sqrt{-g}} \frac{\delta S}{\delta g^{\mu\nu}} \,, \tag{4.15}$$

and comparing this to the energy-momentum tensor of a perfect fluid in the FLRW background (4.1) and assuming a spatial homogeneous scalar field $\phi(x) = \phi(t)$ we can deduce the respective density and pressure densities

$$\rho_\phi = \frac{1}{2} \dot{\phi}^2 + V(\phi) \,, \quad p_\phi = \frac{1}{2} \dot{\phi}^2 - V(\phi) \,. \tag{4.16}$$

The dynamics are governed by the equation of motion for the scalar field in the FLRW background and the Friedmann equation (4.2)

$$\ddot{\phi} + 3H\dot{\phi} + V' = 0 \,, \quad H^2 = \frac{\rho_\phi}{3M_{\mathrm{Pl}}^2} \,. \tag{4.17}$$

Using now (4.10), (4.12) and (4.16) we can write the slow-roll parameter as

$$\epsilon = \frac{1}{2M_{\mathrm{Pl}}^2} \frac{\dot{\phi}^2}{H^2} \,. \tag{4.18}$$

An accelerated expansion is achieved for $\epsilon < 1$ and this requires domination of the potential energy over the kinetic energy

$$\frac{V(\phi)}{\dot{\phi}^2} \gg 1 \,, \tag{4.19}$$

which explains the origin of the name "slow-roll". In that case one also finds that $p_\phi \simeq -\rho_\phi$ and

$$H^2 \simeq \frac{V}{3M_{\rm Pl}^2} \,. \tag{4.20}$$

For the accelerated expansion to last long enough we have to ensure that the second time derivative stays small which is encoded in the second slow-roll parameter defined by

$$\delta = -\frac{\ddot{\phi}}{H\dot{\phi}} \,, \tag{4.21}$$

and $|\delta| \ll 1$ then ensures that the fractional change in ϵ per e-fold of inflation stays small and that one can omit the $\ddot{\phi}$ term in the equation of motion (4.17). For future reference, we also define the related slow-roll parameter

$$\eta = \frac{\dot{\epsilon}}{H\epsilon} = 2\left(\frac{\ddot{\phi}}{H\dot{\phi}} - \frac{\dot{H}}{H^2}\right) = 2(\epsilon - \delta) \,. \tag{4.22}$$

Note that $\epsilon \ll 1$ and $\delta \ll 1$ imply also $\eta \ll 1$. When these slow-roll conditions and (4.20) are satisfied one can alternatively derive slow-roll conditions on the scalar potential, by defining the so-called potential slow-roll parameters

$$\epsilon_V = \frac{M_{\rm Pl}^2}{2}\left(\frac{V'}{V}\right)^2$$
$$\eta_V = M_{\rm Pl}^2 \frac{V''}{V} \,, \tag{4.23}$$

where $\epsilon \simeq \epsilon_V$ and $\eta = -2\eta_V + 4\epsilon_V$ are valid in the slow-roll approximation. In our later studies we will monitor by

$$\epsilon_V, |\eta_V| \ll 1 \,, \tag{4.24}$$

whether the slow-roll conditions are satisfied. In the limit of $\epsilon, \eta \to 0$, where $H^2 = \text{const}$ the space-time is approximated by de Sitter space-time where the scale factor grows exponentially $a(t) \sim e^{Ht}$. Inflation ends by violating one of the slow-roll conditions (4.24) and is quantified by the field value $\phi_{\rm end}$ at which

$$\max\{\epsilon_V(\phi_{\rm end}), |\eta_V(\phi_{\rm end})|\} = 1 \,. \tag{4.25}$$

The quantification for the minimal duration of inflation is given by the number of e-folds the scale factor expands between a and a_{end}, which can be expressed by the integral

$$N_e = \ln(a_{\text{end}}/a) = \int_t^{t_{\text{end}}} H \mathrm{d}t \approx \int_{\phi_{\text{end}}}^{\phi} \frac{\mathrm{d}\phi}{\sqrt{2\epsilon_V}}\,, \qquad (4.26)$$

where we assumed the validity of the slow-roll approximation in last equality. To solve the flatness and horizon problem one needs at least $N = 60$ e-folds of inflation [124].

4.3   Beyond Homogeneity

Our treatment so far was purely classical and it is able to explain the homogeneity of the observed CMB as demanded in Section 4.1. However, we do observe inhomogeneities in the CMB as indicated in (4.6). The anisotropies in the CMB are the seeds of all structure we observe today and we remain with the open question what originated these fluctuations. Fortunately, including quantum-mechanical perturbations in the treatment of inflation will answer precisely this question, as we lay out in the rest of this section. This connection gives also hope that a precise analysis of the CMB power spectrum might give opportunities to test inflation models.

4.3.1   Classification of Perturbations

We are now going one step further by including perturbations at the linear order on top of the FLRW-background (4.1) with $k = 0$ denoted by the metric $\bar{g}_{\mu\nu}(t)$. Since these perturbations are small, it sufficient to consider the Einstein Equations only at the linear level, as is usually done in cosmological perturbation theory. We consider the perturbation $h_{\mu\nu}(x)$ on top of this background by

$$g_{\mu\nu}(x) = \bar{g}_{\mu\nu}(t) + h_{\mu\nu}(x)\,, \qquad (4.27)$$

as well as the perturbation of the inflaton field $\delta\phi(t, \boldsymbol{x})$ by

$$\phi(t, \boldsymbol{x}) = \phi(t) + \delta\phi(t, \boldsymbol{x})\,. \qquad (4.28)$$

The background quantities $\bar{g}_{\mu\nu}(t)$ and $\phi(t)$ only carry time-dependence as expected for the homogeneous FLRW background.

Metric Perturbations

The metric perturbation $h_{\mu\nu}$ is usually further decomposed into scalar, transverse vector and traceless-transverse tensor modes (SVT decomposition). This simplifies the further treatment substantially since these modes decouple at

the linear level and can be studied independently of each other. Applying this decomposition to the metric gives

$$\mathrm{d}s^2 = (1 + E)\mathrm{d}t^2 - 2a(\partial_i F - G_i)\mathrm{d}x^i\mathrm{d}t$$
$$- a^2 \left[(1 + A)\delta_{ij} + \partial_i\partial_j B + \partial_i C_j + \partial_j C_i + D_{ij}\right]\mathrm{d}x^i\mathrm{d}x^j\,, \qquad (4.29)$$

where we count four scalars (E, F, A, B), two transverse vectors $(\partial_i G_i = 0$ and $\partial_i C_i = 0)$, and one traceless-transverse tensor $(D_{ii} = \partial_i D_{ij} = 0)$. This counts up to the ten degrees of freedom encoded in $h_{\mu\nu}$.

The next step would be to derive the linearized and SVT-decomposed Einstein equations from (4.29). We will do without this elaborate task and instead refer to the textbook [124]. One important lesson from the equations of motion for the vector modes G_i and C_i is, however, that these mode are decaying and therefore cannot be produced during inflation. Hence, it will be enough to focus on the scalar modes and the tensor mode. The scalar modes present in (4.29) turn out be not gauge-invariant and require therefore further scrutiny.

Some of these modes are considered unphysical in the sense that they can be related to a mere coordinate change of the FLRW background coordinates. The splitting between what we call the background and perturbation is therefore not unique and one has to be careful with identifying physical observables. The gauge transformation acting on the scalar perturbations in (4.29) is inherited from from the general coordinate invariance of General Relativity

$$x^\mu \to x'^\mu = x^\mu + \epsilon^\mu(x)\,, \qquad (4.30)$$

$$g'_{\mu\nu}(x') = \frac{\partial x^\lambda}{\partial x'^\mu}\frac{\partial x^\kappa}{\partial x'^\nu}g_{\lambda\kappa}(x)\,, \qquad (4.31)$$

with $\epsilon^\mu(x)$ small. Instead of working with gauge transformations acting on the coordinates, it is helpful to reformulate this transformation as acting on the perturbation $h_{\mu\nu}$ while keeping the background metric $\bar{g}_{\mu\nu}(t)$ unchanged. The corresponding gauge transformation $h_{\mu\nu} \to h_{\mu\nu} + \Delta h_{\mu\nu}$ can then be derived using (4.30) and (4.31)

$$\Delta h_{\mu\nu}(x) = -\bar{g}_{\lambda\mu}(x)\frac{\partial \epsilon^\lambda(x)}{\partial x^\nu} - \bar{g}_{\lambda\nu}(x)\frac{\partial \epsilon^\lambda(x)}{\partial x^\mu} - \frac{\partial \bar{g}_{\mu\nu}(x)}{\partial x^\lambda}\epsilon^\lambda\,, \qquad (4.32)$$

where we are keeping only terms at linear order in $\epsilon(x)$ and $h_{\mu\nu}(x)$. To analyze the metric perturbations in the SVT-decomposition, we decompose the spatial part of the coordinate transformation (4.30) as

$$\epsilon_i = \partial_i\epsilon^S + \epsilon_i^V\,, \quad \partial_i\epsilon_i^V = 0\,. \qquad (4.33)$$

Writing now (4.32) component wise with the above decomposition we obtain

$$\Delta h_{00} = -2\dot{\epsilon}_0\,, \qquad (4.34)$$

$$\Delta h_{i0} = -\partial_i\dot{\epsilon}^S - \partial_i\epsilon_0 + 2H(\partial_i\epsilon^S + \epsilon_i^V)\,, \qquad (4.35)$$

$$\Delta h_{ij} = -\partial_j\epsilon_i^S - \partial_i^S\epsilon_j - \epsilon_i^V - \epsilon_j^V + 2a\dot{a}\delta_{ij}\epsilon_0\,. \qquad (4.36)$$

These can be now compared with (4.29) to obtain the transformation rules for the SVT variables. One directly finds that the traceless-transverse tensor is gauge-invariant

$$\Delta D_{ij} = 0 \,. \tag{4.37}$$

The transverse vector variables transform according to

$$\Delta C_i = -\frac{1}{a^2}\epsilon_i^V \,, \tag{4.38}$$

$$\Delta G_i = \frac{1}{a}\left(-\dot{\epsilon}_i^V + 2H\epsilon_i^V\right) , \tag{4.39}$$

and finally the scalars by

$$\Delta A = 2H\epsilon_0 \,, \qquad\qquad \Delta B = -\frac{2}{a^2}\epsilon^S \,, \tag{4.40}$$

$$\Delta E = 2\dot{\epsilon}_0 \,, \qquad\qquad \Delta F = \frac{1}{a}\left(-\epsilon_0 - \dot{\epsilon}^S + 2H\epsilon^S\right) . \tag{4.41}$$

This clearly exposes that not all of the metric perturbations in (4.29) are gauge-invariant. To get rid of the gauge redundancy exposed here, we can either work with gauge invariant quantities or by fixing a gauge. For example one can work with the combination $\tilde{G}_i = G_i - a\dot{C}_i$ of the vector modes such that $\Delta\tilde{G}_i = 0$. Similarly one can construct two gauge invariant scalar metric perturbations, which are also known as Bardeen potentials [128], which in notation of (4.29) read

$$\Psi_B = -\frac{1}{2}\left[A - a^2 H\left(\dot{B} - 2\frac{F}{a}\right)\right] , \tag{4.42}$$

$$\Phi_B = \frac{1}{2}\left[E - \frac{\mathrm{d}}{\mathrm{d}t}\left(a^2\left(\dot{B} - 2\frac{F}{a}\right)\right)\right] . \tag{4.43}$$

Matter Perturbations

The Einstein Equations couple the metric perturbations to the matter perturbations given by $\delta T_{\mu\nu}$, i.e. the perturbation of the energy-momentum tensor. The primordial quantum-mechanical perturbations $\delta\phi$ of the of the inflaton field we lead ultimately to the inhomogeneities we observe in the CMB. Therefore, $\delta T_{\mu\nu}$ should also be SVT-decomposed for our purpose. This will furthermore turn out useful to define gauge-invariant scalar modes with the special feature of being conserved outside the horizon, as we will see shortly.

Let us start with the background, so zeroth-order, energy-momentum tensor $\bar{T}_{\mu\nu}$ in the FLRW ansatz which is modeled by a perfect fluid

$$\bar{T}_{\mu\nu} = (\bar{\rho} + \bar{p})\bar{u}_\mu\bar{u}_\nu + \bar{p}\bar{g}_{\mu\nu} \,, \tag{4.44}$$

where the barred quantities are the unperturbed energy density, pressure and the velocity four vector. These quantities are purely time-dependent owing to the spatial translational and rotational symmetry of the background. The perturbations of the stress-energy tensor are decomposed according to

$$\delta T_{00} = -\bar{\rho} h_{00} + \delta\rho \,, \tag{4.45}$$

$$\delta T_{i0} = \bar{p} h_{i0} - (\bar{\rho} + \bar{p}) \left(\partial_i \delta u + \delta u_i^V \right) \,, \tag{4.46}$$

$$\delta T_{ij} = \bar{p} h_{ij} + a^2 \left(\delta_{ij} \delta p + \pi_{ij} \right) \,, \tag{4.47}$$

where we have introduced the anisotropic stress π_{ij} and have decomposed the three-velocity by $\delta u_i = \partial_i \delta u + \delta u_i^V$. Similarly as we have done for the metric perturbations (4.32), we can derive the gauge transformation for

$$\Delta \delta T_{\mu\nu} = -\bar{T}_{\lambda\mu}(x) \frac{\partial \epsilon^\lambda(x)}{\partial x^\nu} - \bar{T}_{\lambda\nu}(x) \frac{\partial \epsilon^\lambda(x)}{\partial x^\mu} - \frac{\partial \bar{T}_{\mu\nu}(x)}{\partial x^\lambda} \epsilon^\lambda \,. \tag{4.48}$$

Comparing the components above to eqs. (4.45)-(4.47) and using eqs. (4.34)-(4.36) we can derive the transformation rules

$$\Delta \delta p = \dot{\bar{p}} \epsilon_0 \,, \quad \Delta \delta\rho = \dot{\bar{\rho}} \epsilon_0 \,, \quad \Delta \delta u = -\epsilon_0 \,. \tag{4.49}$$

Note that the anisotropic stress π_{ij} and δu_i^V are gauge-invariant.

Fourier Decomposition

Before we continue, it is useful to define the Fourier transform $A_{\boldsymbol{k}}(t)$ of a general perturbation $A(t, \boldsymbol{x})$ as

$$A_{\boldsymbol{k}}(t) = \int \mathrm{d}^3\boldsymbol{x} A(t, \boldsymbol{x}) e^{i\boldsymbol{k}\cdot\boldsymbol{x}} \,. \tag{4.50}$$

Due to the translational invariance of the FLRW background, Fourier modes with different wavevector $\boldsymbol{k}$ do not couple to each other at the linear level of the equations of motion. Thus, two perturbations $A_{\boldsymbol{k}}$ and $A_{\boldsymbol{k}'}$ will evolve independently from each other at linear level when $\boldsymbol{k} \neq \boldsymbol{k}'$.

4.3.2 Conservation of Perturbations Outside the Horizon

We are particularly interested in the gauge-invariant modes which will leave the comoving Hubble horizon $(aH)^{-1}$ during inflation an reenter shortly before recombination, as these correspond to the scales tested by the anisotropies of the CMB. We refer to those Fourier modes which satisfy $k \ll aH$ as superhorizon modes, where $k = |\boldsymbol{k}|$. The particular feature of these modes is that they are conserved on superhorizon scales, which is particularly useful since it can relate the primordial values of the perturbations to the inhomogeneities of the CMB, and thereby we bypass the unknown evolution of perturbations during the reheating stage, about which we know very little.

We start by introducing the gauge-invariant variable [128]

$$\mathcal{R} = \frac{A}{2} + H\delta u\,, \tag{4.51}$$

also known as the comoving curvature perturbation which measures the spatial curvature of comoving hypersurfaces [122]. It easy to check with (4.40) and (4.49) that $\mathcal{R}$ is gauge-invariant. This quantity is conserved, on superhorizon scales $k \ll aH$ under very general conditions on the matter perturbations as has been proven in [129]. First, we introduce the uniform-density hypersurface

$$\zeta = \frac{A}{2} - \frac{H}{\dot{\bar{\rho}}}\delta\rho\,, \tag{4.52}$$

which is equal to $\mathcal{R}$ on superhorizon scales which can be seen from the following relation derived from the linearized Einstein equations in Fourier space [122]

$$-\zeta = \mathcal{R} + \frac{k^2}{a^2 H^2}\frac{2\bar{\rho}}{3(\bar{\rho} + \bar{p})}\Psi_B\,, \tag{4.53}$$

where we dropped the subscripts $\boldsymbol{k}$ of the Fourier modes for convenience. The continuity equation derived from the local conservation law $\nabla_\mu T^{\mu\nu} = 0$ can be cast to the form [122, 130]

$$\frac{\dot{\zeta}}{H} = -\frac{\dot{\bar{p}}}{(\bar{\rho} + \bar{p})}\delta p_{\text{en}} - \frac{k^2}{3a^2 H^2}\left[\zeta - \Psi_B\left(1 - \frac{2\bar{\rho}}{9(\bar{\rho} + \bar{p})}\frac{k^2}{a^2 H^2}\right)\right]\,, \tag{4.54}$$

where we have defined the entropic pressure perturbation as

$$\delta p_{\text{en}} = \frac{\delta p}{\dot{\bar{p}}} - \frac{\delta\rho}{\dot{\bar{\rho}}}\,. \tag{4.55}$$

Since ζ and $\mathcal{R}$ are equal on superhorizon scales due to (4.53), it follows that the superhorizon modes of $\mathcal{R}$ are conserved

$$\dot{\mathcal{R}} = 0 \quad\text{for}\quad k \ll aH \quad\text{and}\quad \delta p_{\text{en}} = 0\,, \tag{4.56}$$

for adiabatic perturbations on superhorizon scales. The adiabatic condition is satisfied when the ratio $\delta g/\dot{\bar{g}}$ for a general perturbation δg is equal for any perturbation [127]. In particular, applied to the energy density and pressure perturbations it follows that (4.55) vanishes. Single-field inflation can only give rise to adiabatic perturbations but it cannot give rise to a relative density contrast of different perturbations violating (4.55). In other words, all inhomogeneities like that of dark matter or radiation are then tied to the curvature perturbation $\mathcal{R}$ [122]. Up to this point, there is no evidence for non-adiabatic, or so-called isocurvature perturbations in the CMB [131].

The conservation law (4.56) for adiabatic perturbations allows us, as previously advertised, to connect the primordial power spectrum of $\mathcal{R}$ which is

initially generated by quantum fluctuations to the anisotropies of the CMB. These modes are initially on subhorizon scales, leave the Hubble horizon during inflation when $k_* = a_* H_*$ and reenter the Hubble horizon before recombination (see also Fig. 4.1). Fortunately, the perturbations which we can test with CMB observations are subject to the conservation law (4.56).
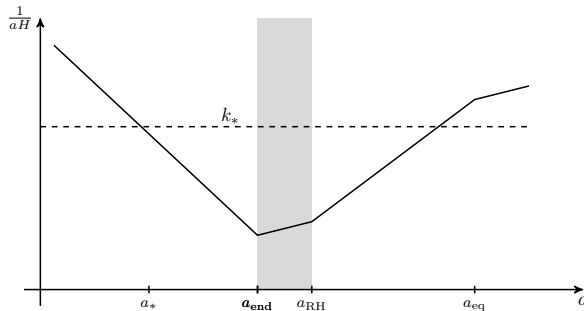
Figure 4.1: Evolution of the comoving Hubble radius (solid line) and a perturbation (dashed line) with corresponding comoving wavenumber $k_* = a_* H_*$. The gray area indicates the era of reheating. The scale factor a_{end} denotes the end of inflation, a_{RH} denotes the start of radiation domination and a_{eq} denotes matter-radiation equality.

4.3.3 Quantum Fluctuations as Initial Conditions

The next step is to compute the scalar perturbation $\mathcal{R}$ at horizon exit and connect it to primordial quantum fluctuations as initial conditions. These quantum fluctuations are then stretched out during inflation and give rise to the cosmological perturbations which are imprinted in the CMB. The starting point is to expand the action (4.13) up to second order in the fluctuations. Up to a total derivative, one obtains the so-called Mukhanov action [132]

$$S_2 = \frac{M_{\mathrm{Pl}}^2}{2} \int \mathrm{d}\tau \mathrm{d}^3 x \left(v'^2 - (\partial_i v)^2 + \frac{z''}{z} v^2 \right). \tag{4.57}$$

We are left with only one final gauge-invariant scalar perturbation v, where the treatment of tensor perturbations is postponed to Section 4.3.5. It is related to the comoving curvature perturbation by

$$v = z\mathcal{R} = z\left(\frac{A}{2} - \frac{H}{\dot{\bar{\phi}}} \delta\phi \right), \quad z = \frac{a\bar{\phi}'}{\mathcal{H}}, \tag{4.58}$$

where $\mathcal{H} = a'/a$ and primes denote derivatives with respect to the conformal time coordinate τ defined through the line element

$$\mathrm{d}s^2 = a^2(\tau)\left(\mathrm{d}\tau^2 - \mathrm{d}\boldsymbol{x}^2 \right). \tag{4.59}$$

We now promote v to a quantum operator and follow the quantization procedure analogous to that of a simple harmonic oscillator by following [122]. We start by introducing creation and annihilation operators for

$$\hat{v} = \int \frac{\mathrm{d}^3 k}{(2\pi)^3} \left(v_k(\tau) \hat{a}_{\boldsymbol{k}} e^{i\boldsymbol{k}\cdot x} + v_k^*(\tau) \hat{a}_{\boldsymbol{k}}^\dagger e^{-i\boldsymbol{k}\cdot x} \right) . \tag{4.60}$$

The momentum modes satisfy a Klein-Gordon equation in Fourier space

$$v_k'' + \left(k^2 - \frac{z''}{z} \right) v_k = 0 \, , \tag{4.61}$$

with the term in brackets defining a time-dependent frequency. The creation and annihilation operator should satisfy the usual commutation relation

$$\left[\hat{a}_{\boldsymbol{k}} , \hat{a}_{\boldsymbol{k}'}^\dagger \right] = (2\pi)^3 \delta(\boldsymbol{k} - \boldsymbol{k}') \, , \tag{4.62}$$

which entails that the mode functions should be normalized according to

$$i(v_k^* v_k' - (v_k^*)' v_k) = 1 \, . \tag{4.63}$$

The vacuum state $|0\rangle$ is defined as usual by

$$\hat{a}_{\boldsymbol{k}} |0\rangle = 0 \, , \tag{4.64}$$

which imposes a further condition on v_k. To define the vacuum state we consider that modes in the far past $\tau \to -\infty$ are deeply subhorizon and behave as in Minkowski vacuum. In this limit (4.61) simplifies to standard mode equation for a harmonic oscillator

$$v_k'' + k^2 v_k = 0 \, . \tag{4.65}$$

As initial condition in the far past we therefore impose the standard normalization in Minkowski space

$$\lim_{\tau \to -\infty} v_k = \frac{e^{-ik\tau}}{\sqrt{2k}} \, . \tag{4.66}$$

We can solve (4.61) in the de Sitter limit, i.e. when $\epsilon \to 0$ and $H = \text{const}$, and furthermore

$$\lim_{\epsilon \to 0} \frac{z''}{z} = \frac{2}{\tau^2} \, , \tag{4.67}$$

which simplifies the mode equation (4.61) in this limit to

$$v_k'' + \left(k^2 - \frac{2}{\tau^2} \right) v_k = 0 \, . \tag{4.68}$$

The above equation can be solved with the asymptotic normalization (4.66) and one finds the solution

$$v_k = \frac{e^{-ik\tau}}{\sqrt{2}} \left(1 - \frac{i}{k\tau} \right) \, , \tag{4.69}$$

also known as Bunch-Davies mode functions [133], which are related to the curvature perturbation $\mathcal{R}$ by (4.58).

4.3.4   Power Spectrum of Scalar Perturbations

The CMB temperature map test the statistical properties of the scalar perturbations. The power spectrum of these perturbations contains all statistical information if they follow Gaußian statistics. Therefore, it is important to compute this power spectrum of the $\mathcal{R}$-perturbation which is defined by the ensemble average

$$\langle \mathcal{R}_{\boldsymbol{k}}(t_*)\mathcal{R}_{\boldsymbol{k}'}(t_*)\rangle = (2\pi)^3\delta(\boldsymbol{k}+\boldsymbol{k}')P_{\mathcal{R}}(k)\,, \tag{4.70}$$

where the delta distribution is a reflection of translational invariance of the background. Note that non-Gaußianities are suppressed in single-field inflation models [134] and so far no clear evidence for the existence of non-Gaußianities has been found in the CMB [135].

It is convenient to also introduce the dimensionless power spectrum

$$\Delta_{\mathcal{R}}(k) = \frac{k^3}{2\pi^2}P_{\mathcal{R}}(k)\,. \tag{4.71}$$

If the power spectrum is exactly scale-invariant this means that $k^3 P_{\mathcal{R}}(k)$ is constant because the factor k^3 cancels the volume dependence of $P_{\mathcal{R}}(k)$. Therefore, it is sensible to analyse the real scale-dependence of scalar modes with the dimensionless power spectrum (4.71). We now would like to solve the equation (4.61) at linear order in the slow-roll parameters to compute the power spectrum (4.71) in this approximation. Our previous result (4.69) was derived in exact de Sitter space, so to zeroth order in slow-roll parameters. For this calculation it is useful to rewrite the slow-roll parameters (4.11) and (4.22) in conformal coordinates (4.59)

$$\epsilon = \left(1 - \frac{\mathcal{H}'}{\mathcal{H}^2}\right)\,, \quad \eta = \frac{1}{\mathcal{H}}\frac{\epsilon'}{\epsilon}\,. \tag{4.72}$$

The above relation for ϵ can be integrated and using that ϵ is constant to the order we work in

$$\int \mathrm{d}\tau\,\frac{\mathcal{H}'}{\mathcal{H}^2} = \int \mathrm{d}\tau(\epsilon - 1) \approx \tau(\epsilon - 1)\,, \tag{4.73}$$

which yields to order $\mathcal{O}(\epsilon)$

$$\mathcal{H} \approx -\frac{1}{\tau}(1 + \epsilon)\,. \tag{4.74}$$

Using (4.72) and (4.74) we can compute the time dependent term in (4.61)

$$\frac{z''}{z} = \frac{1}{\tau^2}\left(2 + 3\epsilon + \frac{3}{2}\eta\right) =: \frac{\nu^2 - \frac{1}{4}}{\tau^2}\,, \tag{4.75}$$

which has the correct de Sitter limit (4.67). We also have defined the parameter

$$\nu = \frac{3}{2} + \epsilon + \frac{\eta}{2} \,, \tag{4.76}$$

such that the second equality in (4.75) holds at leading order. The convenience of this definition is that the mode equation (4.61) written with (4.75), has a general solution given by a linear combination of the Hankel functions $H_\nu^{(i)}$ of the first two kinds [122]

$$v_k(\tau) = \frac{\sqrt{\pi}}{2}\sqrt{-\tau}\left[c_1 H_\nu^{(1)}(-k\tau) + c_2 H_\nu^{(2)}(-k\tau)\right] \,. \tag{4.77}$$

The coefficients can be determined by comparing the limit of the far past

$$\lim_{(k\tau)\to-\infty} H_\nu^{(1,2)}(-k\tau) = \frac{2}{\sqrt{\pi}}\frac{1}{\sqrt{-k\tau}}e^{\mp i(k\tau+\alpha)} \,, \tag{4.78}$$

where $\alpha = \pi/2(\nu+1/2)$ is an irrelevant phase shift, to the Minkowski boundary condition (4.66). One finds therefore that $c_1 = 1$ and $c_2 = 0$ which results in

$$v_k(\tau) = \frac{\sqrt{\pi}}{2}\sqrt{-\tau}H_\nu^{(1)}(-k\tau) \,. \tag{4.79}$$

This finally allows to compute the power spectrum (4.70) by the relation

$$P_{\mathcal{R}}(k) = \frac{|v_k|^2}{z^2} \,. \tag{4.80}$$

As laid out in Section 4.3.2, the benefit of working with the curvature perturbation $\mathcal{R}$ is that it is conserved after horizon crossing, so we can compute its value at that time t_* where $k_* = a(t_*)H(t_*)$ and then rely on its constancy for $|k\tau| \ll 1$. For the superhorizon limit $|k\tau| \to 0$ it useful to use the limit [122]

$$\lim_{k\tau\to 0} H_\nu^{(1)}(-k\tau) = \frac{i}{\pi}\Gamma(\nu)\left(\frac{-k\tau}{2}\right)^{-\nu} \approx i\sqrt{\frac{2}{\pi}}(-k\tau)^{3/2} \,, \tag{4.81}$$

where in the second equality we used the de Sitter limit $\epsilon = \eta = 0$. Considering now the dimensionless version (4.71) of the power spectrum, we can combine the results (4.79) - (4.81) to derive the value of the power spectrum at horizon crossing

$$\Delta_{\mathcal{R}}(k_*) \approx \frac{1}{8\pi^2 M_{\rm Pl}^2}\left(\frac{1}{\epsilon}\frac{1}{a^2\tau^2}\right)\bigg|_{k=a_* H_*} = \frac{1}{8\pi^2 M_{\rm Pl}^2}\left(\frac{H_*^2}{\epsilon_*}\right) \,. \tag{4.82}$$

In slow-roll approximation the Hubble rate is approximated by the potential energy of the inflaton (cf. (4.20)). Furthermore, using the potential slow-roll parameter (4.23) we define the amplitude of the scalar power spectrum

$$A_s := \Delta_{\mathcal{R}}(k_*) = \frac{1}{24\pi^2 M_{\rm Pl}^4}\left(\frac{V_*}{\epsilon_{V*}}\right) \,. \tag{4.83}$$

Scale-dependence of Scalar Fluctuations

The scale-dependence of the scalar power spectrum is encoded in the so-called spectral tilt defined by

$$n_s - 1 = \frac{\mathrm{d} \ln \Delta_{\mathcal{R}}}{\mathrm{d} \ln k} \,. \tag{4.84}$$

To analyze the scale-dependence, or k-dependence, we can utilize (4.81) and be reminded of the additional k^3 in (4.71), to obtain the scaling relation

$$\Delta_{\mathcal{R}} \sim k^{3-2\nu} \,. \tag{4.85}$$

The spectral tilt is then determined by the slow-roll parameters

$$n_s - 1 = 3 - 2\nu = -2\epsilon - \eta = 2\eta_{V*} - 6\epsilon_{V*} \,. \tag{4.86}$$

To summarize, the power spectrum is often parameterized in a power law around the pivot scale k_*, i.e.

$$\Delta_{\mathcal{R}}(k) = A_s(k_*) \left(\frac{k}{k_*} \right)^{n_s(k_*)-1} \,, \tag{4.87}$$

where we neglect the running (k-dependence) of the spectral tilt.

4.3.5 Primordial Gravitational Waves

So far we have only considered perturbations classified as scalar modes. However, as we have seen in in (4.29) there us is also perturbation described by a transverse-traceless tensor D_{ij}. It can be understood as a spin-2 degree of freedom, so corresponds to primordial gravitational waves generated from inflation. A substantial simplification with respect to scalar perturbations is that these tensor modes are already gauge-invariant. Focusing only on the tensor modes, (4.29) reads in conformal coordinates

$$\mathrm{d}s^2 = a^2(\tau) \left[\mathrm{d}\tau^2 - (\delta_{ij} + D_{ij}) \, \mathrm{d}x^i \mathrm{d}x^j \right] \,. \tag{4.88}$$

Plugging this into the Einstein-Hilbert action and expanding to second order in the tensor perturbations we obtain [132]

$$S_2^T = -\frac{M_{\mathrm{Pl}}^2}{8} \int \mathrm{d}^3 x \mathrm{d}\eta \, a^2 \left[(D'_{ij})^2 - (\nabla D_{ij})^2 \right] \,. \tag{4.89}$$

We proceed by a Fourier decomposition and an expansion in the two polarization tensors

$$D_{ij}(\tau, \boldsymbol{x}) = \sum_{s=\{+,\times\}} \int \frac{\mathrm{d}^3 k}{(2\pi)^3} \epsilon_{ij}^s(\boldsymbol{k}) h_{\boldsymbol{k}}^s(\tau) e^{-i\boldsymbol{k}\cdot\boldsymbol{x}} \,, \tag{4.90}$$

where the massless spin-2 excitation carries two degrees of freedom of helicities +2 and -2, so it has two independent polarization tensors ϵ_{ij}^{+} and $\epsilon_{ij}^{\times}$. They have the property[2] $\epsilon_{\ i}^{s\ j}(\boldsymbol{k})\epsilon_{\ j}^{s\ i}(-\boldsymbol{k}) = \delta_{ss'}$ so that the action becomes

$$S_2^T = -\frac{M_{\mathrm{Pl}}^2}{8} \sum_{s=\{+,\times\}} \int \mathrm{d}^3 k \mathrm{d}\eta\, a^2 \left[h_{\boldsymbol{k}}^{s\prime} h_{-\boldsymbol{k}}^{s\prime} - k^2 h_{\boldsymbol{k}}^{s} h_{-\boldsymbol{k}}^{s} \right] . \tag{4.91}$$

Introducing a new variable

$$v_{\boldsymbol{k}}(\tau) = \frac{M_{\mathrm{Pl}} a}{2} h_{\boldsymbol{k}}^{s}(\tau) , \tag{4.92}$$

the action reads up to total derivatives

$$S_2^T = -\frac{1}{2} \int \mathrm{d}^3 k \mathrm{d}\eta \left[v_{\boldsymbol{k}}^{s\prime} v_{-\boldsymbol{k}}^{s\prime} - \left(k^2 - \frac{a''}{a} \right) v_{\boldsymbol{k}}^{s} v_{-\boldsymbol{k}}^{s} \right] . \tag{4.93}$$

The momentum modes satisfy the equation of motion

$$v_{\boldsymbol{k}}^{s\,\prime\prime} + \left(k^2 - \frac{a''}{a} \right) v_{\boldsymbol{k}}^{s} = 0 . \tag{4.94}$$

Each polarization therefore satisfies a similar mode equation as in the scalar case (4.61) but with a simpler time dependence a''/a, which can be approximated in slow-roll parameters by

$$\frac{a''}{a} \approx \frac{1}{\tau^2}(2 + 3\epsilon) =: \frac{\nu_T^2 - \frac{1}{4}}{\tau^2} . \tag{4.95}$$

As before, we have defined the index

$$\nu_T = \frac{3}{2} + 3\epsilon , \tag{4.96}$$

such that we can solve (4.94) with the same methods as previously shown in section 4.3.4. One finds that the power spectrum for a single polarization of primordial gravitational waves is

$$\Delta_h^2(k) = \frac{1}{\pi^2 M_{\mathrm{Pl}}^2} H_*^2 . \tag{4.97}$$

We could proceed by defining a spectral tilt for tensor modes as in the previous section 4.3.4, but since this is not measured by observations so far, we do not need it in this thesis. However, what can be inferred from the CMB observation is an upper limit on the ratio of the tensor amplitude to the scalar amplitude. This quantity is called tensor-to-scalar ratio and is defined as

$$r := \frac{2\Delta_h^2(k_*)}{\Delta_{\mathcal{R}}^2(k_*)} = 16\epsilon_* . \tag{4.98}$$

The factor of two accounts for the sum of the two polarizations for gravitational waves.

---

[2]This can be derived for a plane wave traveling in z-direction.

4.4   Effect on the Cosmic Microwave Background

We now would like to make contact to observations. In the previous two sections, we have defined three important quantities: the amplitude of scalar fluctuations A_s (4.83), the spectral tilt for scalar fluctuations n_s (4.86) and the tensor-to-scalar ratio r (4.98). Through these formulas, their values can be related to the shape of the inflaton potential encoded in the potential slow-roll parameters (4.23). Since these three quantities are constrained by CMB observation this offers the opportunity to test inflation models.

The power spectrum of scalar perturbations is imprinted on the last scattering surface by making some regions overdense, while other regions are underdense. This leads to different amounts of redshifts of the escaping photons making up the CMB. This phenomenon is known as the Sachs-Wolfe effect [136] and it basically relates the anisotropy in the temperature δT in the direction of sight $\hat{e}$ to the primordial curvature perturbation [127]

$$\frac{\delta T(\hat{e})}{T_0} \sim \mathcal{R} \, . \tag{4.99}$$

The above is only true for the largest scales we can observe in the CMB. These just entered the horizon shortly before recombination and where not subjected to subhorizon evolution. Therefore, one can say that with observation of these large scales we test the primordial spectrum $P_\mathcal{R}$ through (4.99) very directly. On smaller scales, or equivalently smaller angles on the sky, we need to take into account the evolution between horizon entry and recombination. In contrast to the epoch of reheating, we know the equations of motion for the perturbations, since the scales of interest enter during radiation or matter domination.

To make this connection a bit clearer, we consider an harmonic expansion of the CMB temperature map in spherical harmonics

$$\frac{\delta T(\hat{e})}{T_0} = \sum_{l,m} a_{lm} Y_{lm}(\hat{e}) \, . \tag{4.100}$$

The angular CMB power spectrum for temperature correlations for the multipoles l is then

$$C_l^{TT} = \frac{1}{2l+1} \sum_m \langle a_{lm}^* a_{lm} \rangle \, . \tag{4.101}$$

The multipole moments a_{lm} are related to the primordial curvature perturbation by [122]

$$a_{lm} = 4\pi(-i)^l \int \frac{\mathrm{d}^3 k}{(2\pi)^3} \, T_\theta(k,l) \mathcal{R}_{\boldsymbol{k}} Y_{lm}(\hat{\boldsymbol{k}}) \, , \tag{4.102}$$

where T_θ is the transfer function taking into account the subhorizon evolution and it is independent of m due to rotational invariance. We can now compute (4.101) and obtain

$$C_l^{TT} = \frac{2}{\pi} \int_0^\infty \mathrm{d}k\, k^2\, T_\theta^2(k,l) P_\mathcal{R}(k)\,. \tag{4.103}$$

We see now the relation between the mulitpole expansion of the CMB power spectrum C_l^{TT} to the primordial power spectrum $P_\mathcal{R}$. From measuring C_l^{TT} the Planck mission [131] is able to constraint features of the primordial power spectrum like n_s and A_s. The only missing ingredient is the transfer function $T_\theta(k,l)$ and its calculation can be found e.g. in the textbook [126].

4.4.1 Polarization of the Cosmic Microwave Background

So far we only considered one information of the CMB photons, i.e. their wavelength. Some additional information on the primordial spectra can be gained by measuring the polarization of CMB photons. The CMB photons obtain their polarization through Thomson scattering on free electrons as they emerges from the last scattering surface during recombination [127]. There are two types of polarizations which are usually classified as $E_{\boldsymbol{k}}$ and $B_{\boldsymbol{k}}$ modes, corresponding to curl-free and divergence-free polarization vectors, respectively. One can therefore define on top of the TT-correlations (4.101) also e.g. EE correlation C_L^{EE} or the cross-correlations C_L^{TE}. It is important to note that scalar modes can create only E-modes. B-modes, on the other hand, are only created by primordial gravitational waves [137, 138]. The measurement of B-modes offers therefore the interesting possibility to confirm the existence of primordial gravitational waves and to also determine the power spectrum of tensor modes (4.97) (see e.g. the review [139]). As of today, only observational constraints on primordial gravitational waves have been reported in [131, 140] and this constraints the tensor-to-scalar ratio r in degeneracy with n_s. For this reason the CMB constraints on inflation models are often reported in the n_s-r-plane as we will do later in Chapter 5 and 6, leaving more details on the polarization of the CMB aside.

Chapter 5

Unified Emergence of Mass Scales and Inflation

We are now well equipped to tackle the radiative generation of widely separated mass scales in high-energy physics and the inflaton potential in the framework of classical scale-invariance. To give an overview, a schematic plot of the energy scales discussed here is shown in Figure 5.1. The highest scale shown is the Planck mass which sets the strength of gravitational interactions through $G_N = 1/(8\pi M_{\mathrm{Pl}}^2)$. It is, next to the electroweak scale v_{EW}, the only scale shown in Figure 5.1 whose value we can pinpoint by observations. However, confronting these two scales vis-à-vis, their large hierarchy $v_{\mathrm{EW}}/M_{\mathrm{Pl}} \sim 10^{-16}$ is unnatural in view of the gauge hierarchy problem. To generate both scales from a common origin, as we will do in this chapter, calls for further explanation and we will analyze the coexistence of these two scales, and related fine-tuning, if both their origin is accounted for by the CW-mechanism.

Including inflation into the picture, we have little information on the energy scale of the microscopic theory realizing the slow-roll dynamics. In principle, any energy scale between a few MeV and 10^{16} GeV is expected to be in line with cosmological observations. The lower bound is not very strict and originates from the requirement that the reheating temperature $T_{\mathrm{RH}} > 1$ MeV should be higher than the temperature where BBN is taking place [141]. The energy scale of inflation, which is dominated during slow-roll by the potential energy $V_*^{1/4}$ of the inflaton potential (cf. (4.20)), can be related to the tensor-to-scalar ratio (4.98). Since the scalar amplitude A_s (4.83) is fixed by measurements to high precision one can derive the upper bound on

$$V_*^{1/4} = \left(\frac{3\pi^2 A_s r}{2} \right)^{1/4} M_{\mathrm{Pl}} \lesssim 1.6 \times 10^{16}\,\mathrm{GeV}\,, \tag{5.1}$$

by relating it to the observational upper bound on r [131]. For this reason, the expected energy range for inflation is shown in Figure 5.1 by the fading red bar.

Going to lower scales, the existence of a Majorana mass scale M_N for right-handed neutrinos is expected if the smallness of neutrino masses is explained with the type-I seesaw model [142–146]. The exact value of M_N is not determined, since the seesaw mechanism only explains the smallness of neutrino masses qualitatively, but not quantitatively, because the Dirac-type Yukawa couplings and M_N are free parameters of the model. Therefore, plenty realizations of type-I seesaw models haven been proposed where the Majorana mass M_N ranges from the GUT scale down to the eV-scale. At the lower end of this range one should note however that one runs into conflict with the main motivation of the seesaw mechanism, which is to explain the tininess of neutrino masses with respect to corresponding charged leptons [147]. The discovery of neutrino flavor oscillations [148] has established that neutrinos are massive but since they provide only a measurement of the neutrino mass-squared differences, the absolute mass scale of neutrinos is still unknown. However, Planck measurements of the CMB provide an upper bound on the sum of neutrino masses $m_\nu = \sum m_{\nu,i} < 0.12$ eV [60]. This is the lightest mass scale in this discussion and in Figure 5.1. The blue bar roughly indicates the energy range for M_N, but we have highlighted a special value at $M_N = 10^7$ GeV. At this value the inclusion of right-handed neutrinos can account for the radiative generation of the Higgs mass parameter, while meanwhile giving rise to the small mass of neutrinos through the usual type-I seesaw mechanism. In this approach, dubbed neutrino option [149], one ties the scale of neutrino masses, Higgs mass and Majorana mass scale for right-handed neutrinos together and offers a new perspective on the hierarchy problem. In Section 5.5 we incorporate this idea into the scale-invariant framework which will link the Majorana mass to the same scalar VEV which is also responsible for generating the Planck mass. We will lay out that the hierarchy $M_N/M_{\rm Pl} \sim 10^{-11}$ can arise technically natural and discuss how the hierarchy $v_{\rm EW}/M_{\rm Pl}$ can be stabilized. As a last point, and not indicated by an energy scale in Figure 5.1, we will discuss a possibility to incorporate a DM candidate in this setup, with the main purpose of demonstrating that this does not spoil any other findings discussed in this Chapter.
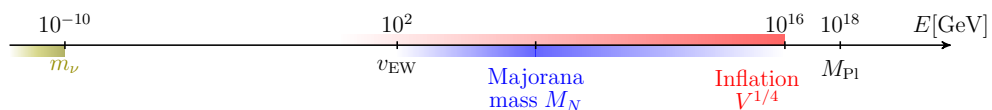
Figure 5.1: A schematic overview of the mass scales on a logarithmic scale discussed in this chapter. The bars with fading colors indicate energy scales which are undetermined.

A parallel goal of this chapter is the simultaneous generation of an inflaton potential realizing successful slow-roll inflation. Also in that respect we stay faithful to our general guiding principle of scale-invariance. As briefly mentioned in the introduction, the constraints on inflation reported by the Planck

collaboration [131], indicate that the spectral tilt n_s is close to one, i.e. the scale-invariant limit, and the tensor-to-scalar ratio r is constrained to be small which can be achieved by very flat inflaton potentials since (4.98) and (4.23) relate r to the gradient V' of the inflaton potential. This can be achieved by two very popular and economical models, which are Starobinsky inflation (or R^2-inflation) [61] and Higgs inflation [150]. Both give rise to sufficiently flat potentials when transformed from the Jordan to Einstein frame. Note that in both models, one includes globally scale-invariant terms into the action, i.e. R^2 and $\beta_H(H^\dagger H)R$ respectively. Their dominance with respect to the Einstein-Hilbert term (γR^2 with $\gamma \sim \mathcal{O}(10^9)$ and $\beta|H|^2 R$ with $\beta \sim \mathcal{O}(10^4)$) can be seen as an indication for the positive impact of scale-invariant terms. In fact, the approaches of Starobinsky and Higgs Inflation have been combined into so-called Scalaron-Higgs-Inflation [151, 152]. Our setup for inflation is related but with the distinction that we exclude terms which are not globally scale-invariant and that the Higgs field will not participate in the inflationary dynamics. The latter is because the inflaton field S in our scenario is also responsible for generating the Planck mass by its VEV v_S. Since the physics of cosmic inflation discussed in Chapter 4 was based on single field inflation coupled to Einstein-Hilbert gravity, we have to extend our discussion to a theory of gravity which contains quadratic orders of curvature tensors and non-minimal couplings to scalars, but we will argue in Section 5.3 that we can effectively treat inflation as a single-field model, such that we can apply some of the formulas derived in Chapter 4 directly in order to present inflationary predictions for this model.

The total Lagrangian of the model discussed in this chapter is divided into four parts

$$\mathcal{L}_\text{T} = \mathcal{L}_\text{GR} + \mathcal{L}_\text{CW} + \mathcal{L}_\text{cSM} + \mathcal{L}_{N\chi}, \tag{5.2}$$

where $\mathcal{L}_\text{GR}$ describes globally scale-invariant gravity, $\mathcal{L}_\text{CW}$ consists of an additional scalar sector to realize radiative symmetry breaking with the CW-mechanism, $\mathcal{L}_\text{cSM}$ is the scale-invariant SM with additional Higgs portal couplings and $\mathcal{L}_{N\chi}$ includes the right-handed neutrinos N_R and the DM candidate χ. Each part will be discussed in more detail as passing through the following sections.

5.1 Gravity with Global Scale-invariance

Scale-invariant gravity has been studied extensively, for example with global scale-invariance [26–39, 39, 153–160] or local Weyl invariance [40–57] (see also Section 3.5). The action for scale-invariant gravity (3.37) can be rewritten such that the three independent squares are

$$S_\text{GR} = \int \mathrm{d}^4 x \, \sqrt{-g} \left(c_1 C_{\mu\nu\alpha\beta} C^{\mu\nu\alpha\beta} + c_2 R_{\mu\nu} R^{\mu\nu} + c_3 R^2 \right), \tag{5.3}$$

where $C_{\mu\nu\alpha\beta}$ is the Weyl tensor, $R_{\mu\nu}$ the Ricci tensor and R is the Ricci scalar. The first term is locally scale-invariant while the other two are only globally invariant. We can simplify the action by using the Gauß-Bonnet invariant

$$\mathcal{G} = C_{\mu\nu\alpha\beta}C^{\mu\nu\alpha\beta} - 2R_{\mu\nu}R^{\mu\nu} + \frac{1}{6}R^2 \,, \tag{5.4}$$

which is a total derivative leading to a boundary term at the level of the action [161]. Using it to replace the second term in (5.3) and dropping the boundary term we obtain

$$S_{\mathrm{GR}} = \int \mathrm{d}^4x \sqrt{-g} \left(\kappa C_{\mu\nu\alpha\beta}C^{\mu\nu\alpha\beta} + \gamma\, R^2 \right) \,, \tag{5.5}$$

where we have redefined the dimensionless constants. A theory of gravity based solely on (5.5) would not pass the many test of GR and its Newtonian limit, i.e. no identification of the gravitational coupling constant G_N can be made. Instead, we have to rely on the inclusion of scalar fields which couple non-minimally to the Ricci scalar via

$$S_\phi = \int \mathrm{d}^4x \sqrt{-g} \left(-g^{\mu\nu}\partial_\mu\phi\partial_\nu\phi + \frac{\beta_\phi}{2}\phi^2 R \right) \,, \tag{5.6}$$

through a dimensionless coupling constant β_ϕ. It is now feasible to generate the Planck mass

$$M_{\mathrm{Pl}}^2 = \beta_\phi v_\phi^2 \,, \tag{5.7}$$

by the scalar VEV $v_\phi = \langle\phi\rangle$. At low-energies we can therefore recover the well-tested phenomenology of General Relativity. The combination of the actions (5.5) and (5.6) will form the base for the realization of inflation. Before that discussion we have to dynamically induce the Planck mass in light of (5.7).

5.2   Symmetry Breaking of Scale-invariance

For the purposes of breaking classical scale-invariance we need at least two scalars S and σ because a two-scalar sector is the most economic way to realize the CW-mechanism in the Gildener-Weinberg approach [107].[1] The scalar sector is described by the classical action

$$S_{\mathrm{CW}} = \int \mathrm{d}^4x \sqrt{-g} \left[-\frac{1}{2}g^{\mu\nu}\partial_\mu S\partial_\nu S - \frac{1}{2}g^{\mu\nu}\partial_\mu\sigma\partial_\nu\sigma - V(S,\sigma) \right.$$
$$\left. +\frac{1}{2}(\beta_S S^2 + \beta_\sigma \sigma^2)\, R \right] \,, \tag{5.8}$$

---

[1]Alternatively, one could realize this with one scalar which is gauged under an additional $U(1)$ such as the scalar QED example of Section 3.1. Note that our notion of minimality in that respect will be reevaluated in Chapter 6 where we also take gravitational degrees of freedom into account.

and we also assume a Z_2 symmetry with the scalar σ being Z_2-odd (more details on this in Section 5.6). The inclusion of the Higgs scalar is postponed to Section 5.4. The most general scale-invariant tree-level potential is then

$$V(S,\sigma) = \frac{1}{4}\lambda_S S^4 + \frac{1}{4}\lambda_\sigma \sigma^4 + \frac{1}{4}\lambda_{s\sigma} S^2\sigma^2 \,. \tag{5.9}$$

In order to simultaneously avoid the domain wall problem [162] and to stabilize the DM candidate χ discussed in Section 5.6, we want to choose the minimum of the scalar potential, such that the Z_2 symmetry remains unbroken, i. e. for $\langle S \rangle \neq 0$ and $\langle \sigma \rangle = 0$. This can be realized according to the Gildener-Weinberg method [107] by assuming an approximate flat direction in the contour parameterized through $\sigma = 0$. The tree-level couplings should therefore satisfy (see also Section 3.2)

$$\lambda_S \ll \lambda_{S\sigma} \quad \text{and} \quad \lambda_S \ll \lambda_\sigma \,. \tag{5.10}$$

With this choice, we see from (5.8), a non-zero VEV $v_S = \langle S \rangle$ will generate the Einstein-Hilbert term with the (reduced) Planck mass $M_{\text{Pl}} \simeq \sqrt{\beta_S}v_S$. We integrate out the quantum fluctuations δS and $\delta\sigma$ from the two scalars by utilizing (2.29). In the Gildener-Weinberg approximation the background fields are set to $S \neq 0$, $R \neq 0$ and $\sigma = 0$ and we obtain the effective potential at one-loop

$$U_{\text{eff}}(S,\sigma,R) = V(S,\sigma,R) + \frac{1}{64\pi^2}\left[\tilde{m}_s^4 \ln\left(\frac{\tilde{m}_s^2}{\mu^2}\right) + \tilde{m}_\sigma^4 \ln\left(\frac{\tilde{m}_\sigma^2}{\mu^2}\right) \right]\,, \tag{5.11}$$

where the field-dependent masses in this background are

$$\tilde{m}_s^2 = 3\lambda_S S^2 + \beta_S R \quad \text{and} \quad \tilde{m}_\sigma^2 = \frac{1}{2}\lambda_{S\sigma} S^2 + \beta_\sigma R \,. \tag{5.12}$$

Here, we have used the $\overline{\text{MS}}$ scheme and furthermore absorbed the constant $-3/2$-term into the renormalization scale μ.[2] Since by construction $\langle \sigma \rangle = 0$, and the field direction perpendicular to it is steep due to large λ_σ (cf. (5.10)), we assume that σ will not play any role during inflation. We proceed by computing v_S. During inflation we can assume that $\beta_S R < 3\lambda_S S^2$ and $\beta_\sigma R < (1/2)\lambda_{S\sigma}S^2$ such that we can expand (5.11) in powers of the Ricci scalar, and furthermore setting $\sigma = 0$,

$$U_{\text{eff}}(S,R,\sigma=0) = U_{\text{CW}}(S) + U_{(1)}(S)\,R + U_{(2)}(S)R^2 + O(R^3)\,, \tag{5.13}$$

---

[2]Note that integration also gives rise to divergences that have to be absorbed into the couplings λ_S, γ, and β_S. This agrees with the earlier computation of e.g. [163, 164] and references cited therein. Furthermore, the β_S and β_σ terms in (5.12) should actually read $\beta_S - 1/6$ and $\beta_\sigma - 1/6$, if one properly does the computation in a curved background [165]. However, since β_S will turn out be large, i.e. $\beta_S \gtrsim 10^2$, for successful inflation and β_σ will play an irrelevant for inflation, we will be ignoring the constants $1/6$ term throughout.

where

$$U_{\mathrm{CW}}(S) = \frac{1}{4}\lambda_S S^4 + \frac{S^4}{64\pi^2}\left[9\lambda_S^2 \ln\left(\frac{3\lambda_S S^2}{\mu^2}\right) + \frac{\lambda_{S\sigma}^2}{4}\ln\left(\frac{\lambda_{S\sigma}S^2}{2\mu^2}\right)\right], \quad (5.14)$$

$$U_{(1)}(S) = \frac{1}{128\pi^2}\left[6\beta_S\lambda_S S^2\left(1 + 2\ln\left(\frac{3\lambda_S S^2}{\mu^2}\right)\right)\right.$$
$$\left. + \beta_\sigma\lambda_{S\sigma}S^2\left(1 + 2\ln\left(\frac{\lambda_{S\sigma}S^2}{2\mu^2}\right)\right)\right], \quad (5.15)$$

$$U_{(2)}(S) = \frac{1}{128\pi^2}\left[\beta_S^2\left(3 + 2\ln\left(\frac{3\lambda_S S^2}{\mu^2}\right)\right)\right.$$
$$\left. + \beta_\sigma^2\left(3 + 2\ln\left(\frac{\lambda_{S\sigma}S^2}{2\mu^2}\right)\right)\right]. \quad (5.16)$$

Since we are assuming a negligibly small but non-zero value of the Ricci scalar R, we obtain the R-independent leading-order estimate for v_S from the potential $U_{\mathrm{CW}}(S)$ through the stationary condition

$$\left.\frac{\partial U_{\mathrm{CW}}(S)}{\partial S}\right|_{S=v_S} = 0, \quad (5.17)$$

and then verify it is indeed a minimum. The induced vacuum energy at the VEV is

$$U_0 := U_{\mathrm{CW}}(v_S) = -\mu^4\frac{\beta_{\lambda_S}}{16}\exp\left[-1 - 16C/\beta_{\lambda_S}\right], \quad (5.18)$$

where β_{λ_S} is the one-loop β-function for λ_S in the absence of further couplings other than seen in (5.8). It reads

$$\beta_{\lambda_S} = \frac{1}{16\pi^2}\left(18\lambda_S^2 + \frac{1}{2}\lambda_{S\sigma}^2\right), \quad \text{and} \quad (5.19)$$

$$C = \frac{1}{4}\lambda_S + \frac{1}{64\pi^2}\left(9\lambda_S^2\ln(3\lambda_S) + \frac{1}{4}\lambda_{S\sigma}^2\ln(\lambda_{S\sigma}/2)\right). \quad (5.20)$$

The negative zero-point energy density (5.18) is a consequence of the spontaneous breaking of global scale-invariance. This zero-point energy density, which contributes to the cosmological constant, is finite in dimensional regularization because of the scale-invariance of the considered model. Since the induced value of U_0 is too large compared to the observed value of the cosmological constant, we choose to subtract the zero-point energy density by an ad-hoc subtraction and redefining the effective potential as

$$\tilde{U}_{\mathrm{CW}}(S) = U_{\mathrm{CW}}(S) - U_0, \quad (5.21)$$

such that we now have $\tilde{U}_{\mathrm{CW}}(v_S) = 0$. The above corresponds to an explicit super-soft breaking of scale invariance at tree level, which is the cost of getting

rid of the cosmological constant problem. To properly address the cosmological constant problem one should probably also take into account gravitational quantum corrections, also coming from the Weyl-tensor squared term. In the rest of this thesis, we set this issue with the cosmological constant problem aside. We can now identify the Planck mass by (5.8) and (5.13)

$$M_{\text{Pl}} = \sqrt{\beta_S + \frac{2U_{(1)}(v_S)}{v_S^2}}\, v_S\,. \tag{5.22}$$

Since $v_S = \mu f_S(\lambda_S, \lambda_{S\sigma})$ (cf. (5.14) and (5.17)), the formula above relates M_{Pl} with the renormalization scale $M_{\text{Pl}} = \mu f_P(\beta_S, \beta_\sigma, \lambda_S, \lambda_{S\sigma})$, where f_S and f_P are dimensionless functions of the coupling constants.

5.3 Effective Action for Inflation

For successful inflation through slow-roll at least one bosonic degree of freedom is necessary [65, 66, 166]. It was realized relatively early [61] that the inclusion of the R^2-term in the action leads to an additional scalar degree of freedom[3], the so-called scalaron, can play the role of the inflaton field. However, the quantum corrections of the scalaron alone to a scalar field S cannot account for the generation of M_{Pl} via the CW-mechanism. Also, in the context of Higgs inflation the CW-mechanism does not suffice to generate a VEV for a scalar S which thereby generates M_{Pl}. It is for these reasons that we need two scalars σ and S. The former is necessary because of its quantum correction in the effective potential such that a global minimum with $v_s \neq 0$ is generated. Of course, the R^2-term is natural in a scale-invariant model, and as we will see later, it helps in pushing the tensor-to-scalar ratio r to smaller values, as is preferred by current observations.

The role of scale-invariance in inflation models is widely studied, e.g. in [38, 57, 154, 156, 157, 167–169] where the inflaton potential is not explicitly generated by the CW-mechanism as in contrast to e.g. [31, 39, 158, 170–174]. Most similar to our setup are the studies in [172, 173], although the inflaton potential is there derived differently. In [172, 173] the transition from Jordan to Einstein frame is performed before it is shown that scale-invariance is broken. This means one implicitly assumes that scale invariance is broken, since the Weyl rescaling to the Einstein without a scale is not possible. In contrast to that, we computed the CW-potential in the Jordan frame which yields the effective Lagrangian (5.23). In this way, we can show that a finite scale is generated in the Jordan frame and the transition to Einstein frame is therefore allowed. In principle, it would be also possible in our approach to compute the predictions for slow-roll inflation in the Jordan frame since they are frame independent [175, 176],

---

[3]This additional degree of freedom is in fact inherited from the metric and can be made an explicit propagating scalar field in the Einstein frame.

but we will not so and continue the computation in the more familiar Einstein frame to use the results of Chapter 4.[4]

For the laid out reasons we start with the relevant effective Lagrangian for inflation[5]

$$\frac{\mathcal{L}_{\text{eff}}}{\sqrt{-g_J}} = -\frac{1}{2}M_{\text{Pl}}^2 B(S)R_J + G(S)R_J^2 - \frac{1}{2}g_J^{\mu\nu}\partial_\mu S\partial_\nu S - \tilde{U}_{\text{CW}}(S)\,, \qquad (5.23)$$

where the subscript J denotes the metric and corresponding curvature invariants in the Jordan frame. It is obtained by the combination of the classical actions (5.5) and the inclusion of one-loop contributions of the effective potential summarized in (5.13) and (5.21). The two functions above are given by

$$B(S) = \frac{1}{M_{\text{Pl}}^2}\left(\beta_S S^2 + 2U_{(1)}(S)\right) \quad \text{and} \quad G(S) = \gamma - U_{(2)}(S)\,. \qquad (5.24)$$

We should note that in (5.23) we have omitted the Weyl tensor term present in (5.5), because it is assumed that irrespectively of the value of κ, the Weyl tensor squared term only has relatively negligible effects on r [183–185]. This point be will reevaluated in Chapter 6. We continue with our discussion by noting that the equation of motion of S does not depend on κ.

We will proceed by removing the R_J^2 term by introduction of an auxiliary scalar field through the substitution

$$G(S)R_J^2 \to 2G(S)R_J\psi - G(S)\psi^2\,. \qquad (5.25)$$

One can easily check that the equation of motion for ψ delivers a constraint which returns (5.23). The next step is to perform a Weyl transformation which transform the metric according to

$$g_{\mu\nu} = \Omega^2\, g_{\mu\nu}^J\,, \quad \text{with} \quad \Omega^2(S,\psi) = B(S) - \frac{4\,G(S)\psi}{M_{\text{Pl}}^2}\,. \qquad (5.26)$$

The Lagrangian (5.23) is then transformed to the Einstein frame

$$\frac{\mathcal{L}_{\text{eff}}^E}{\sqrt{-g}} = \frac{1}{2}\, M_{\text{Pl}}^2\left(R - \frac{3}{2}\, g^{\mu\nu}\, \partial_\mu \ln\Omega^2(S,\psi)\, \partial_\nu \ln\Omega^2(S,\psi)\right)$$
$$- \frac{g^{\mu\nu}}{2\,\Omega^2(S,\psi)}\, \partial_\mu S\, \partial_\nu S - V(S,\psi)\,, \qquad (5.27)$$

---

[4]Note that that transformations between the Jordan and Einstein frames should be taken with care at the quantum level when also taking graviational quantum contributions into account [177, 178]. We are treating gravity here classically so this should be of no concern.

[5]A similar Lagrangian with a priori arbitrary functions B, G, and U has been already studied in [151, 179–182].

where we dropped the subscript J for the metric and the Ricci scalar in the Einstein frame. The scalar potential is transformed to

$$V(S, \psi) = \frac{U_{\mathrm{CW}}(S) + G(S)\psi^2}{\left[\, B(S)M_{\mathrm{Pl}}^2 - 4\, G(S)\psi \,\right]^2}\, M_{\mathrm{Pl}}^4 \,, \tag{5.28}$$

which depends now on two scalar fields S and ψ. The latter, as we see in the second term of (5.27), is promoted to a propagating scalar field in the Einstein frame. Its canonically normalized expression, the scalaron field ϕ [186, 187], is defined as

$$\phi = \sqrt{\frac{3}{2}}\, M_{\mathrm{Pl}} \ln \left| \Omega^2 \right| \,. \tag{5.29}$$

The Einstein-frame Lagrangian now reads

$$\frac{\mathcal{L}_{\mathrm{eff}}^E}{\sqrt{-g}} = \frac{1}{2}\, M_{\mathrm{Pl}}^2\, R - \frac{1}{2}\, g^{\mu\nu}\, \partial_\mu \phi\, \partial_\nu \phi - \frac{1}{2}\, e^{-\Phi(\phi)}\, g^{\mu\nu}\, \partial_\mu S\, \partial_\nu S$$
$$- V(S, \phi) \,, \tag{5.30}$$

where $\Phi(\phi) = \sqrt{2}\,\phi/\sqrt{3}\, M_{\mathrm{Pl}}$, and the $V(S, \phi)$ potential (5.28) now reads

$$V(S, \phi) = e^{-2\,\Phi(\phi)} \left[U_{\mathrm{CW}}(S) + \frac{M_{\mathrm{Pl}}^4}{16\, G(S)} \left(B(S) - e^{\Phi(\phi)} \right)^2 \right] \,. \tag{5.31}$$

We arrive at an effective Lagrangian (5.30) where all metric degrees of freedom are described by the Einstein-Hilbert term, as it was the case in Chapter 4. The novel feature of (5.30) with respect to our previous considerations is that two scalar fields are present with a relatively involved potential (5.31) which could play the role of the inflaton.

5.3.1 Valley Approximation

We could proceed by studying inflation using multifield techniques (see e.g. [188]) for the 2d-potential (5.31). Instead of this rather involved approach, we will argue that it is possible to obtain an effective one-field description and to derive predictions for CMB observables. The contour plot of the potential (Fig. 5.2) indicates that the potential exhibits a clear valley structure along which the potential is relatively flat and suitable for slow-roll inflation. We will assume that the inflationary trajectory during slow-roll evolution in the S-ϕ plane is confined to this valley and can be parameterized by a single field. In fact, this behavior was confirmed in [31] for a similar model in which the classical trajectories with different initial conditions converge to an inflationary attractor line, i. e. the valley contour. The existence of this valley structure is guaranteed as long as a large hierarchy between the two mass eigenvalues of the scalar mass matrix derived from (5.31) exists. Then, the gradient along the valley
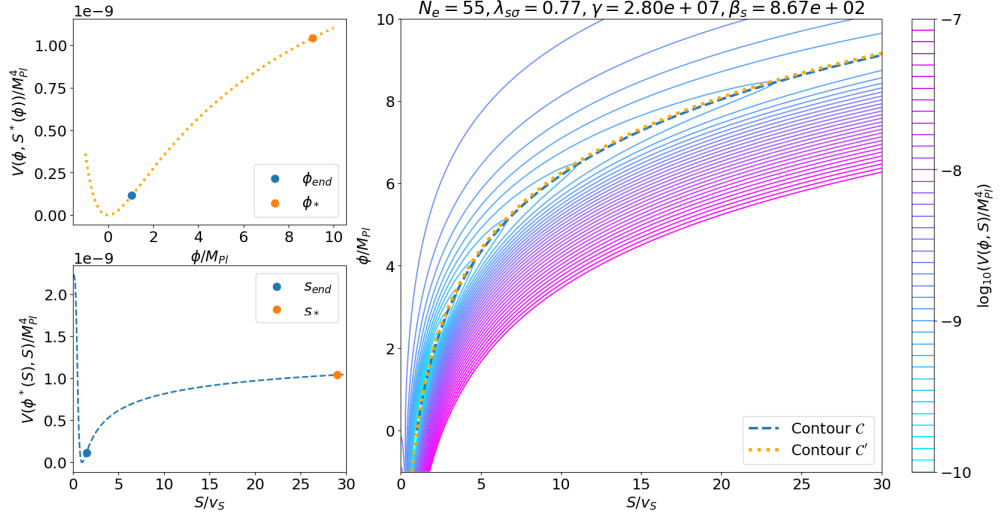
Figure 5.2: Scalar potential for benchmark point 3 of Table 5.1. The two contours defined in Eqs. (5.33) and (A.1) are shown on top of the contour plot of $V(S, \phi)$ (5.31) (right) and the corresponding one-dimensional inflaton potentials along those contours (left).

is hierarchically smaller than the gradient perpendicular to it. To parametrize the contour of the valley one can use two different approaches and we compare them in Appendix A and discuss the respective viability.

We discuss one of the approaches here which is based on the observation (Fig. 5.2) that there is precisely one local extremum in the scalaron direction for each $S > v_s$ which can be obtained by

$$\frac{\partial V(S, \phi)}{\partial \phi}\bigg|_{\phi=\tilde{\phi}(S)} = 0 \quad \Rightarrow \quad \tilde{\phi}(S) = \sqrt{\frac{3}{2}} M_{\text{Pl}} \ln \left(B(S) + \frac{16 G(S) U_{\text{CW}}(S)}{B(S) M_{\text{Pl}}^4} \right),$$

$$(5.32)$$

which in turn defines the valley contour in the two-dimensional field space through

$$\mathcal{C} = \{S, \tilde{\phi}(S)\} \quad \text{where} \quad \frac{\partial V(S, \phi)}{\partial \phi}\bigg|_{\phi=\tilde{\phi}(S)} = 0 \,. \tag{5.33}$$

The inflationary trajectory can be assumed to satisfy (5.32) at all times if the scalaron mass satisfies

$$\frac{m_\phi^2}{H_{\text{inf}}^2} \gg 1 \,, \tag{5.34}$$

where m_ϕ is evaluated along the contour $\mathcal{C}$ and H_{inf} is the inflationary Hubble parameter during. If (5.34) holds, the heavy positive scalaron mass is able

to stabilize the contour $\mathcal{C}$ during the slow-roll phase and any motion leaving the contour $\mathcal{C}$ can be neglected. Inserting $\tilde{\phi}(S)$ into (5.31) we obtain the one-dimensional inflaton potential along this contour,

$$V_{\mathrm{inf}}(S) = V(S, \tilde{\phi}(S)) = \frac{U_{\mathrm{CW}}(S)}{B(S)^2 + 16\, G(S) U_{\mathrm{CW}}(S)/M_{\mathrm{Pl}}^4}\,. \qquad (5.35)$$

The kinetic terms in (5.30) now read

$$e^{-\Phi(\tilde{\phi}(S))}\, g^{\mu\nu} \partial_\mu S \partial_\nu S + g^{\mu\nu} \partial_\mu \tilde{\phi}(S) \partial_\nu \tilde{\phi}(S) \Rightarrow F(S)^2 g^{\mu\nu} \partial_\mu S \partial_\nu S\,, \qquad (5.36)$$

where the non-standard normalization is

$$F(S) = \frac{1}{[1 + 4\, A(S)]\, B(S)} \left\{ [1 + 4\, A(S)]\, B(S) + \frac{3}{2}\, M_{\mathrm{Pl}}^2 \left([1 + 4\, A(S)]\, B'(S) \right.\right.$$
$$\left.\left. + 4\, A'(S) B(S))^2 \right\}^{1/2} \text{ with } A(S) = \frac{4 G(S) U_{\mathrm{CW}}(S)}{B(S)^2 M_{\mathrm{Pl}}^2}\,. \qquad (5.37)$$

Finally, we arrive at the effective one-field description with the Lagrangian,

$$\frac{\mathcal{L}_{\mathrm{eff}}^E}{\sqrt{-g}} = -\frac{1}{2}\, M_{\mathrm{Pl}}^2\, R + \frac{1}{2}\, F(S)^2\, g^{\mu\nu}\, \partial_\mu S\, \partial_\nu S - V_{\mathrm{inf}}(S)\,, \qquad (5.38)$$

and a canonically normalized inflaton field $\hat{S}$ can be obtained by integration

$$\hat{S}(S) = \int_{v_S}^S dx\, F(x)\,. \qquad (5.39)$$

If the condition (5.34) is satisfied we can safely use the effective one-field description (5.38) to study slow-roll inflation. An important step is to compute the potential slow-roll parameters (4.23). These equations have been derived for a canonically normalized scalar field and in the present model (5.36) we have to take the additional $F(S)$-term into account. These modify (4.23) to

$$\epsilon_V(S) = \frac{M_{\mathrm{Pl}}^2}{2\, F^2(S)} \left(\frac{V_{\mathrm{inf}}'(S)}{V_{\mathrm{inf}}(S)} \right)^2\,, \qquad (5.40)$$

$$\eta_V(S) = \frac{M_{\mathrm{Pl}}^2}{F^2(S)} \left(\frac{V_{\mathrm{inf}}''(S)}{V_{\mathrm{inf}}(S)} - \frac{F'(S)}{F(S)} \frac{V_{\mathrm{inf}}'(S)}{V_{\mathrm{inf}}(S)} \right)\,. \qquad (5.41)$$

The number of e-folds (4.26) in this case is computed by

$$N_e = \int_{S_*}^{S_{\mathrm{end}}} \frac{F^2(S)}{M_{\mathrm{Pl}}^2} \frac{V_{\mathrm{inf}}(S)}{V_{\mathrm{inf}}'(S)}\,, \qquad (5.42)$$

where S_* denotes the field value at the time of CMB horizon exit of the scale k_*. The field value at the end of inflation S_{end} is obtained by the condition (4.25). With this at hand, we can compute the scalar power spectrum amplitude A_s,

the scalar spectral index n_s and the tensor-to-scalar ratio r with (4.83), (4.86) and (4.98). The quantities with an asterisk are evaluated at $S = S_*$. The parameters of our model relevant for inflation are the quartic couplings $\lambda_S, \lambda_{S\sigma}$, non-minimal coupling β_S and the R^2 coefficient γ (cf. (5.5) and (5.8)). The renormalization scale μ in the effective potential (5.11) is fixed through the identification of M_{Pl} in (5.22). Note that all these parameters (except μ) are dimensionless as they should be for a scale-invariant theory. The other two present parameters λ_S and β_σ are irrelevant for inflation or the determination of M_{Pl} in leading order because of the flat direction condition (5.10) which ensures that the field σ plays no role for inflation. For this reason we will present all further model prediction for fixed values of $\lambda_S = 0.005$ and $\beta_\sigma = 1$. The mentioned CMB observables A_s, n_s and r are measured or constrained by the latest data from the Planck mission [131]. For our purpose we assume $N_e \simeq 50 \cdots 60$ e-folds from CMB horizon exit until the end of inflation and constrain the parameter space spanned by $\lambda_{S\sigma}, \beta_S$ and γ, such that the well measured scalar spectrum amplitude constraint is fulfilled [131]

$$\ln\left(10^{10} A_s\right) = 3.044 \pm 0.014 \, . \tag{5.43}$$
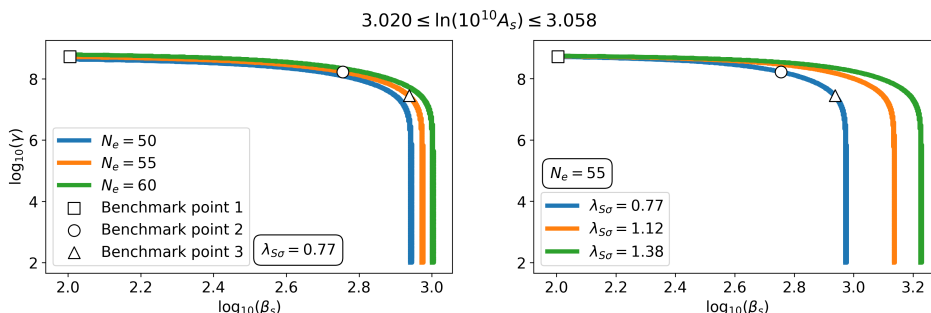
Figure 5.3: The lines indicate pairs of the parameters γ and β_S for which the A_s-constraint (5.43) is satisfied, for a varying number of e-folds N_e (left) or varying $\lambda_{S\sigma}$ (right). All shown points are obtained for $\beta_\sigma = 1$ and $\lambda_S = 0.005$ and the three benchmark points summarized in Table 5.1.

This tight constraint can be used to effectively remove one free parameter of the model. Fig. 5.3 shows that there is a relation between β_S and γ once A_s, N_e and $\lambda_{S\sigma}$ have been fixed. We can use this and express the β_S dependence of the CMB observables n_s and r in terms of γ only. One can also see that there are maximally allowed values ($\beta_{S,\mathrm{max}} \sim 10^3$ and $\gamma_{\mathrm{max}} \sim 10^9$) due to this constraint, where the exact maximal values depend on N_e and $\lambda_{S\sigma}$. Utilizing the constraint (5.43) (corresponding to points shown in Fig. 5.3) we are able to illustrate the parameter dependence of this model through γ only in the $n_s - r$ plane in Fig. 5.4. From Fig. 5.4 we see that the predictions of this model interpolate between two familiar inflation models. The lower end of the

prediction corresponds to that of R^2 inflation [61,189,190], while the upper end is reminiscent of linear chaotic inflation [191].[6]
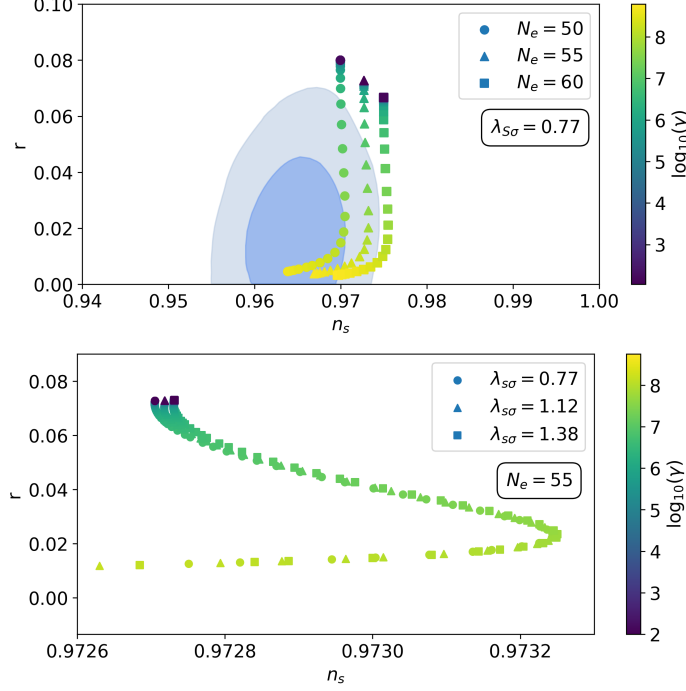
Figure 5.4: Predictions for the scalar spectral index n_s and the tensor-to-scalar ratio r with varying number of e-folds N_e (top) and varying $\lambda_{S\sigma}$ (bottom). All shown points are obtained for $\beta_\sigma = 1$ and $\lambda_S = 0.005$ and satisfy the A_s-constraint (5.43). The β_S-dependence is fixed in light of Fig. 5.3. In the top panel we included the Planck TT,TE,EE+lowE+lensing+BK15 68% and 95% CL regions [131].

#	β_S	γ	Contour $\mathcal{C}$					Contour $\mathcal{C}'$				
			n_s	r	A_s	s_{end}/μ	s_*/μ	n_s	r	A_s	ϕ_{end}/μ	ϕ_*/μ
1	1.01×10^2	5.24×10^8	0.967	0.004	3.032	0.09	0.11	0.965	0.004	3.088	0.83	4.75
2	5.69×10^2	1.68×10^8	0.972	0.010	3.041	0.11	0.45	0.972	0.010	3.075	2.02	13.46
3	8.67×10^2	2.80×10^7	0.973	0.034	3.038	0.13	2.56	0.973	0.034	3.040	2.74	23.46

Table 5.1: Parameters for the three benchmark points marked in Fig. 5.3. For all points we have fixed $\lambda_{S\sigma} = 0.77$, $\lambda_S = 0.005$ and $\beta_\sigma = 1$ and the VEV in each case is $v_S = 0.088\mu$. The last six columns show the predictions for the CMB observables and the related field values for the inflationary contours $\mathcal{C}$ or $\mathcal{C}'$ for $N_e = 55$ e-folds. The valley approximation is discussed in Appendix A .

---

[6]The results of linear inflation were also reproduced in another context in [192,193].

5.4   Embedding into the SM

So far, all discussion of this model was completely decoupled from the SM. However, we have introduced two new scalar fields which are singlets under the SM gauge group in (5.8). Of course, the SM also includes the Higgs and it allows for new terms in the scalar potential. Since $H^\dagger H$ is gauge invariant two portal couplings are allowed which are also scale-invariant. Furthermore, also the Higgs is allowed to have non-minimal coupling β_H. To embed the discussed model into the SM, we have to add the following terms to the Lagrangian

$$\frac{\mathcal{L}_{\text{cSM}}}{\sqrt{-g}} = \mathcal{L}_{\text{SM}}|_{m=0} - \frac{1}{4}(\lambda_{HS}S^2 + \lambda_{H\sigma}\sigma^2)H^\dagger H + \frac{1}{2}\beta_H(HH^\dagger)R\,. \qquad (5.44)$$

The first term denotes the scale-invariant SM Lagrangian with the quadratic Higgs term $m^2 H^\dagger H$ suppressed. The additional couplings β_H, λ_{HS} and $\lambda_{H\sigma}$ are new with respect to (5.8) and can thereby couple the Higgs field to the process of inflation and to the generated scale v_S. First, we assume that $\beta_H \approx 0$ and therefore the Higgs plays no role in this inflation scenario. The portal couplings λ_{HS} and $\lambda_{H\sigma}$ have to be tuned extremely small.[7] Otherwise, it will give rise to a too large Higgs mass proportional to

$$m^2 = \frac{\lambda_{HS}}{2}v_S^2\,. \qquad (5.45)$$

The amount of fine-tuning on the portals λ_{HS} and $\lambda_{H\sigma}$ will be discussed in the next section. We note here, that we will not rely on fine-tuning to a *specific* value of the portal couplings as to account for electroweak symmetry breaking through the mass term (5.45). Therefore, we have to rely on an alternative approach to account for electroweak symmetry breaking by the so-called neutrino option.

5.5   Neutrino Option

The true origin of the quadratic Higgs mass parameter is puzzling so far, in particular in light of the related gauge hierarchy problem. It has been proposed under the name neutrino option in [149, 194] that it could be related to the Majorana mass scale of right-handed neutrinos and that offers a new perspective on the hierarchy problem.[8] This idea is based on the type-I seesaw mechanism [142–146] in a specific parameter region where it can account for the light active neutrino mass and also the Higgs mass parameter. For this matter, we extend the model according to the scale-invariant realization of the type-I seesaw model where instead of explicit mass terms we count on Yukawa couplings to the

---

[7]Note that if λ_{HS} is tiny but $\lambda_{H\sigma}$ is sizable, it will regenerate λ_{HS} at one loop level with corrections proportional to $\Delta\lambda_{HS} \sim \lambda_{H\sigma}\lambda_{S\sigma}/16\pi^2$.

[8]Similar considerations had been already made in [195–198].

scalars we already introduced in (5.8). We introduce right-handed neutrinos N_R which are allowed to have a Majorana-type Yukawa coupling y_M to the scalar S and the Dirac-type Yukawa y_ν to the SM lepton doublet L and the Higgs doublet. Furthermore, we include χ as additional right-handed Majorana neutrinos to accommodate dark matter into the model which will be the subject of the next section. Having the discrete Z_2 symmetry which was mentioned below (5.8), with σ and χ as the only Z_2-odd fields, in mind, we can add the following interactions for the new fermions

$$\frac{\mathcal{L}_{N\chi}}{\sqrt{-g}} = \frac{1}{2}\bar{N}_R i\slashed{\partial} N_R - \frac{1}{2}y_M S\bar{N}_R N_R^C + \frac{1}{2}\bar{\chi}i\slashed{\partial}\chi - \frac{1}{2}y_\chi S\bar{\chi}\chi^C$$
$$- \left(y_{N\chi}\sigma\bar{N}_R\chi + y_\nu\bar{L}\tilde{H}N_R + \text{h.c.}\right) . \tag{5.46}$$
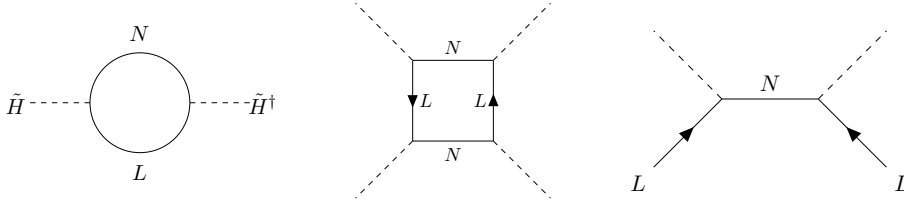
Figure 5.5: Neutrino contributions to the Higgs mass term (left) and Higgs quartic coupling (middle). The Feynman diagram in right panel generates light active neutrino masses through the type-I seesaw mechanism.

In general, the Yukawa couplings y_M, y_χ, $y_{N\chi}$ and y_ν should be interpreted as matrices in the generation space, but since this structure will be of no importance in this work we will treat them as representative real numbers. In Section 5.2 it was established that scale-invariance is broken by a finite $\langle S \rangle = v_S$ which therefore leads through the introduced Yukawa interaction to a Majorana mass $M_N = y_M v_S$ for the right-handed neutrinos and also $m_\chi = y_\chi v_S$. The central idea of the neutrino option is to take advantage of the one-loop corrections involving right-handed neutrinos (see Fig. 5.5) to the Higgs mass term which scale as [149, 194]

$$\Delta m^2 \simeq \frac{y_\nu^2 M_N^2}{8\pi^2} , \tag{5.47}$$

and the Fermi statistics fix the correct sign in front of m^2 in the effective potential. In the EFT picture, this means that the heavy right-neutrinos are integrated out at the scale $\mu = M_N$ and the theory is matched to the SM EFT by including the threshold correction (5.47) at the matching scale. The parameter space which satisfies this matching is indicated by the dashed black line in Fig. 5.6. At lower scales, the standard SM RG-running is assumed. Thereby one can say in other words that the Higgs potential is generated radiatively through

interaction with right-handed neutrinos. For completeness, we should note that the matching also induces some corrections to the quartic Higgs coupling (middle panel of Fig. 5.5) which scale as [149, 194]

$$\Delta \lambda_H \simeq \frac{y_\nu^4}{64\pi^2}\,, \tag{5.48}$$

and are negligible for small y_ν. The interesting parameter space for the neutrino option is

$$M_N \sim 10^7 \text{GeV}\,, \qquad y_\nu \sim 10^{-4}. \tag{5.49}$$

Under inspection of (5.47) and Fig. 5.6 we see that in this ballpark this will lead to $m \sim 10^2$ GeV and thereby fixes electroweak symmetry breaking. The underlying idea of the neutrino option is that (5.47) is the major origin of the Higgs mass parameter and this of course leads to scale-invariance as an underlying guiding principle since it sets the tree-level mass of the Higgs m naturally to zero. The embedding of the neutrino option, which in the original construction in [149, 194] is not scale-invariant due to an explicit Majorana mass M_N, was therefore embedded into a scale-invariant model in [95, 96, 160]. Then, the origin of m is purely explained by (5.47) in light of the neutrino option. In the case of broken scale-invariance, the right-handed neutrinos acquire mass $M_N = y_m v_s$ and the interactions in (5.46) will lead to the type-I seesaw mechanism (see right panel of Fig. 5.5). The light neutrino masses are then obtained by the suppression of the electroweak scale v_{EW} through the Majorana mass

$$m_\nu \simeq \frac{y_\nu^2 v_{\text{EW}}^2}{M_N}\,. \tag{5.50}$$

Fixing this mass scale to be of order $m_\nu \sim 0.1$ eV and using (5.47) to generate the Higgs mass parameter one is lead to the parameters shown in (5.49) (see also Fig. 5.6).

We like to give more details on the embedding of this idea in our model. The VEV v_S leads to the generation of the Planck scale (5.22) and is therefore expected to lay at rather high energies. The origin of M_N is therefore tied to the origin of M_{Pl}. In fact, using (5.22) we can write down the relation

$$M_N = y_M v_S = y_M M_{\text{Pl}} \left(\beta_S - 2U_{(1)}(v_S)/v_S^2\right)^{-1/2}\,. \tag{5.51}$$

Since $\beta_S \gg 2U_{(1)}(v_S)/v_S^2$ is satisfied in the parameter space we consider, this simplifies to

$$y_M \simeq \frac{m_N \beta_S^{1/2}}{M_{\text{Pl}}} \simeq 10^{-10} \times \left(\frac{\beta_S}{10^3}\right)^{1/2}\,. \tag{5.52}$$

For the values of β_S we consider (see e.g. Fig. 5.4) this therefore fixes the Yukawa couplings to very small values $y_M \sim 10^{-10}$. However, the smallness of
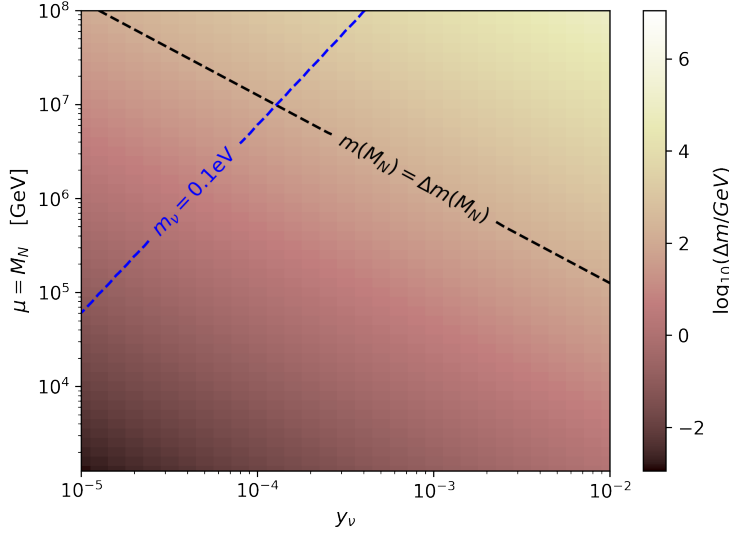
Figure 5.6: The threshold correction to the Higgs mass parameter (5.47) due to the Majorana mass M_N of right-handed neutrinos. Along the black dashed line the matching condition is satisfied, where the threshold correction at the matching scale $\mu = M_N$ equals the running Higgs mass parameter of the SM $m(m_N)$ at the matching scale. The blue line indicates the light neutrino mass scale obtained by the seesaw mechanism (5.50). Both conditions are satisfied at the intersection of the two lines at $y_\nu \simeq 10^{-3.9}$ and $M_N \simeq 10^7$ GeV.

y_M is technically natural in the sense of 't Hooft [23], because it restores the $U(1)_{B-L}$ symmetry as y_M (and $y_{N\chi}$) go to zero.

We have to return to the discussion of the portal couplings between the SM and the additional sector, since our assumption is that the Higgs mass is generated solely by (5.47). The interactions introduced in (5.46) will lead to new quantum corrections to λ_{HS} by the Feynman diagram in the left panel of Fig. 5.7. This one-loop correction scales as

$$(\Delta\lambda_{HS})_N = \frac{y_\nu^2 y_M^2}{16\pi^2} \,, \tag{5.53}$$

where the subscript N denotes that this corrections is due to the right-handed neutrinos. In the previous section we have argued that we have to tune the portals λ_{HS} and $\lambda_{H\sigma}$ to small values as to not spoil the neutrino option. In light of (5.53), we have to assume though that the natural value is of order $y_\nu^2 y_M^2$ through RG-running. However, since the two Yukawa couplings in this scenario are rather small, $y_\nu \sim 10^{-4}$ and $y_M \sim 10^{-10}$, the idea of the neutrino option is not jeopardized by a large λ_{HS} which otherwise generates a large Higgs mass directly from v_S by

$$(\Delta m)_N = (\lambda_{HS})_N \, v_S \simeq \sqrt{\frac{y_\nu^2 y_M^2}{16\pi^2}} v_S \,. \tag{5.54}$$

From $y_\nu \sim 10^{-4}$, $y_M \sim 10^{-10}$ and $v_S \sim 10^{16}$ GeV (this follows from $M_{\mathrm{Pl}} \simeq \beta_S v_s$ and $\beta_S \sim 10^2$) one can therefore estimate that $(\Delta m)_N \ll 10^2$ GeV. Similar arguments have to be made for a small $y_{N\chi}$ which couples the right-handed neutrinos to the dark matter candidate χ. Through the two-loop diagram shown in Fig. 5.7 it will generate a further correction to the Higgs mass which is estimated by

$$(\Delta m)_\chi \simeq \frac{y_\nu y_{N\chi} m_\sigma}{16\pi^2} \, . \tag{5.55}$$

Demanding as before $(\Delta m)_\chi \ll 10^2$ GeV leads to $y_{N\chi} \ll 10^{-8}$.

Frome these considerations we can argue that the set of couplings λ_{HS}, $\lambda_{H\sigma}$, y_M, y_χ and $y_{N\chi}$ remain small at higher orders in perturbation theory if they are all set small enough at tree-level. Their smallness is preserved under RG-running. In some sense, the small values for these couplings are therefore natural, even though no enhancement of symmetry is associated.[9]

A last point we would like to mention here is that leptogenesis [200, 201], i.e. the generation of the baryon asymmetry of the Universe, works successfully within the framework of the neutrino option [97, 202]. Under the assumption that the right-handed neutrinos N can be reheated only through the contact with the SM particles, [10] the bound $T_{\mathrm{RH}} \gtrsim 2 \times 10^9$ GeV must be satisfied in order to realize thermal leptogenesis with $m_N \gtrsim 2 \times 10^7$ GeV [203]. This lower bound on T_{RH} is indicated in Fig. 5.9 (black dotted line). For the three benchmark points in Table 5.1, we find that thermal leptogenesis works only if inflation last longer than $N_e \gtrsim 54$ e-folds.
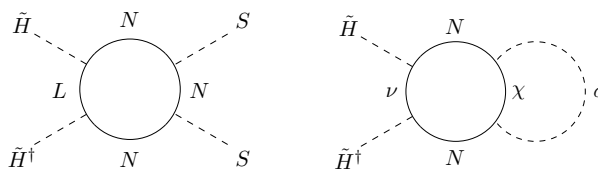
Figure 5.7: Neutrino contribution to the Higgs portal coupling λ_{HS} (left) and dark matter two-loop contribution (right) to the Higgs mass.

5.6   Reheating and Dark Matter

This section can be seen as an addendum to the overall story of this thesis and can be skipped by readers who are interested mainly in the discussion of the generation of hierarchical energy scales. We do not intend to specify a reheating

---

[9]See however [199], where a protection through an enhanced Poincare symmetry is discussed.

[10]The direct reheating through the coupling y_M of N to S is very small due to (5.52).

mechanism or advocate for a particular DM model. It should be rather seen as a general proof of concept that dark matter can be accommodated without spoiling the advocated scale-invariant framework where the generation of all scales is accounted for dynamically. Nevertheless, we give a brief overview of the results obtained in [204].

The process of reheating starts at the end of inflation when the energy density stored in the inflaton is converted to radiation (see e.g. [205, 206] for reviews). In general, we do not know much about this process and the evolution of the universe during that time, as indicated also in Fig. 4.1. We will follow the results of [207, 208] to take into account the effect of the reheating phase to some extent without specifying the underlying reheating mechanism. The basic unknown quantities in this approach are the expansion rate $a_{\rm end}/a_{\rm RH}$ during the reheating and the energy density $\rho_{\rm RH}$ at the end of reheating. These two uncertainties are combined to a single parameter [208]

$$R_{\rm rad} = \frac{a_{\rm end}}{a_{\rm RH}} \left(\frac{\rho_{\rm end}}{\rho_{\rm RH}} \right)^{1/4} , \qquad (5.56)$$

where $\rho_{\rm end} = \rho_S(S_{\rm end})$ is the energy density of the inflaton field at the end of inflation. The reheating temperature $T_{\rm RH}$ is defined through

$$\rho_{\rm RH} = \frac{\pi^2}{30} g_{\rm RH} T_{\rm RH}^4 , \qquad (5.57)$$

where $g_{\rm RH}$ accounts for the relativistic degrees of freedom at the end of reheating. We assume that $R_{\rm rad}$ can be written as [208]

$$\ln R_{\rm rad} = \frac{1 - 3\bar{w}}{12(1 + \bar{w})} \ln \left(\frac{\rho_{\rm RH}}{\rho_{\rm end}} \right) , \qquad (5.58)$$

where $\bar{w}$ is the average equation of state parameter during reheating.

We can now constrain the number of e-folds $N_e = \ln (a_{\rm end}/a_*)$ between the horizon exit of the pivot scale set by the Planck mission [131] and the end of inflation. All quantities marked with an asterisks are meant to be evaluated at horizon exit defined by $k_* = a_* H_*$. One finds [208, 209][11]

$$N_e = \ln \left(\frac{a_{\rm end}}{a_*} \right) = \ln \left(\frac{a_{\rm RH} \, \rho_{\rm RH}^{1/4}}{\sqrt{3} a_0 \, H_0} \right) - \ln \left(\frac{k_*}{a_0 H_0} \right) + \frac{1}{4} \ln \left(\frac{V_{\inf *}^2}{M_{\rm Pl}^4 \, \rho_{\rm end}} \right)$$
$$+ \ln (R_{\rm rad}) , \qquad (5.59)$$

where $g_{\rm RH} = 106.75 + (7/8)12 = 117.25$, $a_0 = 1$ and $H_0 = h \times 2.13 \times 10^{-42}$ GeV and $k_* = 0.002\,{\rm Mpc}^{-1}$ [210]. The first term of (5.59) can be computed by using (5.57)) and the conservation of entropy $a_{\rm RH}^3 \, s_{\rm RH} = a_0^3 \, s_0$, giving $a_{\rm RH}/a_0 =$

---

[11]This equation is derived from $a_{\rm end}/a_* = R_{\rm rad} \left(a_{\rm RH} \rho_{\rm RH}^{1/4}/\sqrt{3} a_0 H_0 \right) \left(\sqrt{3} H_*/\rho_{\rm end}^{1/4} \right) (a_0 H_0/k_*)$

$(q_0/q_{\mathrm{RH}})^{1/3} T_0/T_{\mathrm{RH}}$, where $q_0 = 43/11$, and $q_{\mathrm{RH}} = g_{\mathrm{RH}}$ are the degrees of freedom that enter via entropy at the present day and at the end of the reheating phase, respectively. Then, using the CMB temperature today $T_0 = 2.725\,K$ one finds [131, 211] for this term

$$\ln\left(\frac{a_{\mathrm{RH}}\,\rho_{\mathrm{RH}}^{1/4}}{\sqrt{3}a_0\,H_0}\right) = 66.89 - \frac{1}{12}\ln g_{\mathrm{RH}}\,. \qquad (5.60)$$

The energy density at the end of inflation can be expressed with the help of slow-roll parameter as

$$\rho_{\mathrm{end}} = \frac{V_{\mathrm{end}}(3 - \epsilon_*)}{(3 - \epsilon_{\mathrm{end}})}\,, \qquad (5.61)$$

where $V_{\mathrm{end}} = V_{\mathrm{inf}}(S_{\mathrm{end}})$ with the inflaton potential (5.35). The average equation of state parameter $\bar{w}$ can be deduced from the curvature of the inflaton potential V_{inf} near the minimum. Under examination of (5.24), (5.15), (5.16) and (5.36) we can deduce the scaling of the inflaton potential near the minimum $S = v_S$ by

$$V_{\mathrm{inf}}(S) \simeq U_{\mathrm{CW}}(S) = (3\lambda_S v_S^2 + \dots)\hat{S}^2 + O(\hat{S}^3) \qquad (5.62)$$

where $\hat{S} \simeq S - v_S$ and the dots stand for the higher order contribution coming from the effective potential (5.14). From the formula [212]

$$\bar{w} = \frac{p - 2}{p + 2}\,, \qquad (5.63)$$

where p is defined as the scaling exponent $V \sim \hat{S}^p$. Therefore, we find from (5.62) that $p = 2$ and hence $\bar{w} = 0$. Once the slow roll parameters of a given inflation model are computed, the only quantity on the right hand side of (5.59) that is not determined so far is the reheating temperature T_{RH}. Eq. (5.59) can be understood as a constraint on N_e, assuming that $\rho_{\mathrm{RH}} \in [1\,(\mathrm{TeV})^4, \rho_{\mathrm{end}}]$ is satisfied [131]. On the other hand, since the number of e-folds needed to solve the Big Bang puzzles is $49 < N_e < 59$ [131], (5.59) gives a constraint on T_{RH} assuming that $\rho_{\mathrm{RH}} \in [1\,(\mathrm{TeV})^4, \rho_{\mathrm{end}}]$ is also satisfied.

The relation between N_e and T_{RH} in (5.59) can be used to demonstrate how varying N_e affects the CMB observables r and n_s via the corresponding reheating temperatures in Fig. 5.8 for the benchmark points of Table 5.1.

Dark Matter Production

In (5.46) the fermion χ was introduced as a DM candidate and it has not yet been specified how it can be produced. Utilizing the freeze-in production [213] mechanism, the DM candidate can be produced during or after reheating (see also [214–216]). The two Z_2-odd particles χ and the scalar σ are stable since
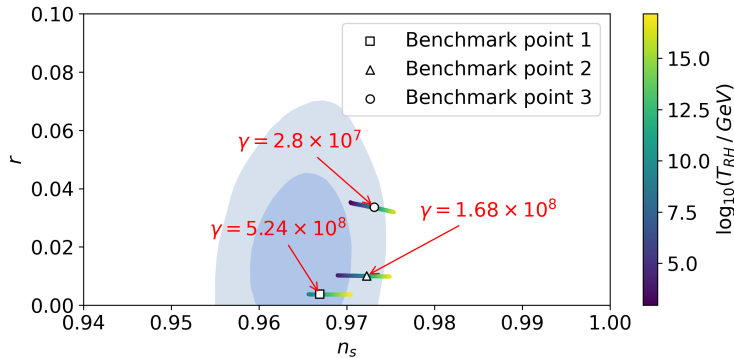
Figure 5.8: Predictions for the scalar spectral index n_s and the tensor-to-scalar ratio r with varying number of e-folds $N_e \in [50, 60]$ and (slightly) varying β_S to account for the A_s-constraint (5.43). The reheating temperature T_{RH} is shown using its dependency on the number of e-folds N_e through (5.59). For all shown points we have fixed $\lambda_S = 0.005$, $\lambda_{S\sigma} = 0.77$, $\beta_\sigma = 1$ and γ as seen labeled in the figure. Due to the lower bound on β_S, we only display $N_e \in [53.5, 60]$ for benchmark point 1. We also show the Planck TT,TE,EE+lowE+lensing+BK15 68% and 95% CL regions [131].

the Z_2 symmetry is not spontaneously broken by the VEV v_S, as accounted for by choosing the flat direction according to (5.10). One should note that the scalar σ has a rather heavy mass $m_\sigma \sim 10^{16}$ GeV (cf. (5.12)) and therefore it is too heavy to be produced via decay of the inflaton S. For this reason we focus on the production of χ which can either be produced by the decay of the inflaton $S \to \chi\chi$ or by the scattering process $NN \to \chi\chi$. In Section 5.5 we have argued that $y_{N\chi}$ is very small and so is the cross section for the process $NN \to \chi\chi$ since it scales as $\sigma_{N\chi} \sim y_{N\chi}^4$. One then finds that this process is negligible for the production of dark matter. The focus is therefore on the inflaton decay into two χ which has a decay width

$$\gamma_\chi = \frac{3\,y_\chi^2 m_S}{16\pi}(1 - 4m_\chi^2/m_S^2)^{1/2}\,. \tag{5.64}$$

Note that χ has contact with the SM particles only through N and because of the constraint $y_{N\chi} \ll 10^{-8}$, the contact of χ to SM particles is very suppressed. Under these assumptions one can consider a system comprised of the inflaton[12] S and DM χ only with the coupled Boltzmann equations [214]

$$\frac{dn_S}{dt} = -3Hn_S - \Gamma_S\,n_S\,, \tag{5.65}$$

$$\frac{dn_\chi}{dt} = -3Hn_\chi + B_\chi\Gamma_S\,n_S\,, \tag{5.66}$$

where n stands for the respective number densities, Γ_S is the total decay width of S and $B_\chi = \gamma_\chi/\Gamma_S$ is the branching ratio. The Boltzmann equations (5.65)

---

[12]We assume that S is the dominant part of the inflaton field, which in general is a mixture of S and the scalaron ϕ. Otherwise, if the mixing is large, one should incorporate it into the decay width (5.64).

are not coupled and can be solved [205] with the solutions

$$n_S(a) = \frac{\rho_{\text{end}}}{m_S} \left[\frac{a_{\text{end}}}{a}\right]^3 e^{-\Gamma_S (t-t_{\text{end}})}, \tag{5.67}$$

$$n_\chi(a) = B_\chi \frac{\rho_{\text{end}}}{m_S} \left[\frac{a_{\text{end}}}{a}\right]^3 \left(1 - e^{-\Gamma_S (t-t_{\text{end}})}\right), \tag{5.68}$$

where all quantities with the subscript "end" are evaluated at the end of inflation. The asymptotic value at $t \to \infty$ yields the DM relic abundance

$$\Omega_\chi h^2 = m_\chi B_\chi \frac{\rho_{\text{end}}}{m_S} \left[\frac{a_{\text{end}}}{a_0}\right]^3 \frac{M_{\text{Pl}}^2}{3(H_0/h)^2}. \tag{5.69}$$

The unknown (due to reheating) expansion rate a_{end}/a_0 between the end of inflation and today can be computed similarly to (5.59) and one finds

$$\frac{a_{\text{end}}}{a_0} = \left(\frac{a_{\text{end}}}{a_{\text{RH}}}\right) \left(\frac{\rho_{\text{end}}^{1/4}}{\rho_{\text{RH}}^{1/4}}\right) \left(\frac{a_{\text{RH}} \rho_{\text{RH}}^{1/4}}{\sqrt{3} a_0 H_0}\right) \left(\frac{\sqrt{3} H_0}{\rho_{\text{end}}^{1/4}}\right). \tag{5.70}$$

Using the relations (5.56), (5.57), (5.58), (5.60) and (5.63) one can relate Ω_χ to the reheating temperature

$$\Omega_\chi h^2 = \sqrt{3} \exp(3 \times 66.89) \frac{B_\chi H_0}{M_{\text{Pl}}^2} \left(\frac{\pi^2}{30}\right)^{1/4} \left(\frac{m_\chi}{m_S}\right) T_{\text{RH}} \tag{5.71}$$

$$\simeq 2.04 \times 10^8 B_\chi \left(\frac{m_\chi}{m_S}\right) \frac{T_{\text{RH}}}{1 \, \text{GeV}}, \tag{5.72}$$

which agrees with the findings of [215]. The branching ratio B_χ can be obtained with (5.64) for γ_χ and by assuming that the lifetime $1/\Gamma_S$ of the inflaton can be identified with the time scale at the end of the reheating phase [205, 214], i.e. $1/H(a_{\text{RH}}) = \left(3 M_{\text{Pl}}^2/\rho_{\text{RH}}\right)^{1/2}$.

For example, for the benchmark point 2 in table 5.1 we obtain

$$\Omega_\chi h^2 \simeq 4.4 \times 10^{31} \, y_\chi^3 \simeq 0.12 \quad \text{for} \quad y_\chi \simeq 1.4 \times 10^{-11}, \tag{5.73}$$

and for the mass of the DM candidate $m_\chi = y_\chi v_S \simeq 4.3 \times 10^6$ GeV. Using (5.72) to fix the right DM relic abundance one can plot m_χ against T_{RH} for a benchmark point. This is shown in Figure 5.9, where β_S is varied such that N_e varies between 50 and 60, leading to a variation of T_{RH} in light of (5.59). We have included the lower bound on T_{RH} for viable thermal leptogenesis by right-handed neutrino mass $M_N \gtrsim 10^7$ GeV [203].
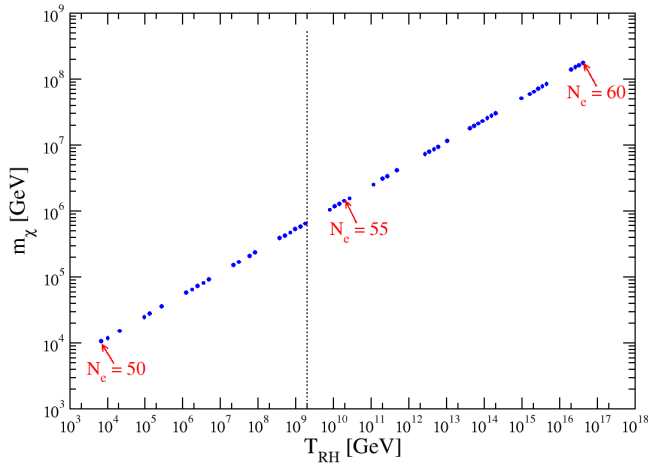
Figure 5.9: Dark matter mass m_χ against reheating temperature $T_{\rm RH}$. The non-minimal coupling β_S is varied around the benchmark value 5.69×10^2 (see benchmark point of Table 5.1) to account for a variation of e-folds N_e. All the other parameters are held fixed and the result is found to be quite insensitive against the change of these parameters. The black dotted line shows the lower bound on $T_{\rm RH}$ for viable thermal leptogenesis with $M_N \gtrsim 2 \times 10^7$ GeV [203].

Chapter 6

Inflation with Massive Spin-2 Ghosts

In the preceding discussion on Planck scale generation (Section 5.2) and inflation (Section 5.3), the effects of the Weyl tensor term in the action were left aside. Therefore, this chapter will pay special attention to this term and the entailing spin-2 ghost.[1] As the name suggests, the Weyl tensor was first constructed and discussed by its eponym Hermann Weyl [218]. It can be considered as the pivotal curvature tensor related to conformal symmetry since by its construction it is invariant under conformal transformations (3.35), i.e. it transforms trivially as

$$C^{\mu}{}_{\nu\lambda\sigma} \rightarrow C^{\mu}{}_{\nu\lambda\sigma} \,. \tag{6.1}$$

The related $C_{\mu\nu\lambda\sigma}C^{\mu\nu\lambda\sigma}$ term, hereinafter C^2-term, is therefore necessarily part of the globally scale-invariant gravity action (5.5). This term is often ignored in the literature even when other higher order terms are considered like in $f(R)$-models or more specifically in the Starobinsky model [61]. The principle reason for this is to avoid the threat of unitary violation due to the presence of a spin-2 ghost state as an additional metric degree of freedom when the C^2-term is included in the action. This is the so-called ghost problem which is a subtle and complicated issue beyond the scope of this thesis. However, we will provide an overview of some approaches discussed in the literature to tackle this problem in Section 6.1.

Despite this serious concern, one should not discard the presence of the C^2-term. Of course, in a scale-invariant theory this term cannot be avoided due to the invariance of C^2-term shown in (6.1). But even in a more general setting taking scale-invariance aside, ghosts may still be generated by quantum effects even when higher curvature terms are set to zero at tree-level. This

---

[1]This ghost should not be confused with the Faddeev-Popov ghosts which are unphysical fields introduced to cure the gauge redundancy in Yang-Mills theories, nor with the Boulware-Deser ghost in massive gravity [217].

was shown e.g. in [54, 59, 219] where the one-loop diagrams of matter fields
in a curved background will generate an effective action with a divergent part
which is proportional to C^2. Furthermore as advertised in the Introduction,
the C^2-term renders quadratic gravity renormalizable [58].

These considerations lead to the serious question of what effect the C^2-term
might have on inflationary predictions. This has been partially addressed in
the literature and it has been shown that the inclusion of the Weyl tensor will
have an effect on primordial tensor perturbations which gives corrections to the
tensor-to-scalar ratio r [183–185]. Beyond that, we will show in this chapter that
the spin-2 ghost, and also the scalaron degree of freedom (cf.(5.29)), give rise
to novel contributions to the Coleman-Weinberg potential. Theses additional
radiative contributions are computed explicitly in Section 6.3 and can give rise
to dynamical generation of the Planck scale and the inflaton potential. In some
sense, the spin-2 ghost takes here the analogues role of the gauge field of the
basic scalar QED example for the CW-mechanism discussed in Section 3.1.
Applying this calculation to the model of Chapter 5, we can achieve a similar
mechanism that utilizes only the metric degrees of freedom and one additional
external scalar S. The other scalar σ introduced Chapter 5 is in fact therefore
not strictly necessary. In Chapter 5, σ was necessary to induce sizable quantum
corrections proportional to $\lambda_{S\sigma}$ in the effective potential and therefore generate
a global minimum along the flat direction leading to $\langle\sigma\rangle = 0$ and $\langle S\rangle \neq 0$. This
role is now filled by the spin-2 ghost which will couple to the scalar S through
the non-minimal coupling β.

6.1   The Ghost Problem

In general, when considering equations of motion in physics we are dealing
with at most two time derivatives. The underlying reason for this choice is that
higher-derivatives lead to linear instabilities of the Hamiltonian. This fact was
already noted in 1850 by Ostrogradksy [220] for classical mechanics. In the
quantum version of the so-called Ostrogradsky instability the instability can
be cured by introducing negative norm states, i.e. ghost states, which in turn
violate the conversation of probability [221]. The resulting quantum theory
is doomed to be non-unitary. One might then naturally wonder whether the
same fate applies to quadratic gravity [58] or scale-invariant gravity, due to the
presence of higher derivatives hiding in the C^2-term, cf. (6.10).[2] To establish
unitarity for higher derivative theories, in particular quadratic gravity, many
interesting ideas have been put forward in the literature which are often based
on alternative quantization procedures.

The so-called fakeon prescription [224, 225] is based on an alternative Feyn-
man prescription for the ghost propagator, which quantizes the ghost states as

---

[2]See also [222, 223] for a recent in-depth discussion of unitarity violation in quadratic
gravity and conformal gravity.

a "fake" particles. This entails that the ghost is always purely virtual and does not appear in the asymptotic spectrum of physical states. In [226, 227] a new type of norm for quantum states is imposed that leads to positive quantum mechanical probabilities. Other approaches are centered around a construction of $\mathcal{PT}$-symmetric rather than Hermitian Hamiltonians which comes with a Hilbert space equipped with a positive definite inner product [228, 229]. Donoghue and Menezes [230, 231] adopt the view that the ghost is an unstable particle when the Lee-Wick contour [232] in the calculation of the Feynman propagator is used. Therefore, the ghost state should not included in the asymptotic states of the S-matrix and the only effect that the ghost leaves behind is the violation of microcausality at the mass scale of the ghost, similarly to the fakeon prescription [224, 225].

Leaving the finer details of the incomplete list of works aside, the relevant takeaway is that the presence of the spin-2 ghost does not render globally scale-invariant gravity immediately unphysical. In particular, the list above shows the quantum-mechanical effects of the massive ghost should be taken seriously and so it is important to also compute the ghost contribution to the CW-potential, as we will do in the following two sections.

6.2 The Model and its Degrees of Freedom

We start with the following general action S_T describing globally scale-invariant gravity as already introduced in (5.5) non-minimally coupled to a single additional matter scalar $S(x)$,

$$S_{\mathrm{T}} = S_{\mathrm{GR}} + S_{\mathrm{S}} \,, \tag{6.2}$$

$$S_{\mathrm{GR}} = \int \mathrm{d}^4 x \sqrt{-g} \left(\gamma R^2 - \kappa C_{\mu\nu\rho\sigma} C^{\mu\nu\rho\sigma} \right) , \tag{6.3}$$

$$S_{\mathrm{S}} = \int \mathrm{d}^4 x \sqrt{-g} \left(\frac{1}{2} \partial_\mu S \partial^\mu S - \frac{\beta}{2} S^2 R - \frac{\lambda}{4} S^4 \right) , \tag{6.4}$$

where γ, κ, β, and λ are arbitrary dimensionless constants and the theory is globally scale-invariant. To separate out the gravitational degrees of freedom, we consider the small fluctuations $h_{\mu\nu}$ around Minkowski space with metric $\eta_{\mu\nu}$,

$$g_{\mu\nu} = \eta_{\mu\nu} + h_{\mu\nu} \,, \tag{6.5}$$

and in a similar spirit, we expand the scalar around a constant background field S_{cl},

$$S = S_{\mathrm{cl}} + \hat{S} \,, \tag{6.6}$$

where $\hat{S}$ are the quantum fluctuations around the background value. To study the propagating modes of the action, we expand (6.2) up to second order in the

fields $h_{\mu\nu}$ and $\hat{S}$ and obtain

$$
S_{\mathrm{T}}^{(\mathrm{quad})} = \int \mathrm{d}^4 x \left[\frac{\beta}{8} S_{\mathrm{cl}}^2 \left(h^{\mu\nu} \Box h_{\mu\nu} + 2 h^{\mu\nu} \partial_\nu \partial^\rho h_{\mu\rho} - h_\mu{}^\mu \Box h_\nu{}^\nu - 2 h_\mu{}^\mu \partial_\nu \partial_\rho h^{\nu\rho} \right) \right.
$$

$$
+ \gamma \left(h^{\mu\nu} \partial_\mu \partial_\nu \partial_\rho \partial_\sigma h^{\rho\sigma} + h_\mu{}^\mu \Box^2 h_\nu{}^\nu + 2 h_\mu{}^\mu \Box \partial_\nu \partial_\rho h^{\nu\rho} \right)
$$

$$
+ \frac{\kappa}{6} \left(-3 h^{\mu\nu} \Box^2 h_{\mu\nu} - 6 h^{\mu\nu} \Box \partial_\nu \partial^\rho h_{\mu\rho} - 2 h^{\mu\nu} \partial_\mu \partial_\nu \partial_\rho \partial_\sigma h^{\rho\sigma} \right.
$$

$$
\left. + h_\mu{}^\mu \Box^2 h_\nu{}^\nu + 2 h_\mu{}^\mu \Box \partial_\nu \partial_\rho h^{\nu\rho} \right)
$$

$$
\left. - \frac{1}{2} \hat{S} \beta S_{\mathrm{cl}} \left(\partial_\nu \partial_\mu + \Box \eta_{\mu\nu} \right) h^{\mu\nu} + \frac{1}{2} \hat{S} \left(\Box - 3\lambda S_{\mathrm{cl}}^2 \right) \hat{S} \right], \tag{6.7}
$$

where we have performed partial integration and introduced the d'Alembert operator $\Box = -\eta^{\mu\nu} \partial_\mu \partial_\nu$. In the equation above we have omitted the terms related to the induced cosmological constant proportional to S_{cl}^4 and the tree-level equation of motion for S_{cl}. York decomposition [233] allows us to further separate the gravitational degrees of freedom encoded in $h_{\mu\nu}$ according to their spin

$$
h_{\mu\nu} = \tilde{h}_{\mu\nu} + \partial_\mu V_\nu + \partial_\nu V_\mu + \left(\partial_\mu \partial_\nu - \frac{1}{4} \eta_{\mu\nu} \Box \right) a + \frac{1}{4} \eta_{\mu\nu} h_\rho{}^\rho, \tag{6.8}
$$

where $\tilde{h}_{\mu\nu}$ is a traceless-transverse tensor mode, V_μ is a transverse vector mode and a and the trace $h_\mu{}^\mu(x)$ are scalar modes. As the name suggest these modes have the property $\partial^\mu \tilde{h}_{\mu\nu} = \tilde{h}_\mu{}^\mu = 0$ and $\partial_\mu V^\mu = 0$. It will also turn out to be useful to introduce the scalar quantity [161]

$$
\phi = h_\mu{}^\mu - \Box a, \tag{6.9}
$$

which is gauge-invariant under diffeomorphisms $h_{\mu\nu} \to h_{\mu\nu} + \partial_\mu \xi_\nu + \partial_\nu \xi_\mu$. This field can be identified with the scalaron degree of freedom originating from the R^2-term in Starobinsky inflation [61]. After applying (6.8) and (6.9) all terms containing the gauge-dependent V_μ and a cancel out and the action simplifies to

$$
S_{\mathrm{T}}^{(\mathrm{quad})} = \int \mathrm{d}^4 x \left[\frac{9\gamma}{16} \phi \left(\Box^2 - m_\phi^2 \Box \right) \phi - \frac{\kappa}{2} \delta_{\mu\nu\rho\sigma} \tilde{h}^{\mu\nu} \left(\Box^2 - m_{\mathrm{gh}}^2 \Box \right) \tilde{h}^{\rho\sigma} \right.
$$

$$
\left. - \hat{S} \left(\frac{3}{4} \beta S_{\mathrm{cl}} \Box \right) \phi + \frac{1}{2} \hat{S} \left(\Box - m_S^2 \right) \hat{S} \right], \tag{6.10}
$$

where $\delta_{\mu\nu\rho\sigma} = \frac{1}{2} (\eta_{\mu\rho} \eta_{\nu\sigma} + \eta_{\mu\sigma} \eta_{\nu\rho})$ and we have identified the field-dependent masses

$$
m_\phi^2(S_{\mathrm{cl}}) = \frac{\beta}{12\gamma} S_{\mathrm{cl}}^2, \qquad m_S^2(S_{\mathrm{cl}}) = 3\lambda S_{\mathrm{cl}}^2, \qquad m_{\mathrm{gh}}^2(S_{\mathrm{cl}}) = \frac{\beta}{4\kappa} S_{\mathrm{cl}}^2. \tag{6.11}
$$

In addition to the two scalar degree of freedoms ϕ and S, the spin-2 ghost obtains a field-dependent mass $m_{\text{gh}}(S_{\text{cl}})$ proportional to the classical background field S_{cl}. In this York-decomposed form, one can also easily calculate the propagator for the spin-2 degrees of freedom by performing a Fourier transform and identifying the inverse propagators as the Hessian with respect to $\tilde{h}_{\mu\nu}$

$$i\langle 0|\mathcal{T}\tilde{h}_{\mu\nu}\tilde{h}_{\rho\sigma}|0\rangle = \frac{4}{\beta S_{\text{cl}}^2}\left(\frac{1}{p^2} - \frac{1}{p^2 - m_{\text{gh}}^2}\right)\delta_{\mu\nu\rho\sigma}, \tag{6.12}$$

where $p^2 = p_\mu p^\mu$. Once can see, that next to the massless pole corresponding to the spin-2 graviton there is an additional pole at $p^2 = m_{\text{gh}}^2$ corresponding to the massive spin-2 ghost which has the opposite sign in (6.12) as opposed to the conventional field. The computation for the two scalar propagator from (6.10) is more involved due to the mixing between $\hat{S}$ and ϕ. For our purposes it will be sufficient in the next section to compute the functional determinant of the inverse propagator in the non-diagonal form.

6.3 Derivation of the Effective Potential

We now turn to the contribution of the massive spin-2 and spin-0 sectors in (6.10) to the one-loop effective potential. Since the inverse propagator in (6.10) reveals a kinetic mixing between $\hat{S}$ and ϕ, spin-2 fields and also higher-derivatives it is not possible to use the standard results presented in Section 2.1.1. Instead one can rely on the result derived in (2.23) in which the one-loop contribution to the effective action can be computed by taking the functional determinant of the inverse propagator. To do so, we collect the fluctuations in $\psi = (\tilde{h}_{\mu\nu}, \phi, \hat{S})^T$ and identify the inverse propagator with the Hessian of (6.10) such that we can write

$$\Gamma^{(1)}[S] = \frac{i}{2}\ln\left[\text{Det}\left(\frac{\delta^2 S_{\text{T}}^{(\text{quad})}}{\delta\psi\delta\psi}\right)\right]$$

$$= \frac{i}{2}\ln(\text{Det}M) - \frac{i}{2}\text{Tr}\left[\ln\left(\delta_{\mu\nu\rho\sigma}\left(-\Box^2 + m_{\text{gh}}^2\Box\right)\right)\right]. \tag{6.13}$$

Note that from here on we drop the subscript of S_{cl} for convenience. In the second line in the above equation we have split the spin-0 sector from the rest. The Hessian in the spin-0 sector is

$$M = \begin{pmatrix} \frac{9\gamma}{8}\left(\Box^2 - m_\phi^2\Box\right) & -\frac{3}{4}\beta S\Box \\ -\frac{3}{4}\beta S\Box & \Box - m_S^2 \end{pmatrix}. \tag{6.14}$$

After computing the determinant of the matrix M, the logarithm can be rewritten as

$$\ln(\text{Det}M) = \text{Tr}\left[\ln\left(\Box - m_+^2\right)\right] + \text{Tr}\left[\ln\left(\Box - m_-^2\right)\right] + \cdots \tag{6.15}$$

where the "$\cdots$" stand for terms irrelevant for the effective potential which have no S-dependence. The introduced mass terms are[3]

$$
\begin{aligned}
m_\pm^2 = &\frac{1}{2}\left(m_S^2 + (1+6\beta)m_\phi^2\right) \\
&\pm \frac{1}{2}\sqrt{\left(m_S^2 + (1+6\beta)m_\phi^2\right)^2 - 4m_S^2 m_\phi^2}\,.
\end{aligned}
\tag{6.16}
$$

The functional trace in (6.15) can be evaluated in momentum space where the inverse propagators are diagonal, cf. (2.25). With this, scalar contributions to the effective action are given by

$$
\Gamma_{\text{scal}}^{(1)}[S] = \frac{i}{2}\sum_{j=\pm}\int \frac{\mathrm{d}^4 p}{(2\pi)^4}\ln\left(p^2 - m_j^2\right)\int \mathrm{d}^4 x
\tag{6.17}
$$

From here we get the corresponding effective potential contribution by removing the volume term and changing the sign, cf. (2.13).

$$
\begin{aligned}
U_{\text{scal}}(S) &= -\frac{i}{2}\sum_{j=\pm}\int \frac{\mathrm{d}^4 p}{(2\pi)^4}\ln\left(p^2 - m_j^2\right) \\
&= \sum_{j=\pm}\frac{1}{64\pi^2}m_j^4\left[\ln\left(\frac{m_j^2}{\mu^2}\right) - \frac{3}{2}\right].
\end{aligned}
\tag{6.18}
$$

In the second equality we have employed dimensional regularization in the $\overline{\text{MS}}$-scheme, introducing the renormalization scale μ in the process, and we have absorbed the divergent terms into the renormalized constant λ.

The calculation of the spin-2 part follows in much the same way as for the scalars. This contribution comes from the last term in (6.13), which can be rewritten as

$$
\text{Tr}\left[\ln\left(\delta_{\mu\nu\rho\sigma}\left(-\Box^2 + m_{\text{gh}}^2\Box\right)\right)\right] = \text{Tr}\left[\ln\left(\delta_{\mu\nu\rho\sigma}\left(\Box - m_{\text{gh}}^2\right)\right)\right] + \text{Tr}\ln(-\Box)\,,
\tag{6.19}
$$

where only the massive part, i.e. the spin-2 ghost, of the inverse propagator contributes.[4] However, in order to correctly count the degrees of freedom in momentum space, we must take advantage of the transverse-traceless nature of $\tilde{h}_{\mu\nu}$ to write

$$
\tilde{h}^{\mu\nu}\delta_{\mu\nu\rho\sigma}\tilde{h}^{\rho\sigma} = \tilde{h}^{\mu\nu}P_{\mu\nu\rho\sigma}^{(2)}\tilde{h}^{\rho\sigma}\,,
\tag{6.20}
$$

---

[3]This agrees with the two mass eigenstates computed in the Einstein frame in [30].

[4]Here we dropped the irrelevant contribution $-\frac{i}{2}\text{Tr}\ln(-\Box)$ to the effective potential which is independent of S, as we did in (6.15) Therefore, the overall sign of the ghost contribution to the effective potential in (6.24) is the same as for a normal particle, which is consistent with the β-function of the quartic coupling λ_S (see e.g. the β-functions in [30]).

where

$$P^{(2)}_{\mu\nu\rho\sigma} = \frac{1}{2}\big(\theta_{\mu\rho}\theta_{\nu\sigma} + \theta_{\mu\sigma}\theta_{\nu\rho}\big) - \frac{1}{d-1}\theta_{\mu\nu}\theta_{\rho\sigma} \tag{6.21}$$

$$\text{with}\qquad \theta_{\mu\nu} = \eta_{\mu\nu} - \frac{p_\mu p_\nu}{p^2}\,, \tag{6.22}$$

is a spin-2 projection operator [234]. Making this replacement ensures that we count the correct number of degrees of freedom for a massive spin-2 field in d space-time dimensions, by computing the trace for rank-2 tensor

$$\text{Tr}\big(P^{(2)}_{\mu\nu\rho\sigma}\big) = \delta^{\mu\nu\rho\sigma}P^{(2)}_{\mu\nu\rho\sigma} = \frac{1}{2}(d+1)(d-2)\,, \tag{6.23}$$

which gives five in $d=4$ as expected for a massive spin-2 excitation. With these considerations, we find that the massive spin-2 contribution to the effective potential coming from (6.19) reads

$$\begin{aligned} U_h(S) &= -\frac{i}{2}\lim_{d\to 4}\left[\mu^{4-d}\int\frac{\mathrm{d}^d p}{(2\pi)^d}\frac{1}{2}(d+1)(d-2)\ln\left(\frac{p^2 - m^2_{\text{gh}}}{p^2}\right)\right]\\ &= \frac{5}{64\pi^2}m^4_{\text{gh}}\left[\ln\left(\frac{m^2_{\text{gh}}}{\mu^2}\right) - \frac{1}{10}\right] \end{aligned} \tag{6.24}$$

In the second equality we have again subtracted the divergent part according to the $\overline{\text{MS}}$-scheme.

Finally, the total effective potential is given by

$$U_{\text{eff}}(S) = \frac{\lambda}{4}S^4 + U_{\text{scal}}(S) + U_h(S) + U_0\,, \tag{6.25}$$

where we introduced U_0 as an arbitrary constant background that may be tuned in order to ensure that the classical zero-point energy vanishes at the global minimum, as we did already in (5.21). Note, that once the cosmological constant is canceled in the Jordan frame, it remains zero after transforming to the Einstein frame in our framework.

6.4 Effective Action for Inflation

As we have done similarly in Section 5.3, the effective action for inflation may be written as

$$S_{\text{eff}} = \int \mathrm{d}^4 x\sqrt{-g}\bigg(\frac{1}{2}S\Box S - \frac{\beta}{2}S^2 R + \gamma R^2 - \kappa C_{\mu\nu\rho\sigma}C^{\mu\nu\rho\sigma} - U_{\text{eff}}(S)\bigg), \tag{6.26}$$

where U_{eff} is the quantum effective one-loop potential we computed in the previous section. One can write (6.25) as [3]

$$U_{\text{eff}}(S) = U_0 + \left[C_1 + C_2\ln\left(\frac{S^2}{\mu^2}\right)\right]S^4\,, \tag{6.27}$$

with C_1 and C_2 being dimensionless constants that depend only on the coupling constants λ, β, γ and κ which can be derived from (6.25).

To study the process of spontaneous symmetry breaking, one needs to compute the VEV v_S by minimizing the effective potential

$$\frac{\partial U_{\text{eff}}(S)}{\partial S}\bigg|_{S=v_S} = 0\,, \qquad v_S = \mu \exp\left(-\frac{1}{4} - \frac{C_1}{2C_2}\right).\qquad(6.28)$$

The non-zero value of v_S indicates a spontaneous breakdown of global scale-invariance. One can also calculate now the explicit value of U_0 in (6.27) by requiring that the effective potential vanishes at the global minimum, i.e.

$$U_{\text{eff}}(v_S) = 0\,, \qquad U_0 = \frac{\mu^4}{2}C_2 \exp\left(-1 - \frac{2C_1}{C_2}\right).\qquad(6.29)$$

The Planck mass that is generated after symmetry breaking is obtained by identifying the non-minimal coupling to the VEV v_S in (6.26) with the canonical Einstein-Hilbert term as

$$-\frac{1}{2}\beta S^2 R\bigg|_{S=v_S} = -\frac{1}{2}M_{\text{Pl}}^2 R\,, \qquad M_{\text{Pl}}^2 = \beta v_S^2\,.\qquad(6.30)$$

Compared to the previous results of Chapter 5, the need for an additional scalar next to S is not necessary since now it is possible to achieve radiative symmetry breaking of scale-invariance in the Jordan frame thanks to the contributions of gravitational degrees of freedom. However, we can still calculate the prediction for inflationary observables along the lines of Section 5.3 with the effective potential obtained in (6.27). We established that scale-invariance is broken, so we can introduce an auxiliary field to remove the R^2-term and then transform to the Einstein frame. As in Section 5.3, we find a 2-dimensional potential for the scalar S and the scalaron which exhibits a valley structure which is expected to be the inflationary trajectory. Following the methods of Section 5.3.1, we can solve for the valley contour and finally derive an effective one-field description in the Einstein frame

$$S_{\text{inf}}^{\text{E}} = \int \mathrm{d}^4x \sqrt{-g}\left(-\frac{1}{2}M_{\text{Pl}}^2 R - \kappa C_{\mu\nu\rho\sigma}C^{\mu\nu\rho\sigma} + \frac{1}{2}F(S)^2 S\Box S - U_{\text{inf}}(S)\right).$$
$$(6.31)$$

The modification to the kinetic term is

$$F(S) = \frac{1}{(1+4A)B}\left[(1+4A)B + \frac{3}{2}M_{\text{Pl}}^2\left((1+4A)B' + 4A'B\right)^2\right]^{1/2},\quad(6.32)$$

where the functiosn A and B are defined by

$$A(S) = \frac{4\gamma\, U_{\text{inf}}(S)}{B(S)^2 M_{\text{Pl}}^4}\,, \qquad\qquad B(S) = \frac{\beta S^2}{M_{\text{Pl}}^2}\,,\qquad(6.33)$$

and primes denote derivatives with respect to S. The inflaton potential $U_{\text{inf}}(S)$ in (6.31) is given by

$$U_{\text{inf}}(S) = \frac{U_{\text{eff}}(S)}{B(S)^2 + 16\gamma\, U_{\text{eff}}(S)/M_{\text{Pl}}^4}\,, \qquad (6.34)$$

and depends on the coupling constants λ, β, γ, and κ. One may also obtain the canonically normalized field $\tilde{S}$ by simple integration as in (5.39).

For details on the methods used to study slow-roll inflation numerically, we refer to Section 5.3.1, since the treatment is the same. We use (5.40)-(5.42) to compute the inflationary CMB observables. After the renormalization scale μ is fixed through the Planck mass identification (6.30) we consider the dimensionless parameters in the range

$$\lambda = 0.005 \qquad \beta \in [10^3, 10^4] \qquad \gamma \in [10^3, 10^9] \qquad \kappa \in [10^2, 10^{3.25}]\,. \qquad (6.35)$$

This parameters space is then constrained by the scalar power spectrum amplitude (5.43) and the resulting predictions for spectral tilt n_s and tensor-to-scalar ratios r are shown in Fig. 6.1. Though more parameter space than (6.35) was explored, it did not yield promising predictions while remaining compatible with this constraint. To highlight the effect of the R^2 and C^2 term on the $n_{\text{s}} - r$ predictions, we display values for the corresponding parameters (γ and κ) separately in the upper and lower panel of Fig. 6.1. The results shows that from $N_e = 50$ up to $N_e = 60$ e-folds plenty of parameter space is compatible with the tightest Planck and BICEP/Keck constraints [131, 235].

The point labeled "B1" in Fig. 6.1 corresponds to the following benchmark values.

$$\text{B1}: \lambda = 0.005 \qquad \beta = 5.62 \times 10^2 \qquad \gamma = 1.22 \times 10^8 \qquad \kappa = 837 \qquad (6.36)$$

In order to get an order of magnitude estimate, the related field-dependent masses m_ϕ and m_{gh} in (6.11) evaluated at the VEV of S are

$$m_\phi^{\text{B1}}(S = v_S) \simeq 6.35 \times 10^{13}\,\text{GeV}\,, \qquad (6.37)$$

$$m_{\text{gh}}^{\text{B1}}(S = v_S) \simeq 4.21 \times 10^{16}\,\text{GeV}\,. \qquad (6.38)$$

These masses can be taken as representative for most of the displayed points, with the masses of the points displayed in Fig. 6.1 being roughly contained in the ranges $m_\phi \in \left[10^{13}\,\text{GeV}, 10^{14}\,\text{GeV}\right]$ and $m_{\text{gh}} \in \left[10^{16}\,\text{GeV}, 10^{17}\,\text{GeV}\right]$. An important point is to be made here, which will clarify the importance of the ghost contribution to the effective potential. Since low m_ϕ goes hand in hand with high γ, the upper panel of Fig. 6.1 shows that low m_ϕ leads to relatively small tensor-to-scalar ratios r. To achieve small r for this model, the contribution of the scalaron mass m_ϕ to the effective potential is relatively small. With the scalaron contribution alone it is therefore not possible to achieve successful
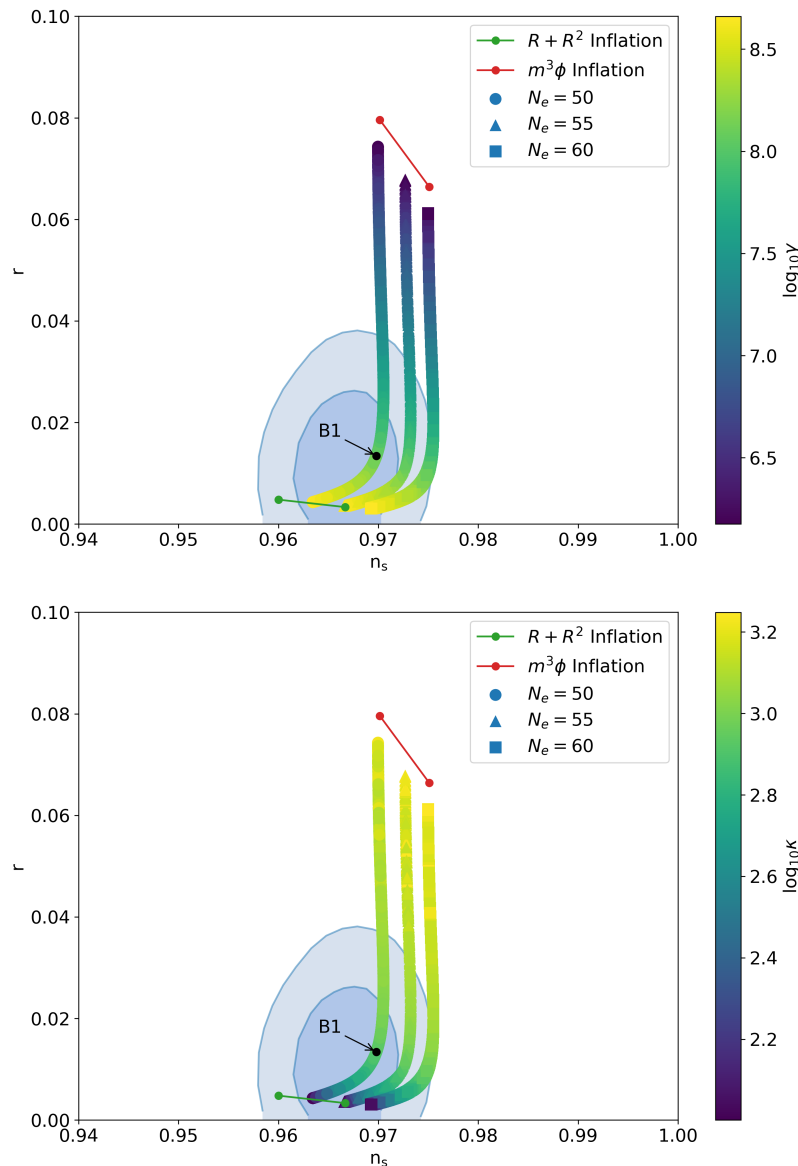
Figure 6.1: Predictions for the scalar spectral index $n_{\rm s}$ and the tensor-to-scalar ratio r with varying numbers of e-folds N_e are displayed. All shown points are taken according to the parameter ranges in (6.35) while satisfying the A_s-constraint (5.43). The color gradient shows γ in the upper and κ in the lower plot. The blue regions indicate the Planck TT,TE,EE+lowE+lensing+BK18+BAO 68% and 95% CL regions from [131, 235]. We also included the predictions of the Starobinsky model (green) and linear inflation (red), where the circles represent the predictions for $N_e = 50$ (left) and $N_e = 60$ (right) e-folds respectively. This exemplifies that our results interpolate between these two results as in Fig. 5.4. The effect of corrections to r due to the C^2 term as discussed in [183–185] are included in Fig. 6.2.

symmetry breaking of scale-invariance and dynamical generation of $M_{\rm Pl}$ while maintaining low r, as favored by observations of inflationary CMB observables. On the other hand, the massive spin-2 ghost is not so strongly tied to low masses at low r. Since it scales as $m_{\rm gh}^2 \propto 1/\kappa$, the lower panel of Fig. 6.1 reveals that $m_{\rm gh}$ is increasing for lower r. The ghost contributions to the effective potential (6.24) is therefore substantial and is crucial for triggering symmetry breaking while maintaining low r, which is a novel consideration with regard to scale-invariant models.
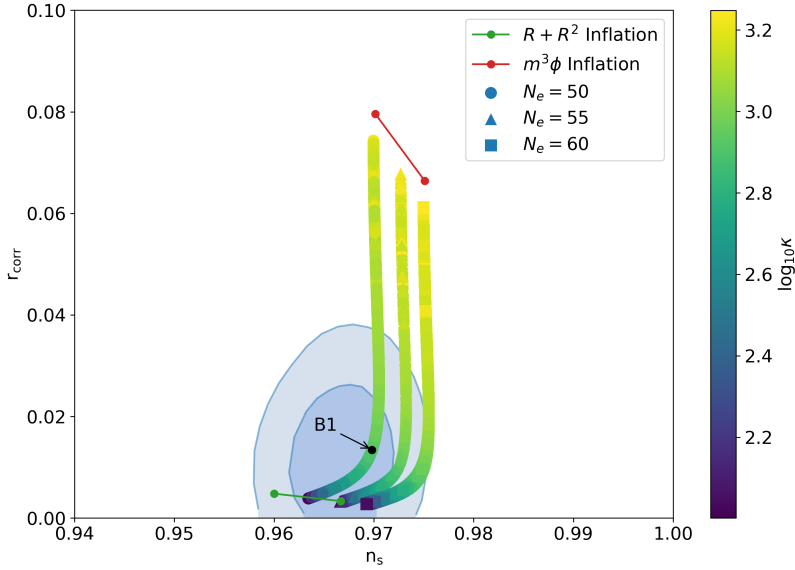
Figure 6.2: Predictions for the scalar spectral index $n_{\rm s}$ and tensor-to-scalar ratio $r_{\rm corr}$ including the corrections due to the C^2 term given in (6.39). The data is displayed in the same way as in the lower panel of Fig. 6.1.

As mentioned in the introduction of this chapter, the C^2-term can contribute non-trivially to primordial tensor perturbations leading to a correction of the tensor-to-scalar ratio [183–185]. It is therefore crucial to discuss how this can influence the findings presented in Fig. 6.1. To calculate this correction we use the slow-roll approximation during inflation[5], i.e. $H^2 \approx U_{\rm inf}/(3M_{\rm Pl}^2)$, and use equation (6.51) in [236] to obtain

$$r_{\rm corr} = r \left(1 + \frac{2\,H^2}{m_{\rm gh}^2} \right)^{-1} \simeq r \left(1 + \frac{2\,U_{\rm inf}(S_*)}{3\,M_{\rm Pl}^2\,m_{\rm gh}^2(S_*)} \right)^{-1}, \qquad (6.39)$$

where r is the tensor-to-scalar ratio without the effect of the C^2-term. The results of Fig. 6.1 are corrected with (6.39) and displayed in Fig. 6.2. We find that these corrections do not change the results substantially and the corrected

---

[5]To ensure a field value that is representative for inflation we choose $S = S_*$ to calculate $U_{\rm inf}(S)$ and $m_{\rm gh}(S)$.

predictions are still fully compatible with the strongest cosmological constraints from Planck and BICEP/Keck. It is safe to conclude that our approach is consistent, i.e. that the direct effects of the inclusion of the C^2 through (6.39) do not jeopardize the effects of the ghost contribution to the effective potential in order to successful dynamical generation of M_{Pl} while maintaining an inflationary potential that leads to low r.

Chapter 7

Conclusion

In this thesis we have questioned the origin of mass scales in high-energy physics. To give a deeper, and maybe more satisfying, answer to this puzzle, we have considered radiative generation of these scales based on the anomalous breaking of scale-invariance as laid out in Chapter 2 and 3. This can be understood as a dynamical origin in the sense that the mass scales follow necessarily out of the theory, i.e. the mass scales can be determined by the dimensionless couplings of theory if their values are defined at some renormalization scale. On top of the gauge symmetries of the SM and general diffeomorphism invariance, we used global scale-invariance of the classical theory in the context of particle physics, gravity and cosmology as the pivotal guiding principle for establishing this dynamical origin and constructed the models discussed in Chapter 5 and 6 in this manner. The emphasis was to provide a global picture of radiatively generated mass scales and their interconnections. We have reevaluated the hierarchy problem in this setting in Sections 3.3, 3.4, 5.4 and 5.5.

Chapter 5 in particular addresses the generation of widely separated scales, which are usually understood to be completely independent of each other, with a change of perspective: How can the Planck mass, Majorana mass, electroweak scale and the neutrino masses be related? To answer this question, we extended the SM with two additional scalar fields and applied the GW approach introduced in Section 3.2. One of the scalars (σ) can then be integrated out due to its heavy tree-level mass leaving the other scalar (S) to fulfill a quadruple role: it breaks scale-invariance by the condensate $v_S = \langle S \rangle$, generates the Planck mass $M_{\mathrm{Pl}} \approx \beta_S v_S^2$, generates the Majorana mass for right-handed neutrinos $M_N = y_M v_s$ and serves as inflaton field. It was then further shown in Section 5.6 that a DM candidate can be incorporated and be produced through inflaton decay. The are also some portals between the hidden sector and the SM which we exploit in Section 5.5 to bridge the large gap between the Planck mass and the electroweak scale using the idea of the neutrino option [149] in which the heavy Majorana neutrinos of the type-I seesaw model are integrated out and matched to the SM EFT. This allows one to soften the huge hierarchy

between the Higgs and Planck masses when both are dynamically generated. To generate the correct Higgs mass and the light active neutrino masses one needs to fix $M_N \sim 10^7$ GeV whereas the majorana mass $M_N = y_M v_s$ can be more easily lowered with respect to $M_{\rm Pl}$ because a small Yukawa coupling y_M is technically natural. There are however some problematic portal terms between the SM and the dark sector so we must assume that the additional scalars are weakly coupled to the SM. The respective portal couplings have to be tuned extremely small, though not to special values, and we have noted that their smallness is stable under RG-running even though no enhancement of symmetry is associated.

The gravitational sector of our studies is globally scale-invariant and can realize an inflating period in the early universe and give rise to primordial fluctuations which are reflected in the CMB anisotropies. In our setup, we showed in Sections 5.2 and 6.4 that scale-invariance is broken in the Jordan frame and that a scale is generated. Consequently, we are allowed to perform a Weyl-rescaling to go from Jordan to Einstein frame. In this frame, the scalaron degree of freedom, originating from the R^2-term, is made explicit. The resulting scalar potential in the Einstein frame is two-dimensional but it exhibits a valley structure along which the potential is very flat, a feature that is itself a reflection of scale-invariance. The slow-roll conditions can be easily satisfied along that valley. Reducing the further analysis to the valley contour, as discussed in Section 5.3.1, this allows for an effective one-field description of inflation. Following this approach we can use the formulas derived in Chapter 4, with some minor modifications, to derive CMB observables related to inflation. Our results are summarized in Fig. 5.4 and show that inflation can be naturally accommodated. The predictions for the spectral tilt $0.964 \lesssim n_s \lesssim 0.975$ and tensor-to-scalar ratio $r \lesssim 0.08$ are well within observational constraints and interpolate between the predictions of Starobinsky inflation and linear chaotic inflation. Our construction also allows for dynamical generation of the Planck mass, which cannot be achieved for example in the popular models of Starobinksy or Higgs inflation. In fact, we have assumed that the Higgs plays no role in our scenario by choosing the non-minimal coupling β_H small.

In Chapter 6 we have carefully analyzed how global scale-invariance can be broken in the Jordan frame. The results of Chapter 5 seem to indicate that two scalars are needed for the CW-mechanism, however, putting the focus on quadratic curvature terms in the action of globally scale-invariant gravity and the resulting metric degrees of freedom, this is must be revaluated. Including these terms renders quadratic gravity renormalizable but potentially non-unitary [58], a fact which is unavoidably given that these quadratic terms are also necessarily generated at the quantum level. Particular emphasis has been put on the Weyl-tensor squared term which gives rise to a problematic massive spin-2 degree of freedom that is the source of said unitarity violation. After briefly listing some of the approaches to restore the unitarity of quadratic gravity in Section 6.1, and being optimistic that in one way or another this

matter will be resolved, we concluded that radiative corrections of the spin-2 ghost have to be taken into account. Therefore, we have computed the one-loop corrections of this field to the effective potential in Section 6.3 and revaluated the CW-mechanism in presence of gravitational degrees of freedom. The subsequent radiative generation of the Planck mass and the inflaton potential then go qualitatively along the lines of Chapter 5 and we find that the one-loop corrections coming from the spin-2 ghost are paramount to triggering the breaking of scale-invariance while also realizing a flat inflaton potential that predicts a low tensor-to-scalar ratio r. Our calculations also allow us to include the quantum contribution from the scalaron. This degree of freedom alone cannot simultaneously account for successful inflation in the observationally favored regime of low r and for dynamical generation of M_{Pl} however. These consideration show that the field content of 5 can be reduced, meaning that the additional scalar σ is not needed to trigger RSB when contributions from the spin-2 ghost are also taken into account. Although not constructed explicitly in this thesis, the more phenomenological aspects discussed in Chapter 5 can also be combined with the framework developed in Chapter 6. In particular, the neutrino option idea can be included as well in order to bridge the large gap to between the Planck and electroweak scales.

Observational constraints on inflation might be the only way to scrutinized the models discussed in this work in the near future, since all additional degrees of freedom with respect to the SM are relatively heavy and far beyond the reach of colliders. Though neutrinoless double beta decay might confirm the Majorana nature of neutrinos, this would give only a hint towards a connection of the electroweak scale and the Majorana mass M_N in light of the neutrino option. Analyzing the inflationary dynamics more carefully, might allow to test the scenario proposed in this thesis in more detail. Although we have treated the inflationary dynamics always in an effective one-field description, and we have argued that this is a good approximation, it might be worthwhile to perform this analysis more carefully as has been done e.g. in [237] because multi-field inflation can give rise to primordial non-Gaußianities in cosmological fluctuations which are suppressed in single-field inflation [134] but give an important effect on the CMB anisotropy as well as on the large scale structure of the Universe (see for instance [135, 238]). There are several experimental projects planned such as LiteBird [239], Euclid [240], LSST [241] to measure the magnitude of non-Gaußianities and constrain their existence. Taking these matters aside, we hope to provide some new insights on the interconnections of radiatively generated mass scales in scale-invariant models, in interplay with cosmic inflation.

Appendix A

Discussion of the Valley Approximation

An alternative method to obtain the valley contour is achieved by looking for local minima in the direction of the field S, yielding the contour $\mathcal{C}'$ and the related inflationary potential,

$$\mathcal{C}' = \{\tilde{S}(\phi), \phi\}, \quad \text{where} \quad \left.\frac{\partial V(S, \phi)}{\partial S}\right|_{S=\tilde{S}(\phi)} = 0, \quad V_{\text{inf}}(\phi) = V(\tilde{S}(\phi), \phi).$$

$$(A.1)$$

Completely analogous to the treatment of contour $\mathcal{C}$, the field normalization (replacing (6.32)) is now given by

$$F^2(\phi) = \left[1 + e^{-\Phi(\phi)}\left(\frac{\partial \tilde{S}(\phi)}{\partial \phi}\right)^2\right].$$

$$(A.2)$$

We now compare the effect of the different methods for obtaining the valley contours $\mathcal{C}$ and $\mathcal{C}'$ on inflationary predictions. This corroborates the discussion in Section 5.3.1 and justifies the method used there.

For the contour $\mathcal{C}'$ we have to solve for $\tilde{S}(\phi)$ numerically by finding the minimum for each value of ϕ in the S-direction. The inflaton field is then identified with the scalaron ϕ and the slow-roll parameters and number of e-folds are defined accordingly to that field parametrization. To exemplify the two mentioned methods above, we show further contour plots in this appendix where we also indicate the two contours in Fig. A.1,A.1 and 5.2 for the three benchmark points of Table 5.1.

On the left hand side of these figures we show the one-dimensional inflationary potentials which are obtained along the contours $\mathcal{C}$ and $\mathcal{C}'$. Comparing these contour plots reveals that for lower values of γ the valley extends more in the S-direction, indicating that contour $\mathcal{C}$ might be the better choice. However, both methods give similar results and approximate the valley contour equally
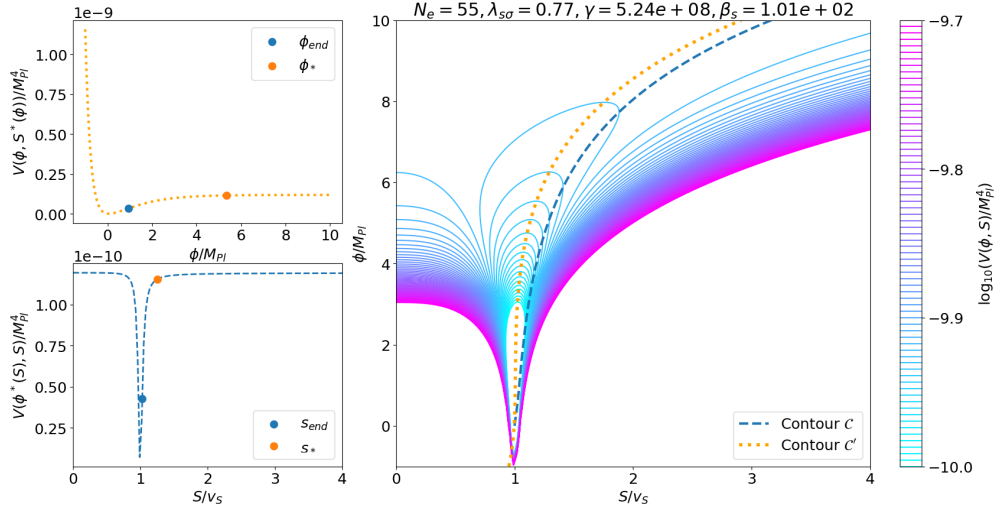
Figure A.1: Scalar potential for benchmark point 1 of Table 5.1. The two contours defined in Eqs. (5.33) and (A.1) are shown on top of the contour plot of $V(S,\phi)$ (5.31) (right) and the corresponding one-dimensional inflaton potentials along those contours (left).

well. For lowers value of γ, we run into numerical problems using the contour $\mathcal{C}'$, indicating that the lowest value where we can test both contours is $\gamma \sim 10^7$. The two contours deviate more from each other as the parameter γ grows larger. In the large γ-limit the inflation field becomes better identified with the scalaron field ϕ since the valley points more in that direction. Here the two contours start to deviate from each other and contour $\mathcal{C}'$ is expected to be the better approximation.

A more quantitative comparison shows us that the difference of the two methods used at large γ leads to different predictions for the CMB observables as can bee seen already in Fig. A.3. The experimental A_s-constraint is satisfied for different pairs of γ and β_S for the two methods. We use the parameter pairs γ and β_S shown in Fig. A.4 to show the effect on predictions for n_s and r considering the two contour methods. The deviation between the two methods is relatively small, which justifies the use of contour $\mathcal{C}$ in Section 5.3.1
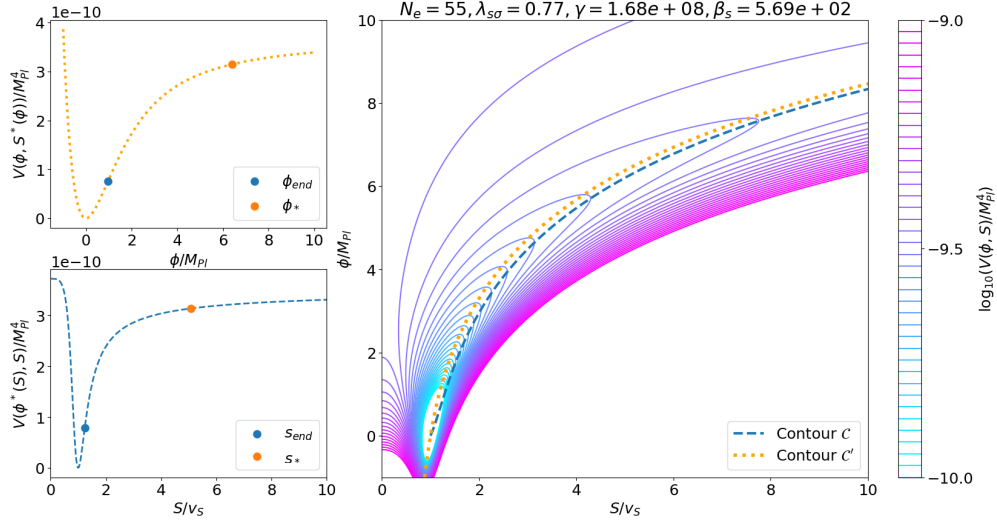
Figure A.2: Scalar potential for benchmark point 2 of Table 5.1. The two contours defined in Eqs. (5.33) and (A.1) are shown on top of the contour plot of $V(S, \phi)$ (5.31) (right) and the corresponding one-dimensional inflaton potentials along those contours (left).
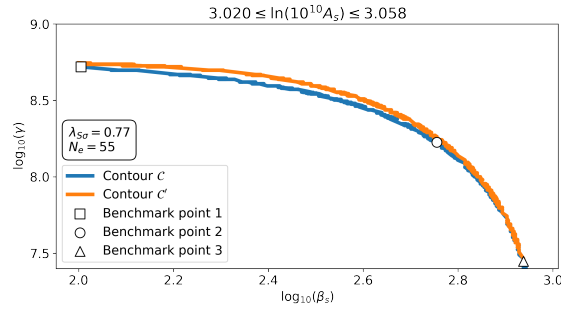
Figure A.3: The lines indicate the parameter combinations of γ and β_S for which the scalar power spectrum amplitude A_s prediction is fixed to the Planck constraint (5.43) for the two inflationary contours defined in Eqs. (5.33) and (A.1). For all points we have fixed $\beta_\sigma = 1$ and $\lambda_S = 0.005$. The three benchmark points defined in table 5.1 and displayed in Fig. A.1, A.2 and 5.2 are marked.
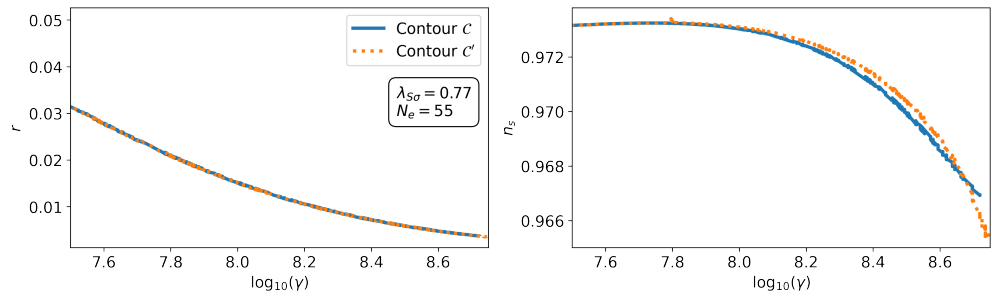
Figure A.4: Inflation parameters computed along the two contours $\mathcal{C}$ and $\mathcal{C}'$: Tensor-to-scalar ratio r (left) and scalar spectral index n_s (right). Note that the relation between γ and β_S is different for contours $\mathcal{C}$ and $\mathcal{C}'$, which can be understood from Fig. A.3.

Acknowledgments

I would like to thank my supervisor Manfred Lindner for the opportunity to pursue research according to my own scientific interest, his guidance throughout my PhD studies and his deep understanding of physics he has shared with. I also thank Tilman Plehn for being the second referee of this thesis, as well as Matthias Bartelmann and Loredana Gastaldo for being part of my PhD committee. My gratitude goes to the participants of conformal Fridays, i.e. Jisuke Kubo, Jeff Kuntz, Philipp Saake and Andreas Trautner. Our weekly discussion during lockdown times where paramount to the research presented in this thesis. I would like to especially thank Kubo for his guidance which was indispensable for my PhD. Special thanks go to Sudip Jana for the fruitful collaboration we had which unfortunately did not make it into this thesis. Many thanks go to Andreas Bally, Maya Hager, Jeff Kuntz and Álvaro Pastor Gutiérrez for proof reading this thesis and providing many helpful comments. Furthermore, I thank all the members of the astroparticle division at the MPIK for the nice research atmosphere in the past four years.

I am deeply grateful to my friends Andreas Bally and Jeffrey Kuntz which made my time in Heidelberg (inside and outside of the institute) to such a wonderful experience. My gratitude goes also to all my other friends which I have met in Heidelberg and Berlin. In the unlikely event that you are reading this, you will know that you are meant (I hope). Lastly, I want to thank my parents for their constant support and guidance.
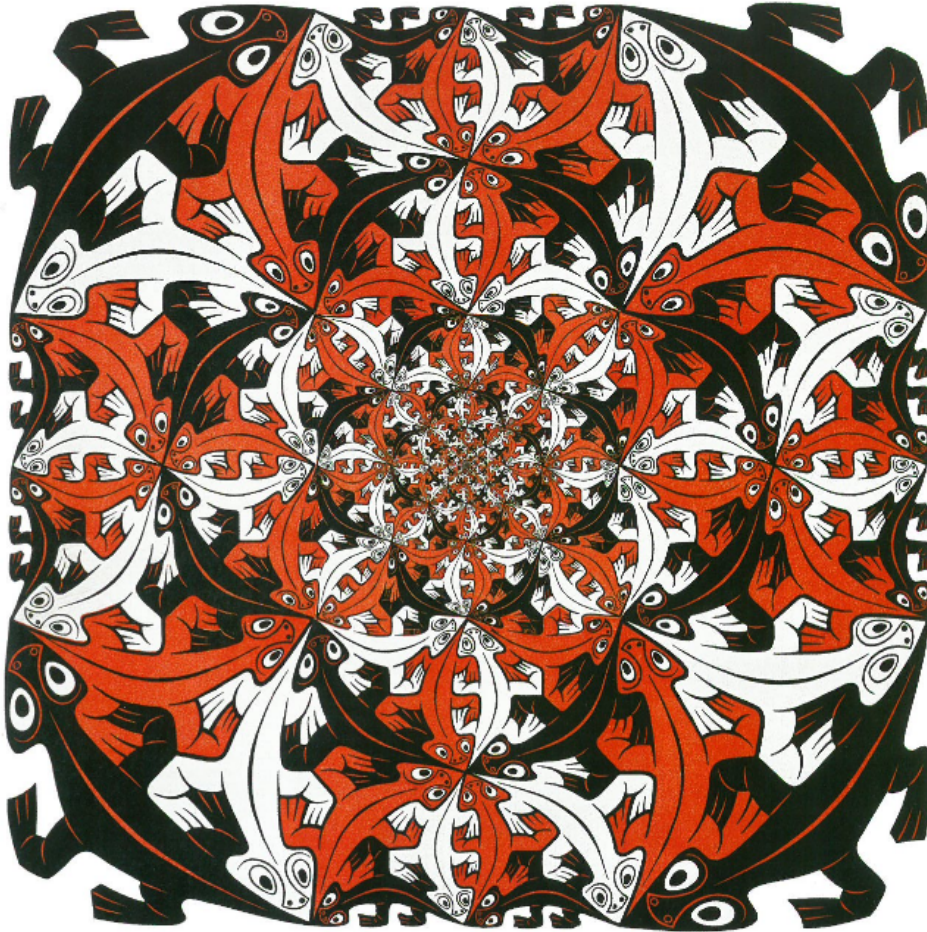
Figure A.5: *Smaller and smaller*, wood-engraving printed from four blocks, 38×38 cm, by M.C. Escher. *"The area of each of the reptile-shaped elements of this pattern is regularly and continuously halved in the direction of the centre, whereas theoretically both infinite smallness of size and infinite greatness of number are reached. However, in practice, the wood-engraver soon comes to an end of his ability to carry on. He is dependent on four factors: 1. the quality of his wood-block, 2. the sharpness of the instrument that he is using, 3. the steadiness of his hand and, 4. his optical ability (good eyesight, plenty of light and a powerful magnifying lens). In this particular case, the halving of the figures is carried through ad absurdum. The smallest animal still possessing a head, a tail and four legs is about 2 millimeters in length. From the point of view of composition, this work is only partially satisfying. In spite of the central limit, it remains only a fragment, because the outer edge of the pattern has been arbitrarily fixed. So a complete composition has not been achieved."* - M.C. Escher [242]. Figure taken from Reference [242].

List of Figures

Disclaimer

This thesis is based on two papers which have been published in peer-reviewed journals and with the original research performed by the author in collaboration with others. In particular:

- The results of Chapter 5 are based on Reference [204] in collaboration with Jisuke Kubo, Jeffrey Kuntz, Manfred Lindner, Philipp Saake and Andreas Trautner.

- The results of Chapter 6 are based on Reference [243] in collaboration with Jisuke Kubo, Jeffrey Kuntz and Philipp Saake.

Bibliography

[1] J.S. Schwinger, *On Quantum electrodynamics and the magnetic moment of the electron*, *Phys. Rev.* **73** (1948) 416.

[2] X. Fan, T.G. Myers, B.A.D. Sukra and G. Gabrielse, *Measurement of the Electron Magnetic Moment*, *Phys. Rev. Lett.* **130** (2023) 071801 [`2209.13084`].

[3] S.R. Coleman and E.J. Weinberg, *Radiative Corrections as the Origin of Spontaneous Symmetry Breaking*, *Phys. Rev. D* **7** (1973) 1888.

[4] M. Sher, *Electroweak Higgs Potentials and Vacuum Stability*, *Phys. Rept.* **179** (1989) 273.

[5] R. Hempfling, *The Next-to-minimal Coleman-Weinberg model*, *Phys. Lett. B* **379** (1996) 153 [`hep-ph/9604278`].

[6] K.A. Meissner and H. Nicolai, *Conformal Symmetry and the Standard Model*, *Phys. Lett. B* **648** (2007) 312 [`hep-th/0612165`].

[7] K.A. Meissner and H. Nicolai, *Effective action, conformal anomaly and the issue of quadratic divergences*, *Phys. Lett. B* **660** (2008) 260 [`0710.2840`].

[8] K.A. Meissner and H. Nicolai, *Conformal invariance from non-conformal gravity*, *Phys. Rev. D* **80** (2009) 086005 [`0907.3298`].

[9] A.J. Helmboldt, P. Humbert, M. Lindner and J. Smirnov, *Minimal conformal extensions of the Higgs sector*, *JHEP* **07** (2017) 113 [`1603.03603`].

[10] R. Foot, A. Kobakhidze and R.R. Volkas, *Electroweak Higgs as a pseudo-Goldstone boson of broken scale invariance*, *Phys. Lett. B* **655** (2007) 156 [`0704.1165`].

[11] C. Englert, J. Jaeckel, V.V. Khoze and M. Spannowsky, *Emergence of the Electroweak Scale through the Higgs Portal*, *JHEP* **04** (2013) 060 [`1301.4224`].

[12] M. Holthausen, J. Kubo, K.S. Lim and M. Lindner, *Electroweak and Conformal Symmetry Breaking by a Strongly Coupled Hidden Sector*, *JHEP* **12** (2013) 076 [1310.4423].

[13] L. Chataignier, T. Prokopec, M.G. Schmidt and B. Świeżewska, *Systematic analysis of radiative symmetry breaking in models with extended scalar sector*, *JHEP* **08** (2018) 083 [1805.09292].

[14] S.L. Glashow, *Partial Symmetries of Weak Interactions*, *Nucl. Phys.* **22** (1961) 579.

[15] S. Weinberg, *A Model of Leptons*, *Phys. Rev. Lett.* **19** (1967) 1264.

[16] A. Salam, *Weak and Electromagnetic Interactions*, *Conf. Proc. C* **680519** (1968) 367.

[17] C.-N. Yang and R.L. Mills, *Conservation of Isotopic Spin and Isotopic Gauge Invariance*, *Phys. Rev.* **96** (1954) 191.

[18] G. 't Hooft, *The Conceptual Basis of Quantum Field Theory*, in *Philosophy of physics*, J. Butterfield and J. Earman, eds., pp. 661–729 (2007), DOI.

[19] P.W. Higgs, *Broken Symmetries and the Masses of Gauge Bosons*, *Phys. Rev. Lett.* **13** (1964) 508.

[20] F. Englert and R. Brout, *Broken Symmetry and the Mass of Gauge Vector Mesons*, *Phys. Rev. Lett.* **13** (1964) 321.

[21] G. 't Hooft, *Renormalization of Massless Yang-Mills Fields*, *Nucl. Phys. B* **33** (1971) 173.

[22] G. 't Hooft, *Renormalizable Lagrangians for Massive Yang-Mills Fields*, *Nucl. Phys. B* **35** (1971) 167.

[23] G. 't Hooft, *Naturalness, chiral symmetry, and spontaneous chiral symmetry breaking*, *NATO Sci. Ser. B* **59** (1980) 135.

[24] W.A. Bardeen, *On naturalness in the standard model*, in *Ontake Summer Institute on Particle Physics*, 8, 1995.

[25] D. Buttazzo, G. Degrassi, P.P. Giardino, G.F. Giudice, F. Sala, A. Salvio et al., *Investigating the near-criticality of the Higgs boson*, *JHEP* **12** (2013) 089 [1307.3536].

[26] Y. Fujii, *Scalar-tensor theory of gravitation and spontaneous breakdown of scale invariance*, *Phys. Rev.* **D9** (1974) 874.

[27] P. Minkowski, *On the Spontaneous Origin of Newton's Constant*, *Phys. Lett.* **71B** (1977) 419.

[28] A. Zee, *A Broken Symmetric Theory of Gravity*, Phys. Rev. Lett. **42** (1979) 417.

[29] H. Terazawa, *Cosmological Origin of Mass Scales*, Phys. Lett. **101B** (1981) 43.

[30] A. Salvio and A. Strumia, *Agravity*, JHEP **06** (2014) 080 [1403.4226].

[31] K. Kannike, G. Hutsi, L. Pizza, A. Racioppi, M. Raidal, A. Salvio et al., *Dynamically Induced Planck Scale and Inflation*, JHEP **05** (2015) 065 [1502.01334].

[32] K. Kannike, M. Raidal, C. Spethmann and H. Veermae, *The evolving Planck mass in classically scale-invariant theories*, JHEP **04** (2017) 026 [1610.06571].

[33] M.B. Einhorn and D.R.T. Jones, *Naturalness and Dimensional Transmutation in Classically Scale-Invariant Gravity*, JHEP **03** (2015) 047 [1410.8513].

[34] J.F. Donoghue and G. Menezes, *Gauge Assisted Quadratic Gravity: A Framework for UV Complete Quantum Gravity*, Phys. Rev. **D97** (2018) 126005 [1804.04980].

[35] J.F. Donoghue and G. Menezes, *Inducing the einstein action in qcd-like theories*, Physical Review D **97** (2018) .

[36] B. Holdom and J. Ren, *Qcd analogy for quantum gravity*, Physical Review D **93** (2016) .

[37] C.T. Hill, *Inertial Symmetry Breaking*, in *Proceedings, 11th International Workshop on the Physics of Excited Nucleons (NSTAR 2017): Columbia, SC, USA, August 20-23, 2017*, 2018, http://lss.fnal.gov/archive/2018/pub/fermilab-pub-18-076-t.pdf [1803.06994].

[38] P.G. Ferreira, C.T. Hill and G.G. Ross, *Weyl Current, Scale-Invariant Inflation and Planck Scale Generation*, Phys. Rev. D **95** (2017) 043507 [1610.09243].

[39] S. Vicentini, L. Vanzo and M. Rinaldi, *Scale-invariant inflation with one-loop quantum corrections*, Phys. Rev. D **99** (2019) 103516 [1902.04434].

[40] F. Englert, E. Gunzig, C. Truffin and P. Windey, *Conformal Invariant General Relativity with Dynamical Symmetry Breakdown*, Phys. Lett. **57B** (1975) 73.

[41] F. Englert, C. Truffin and R. Gastmans, *Conformal Invariance in Quantum Gravity*, Nucl. Phys. **B117** (1976) 407.

[42] E.M. Chudnovsky, *The Spontaneous Conformal Symmetry Breaking and Higgs Model*, Theor. Math. Phys. **35** (1978) 538.

[43] E.S. Fradkin and G.A. Vilkovisky, *Conformal Off Mass Shell Extension and Elimination of Conformal Anomalies in Quantum Gravity*, Phys. Lett. **73B** (1978) 209.

[44] L. Smolin, *Towards a Theory of Space-Time Structure at Very Short Distances*, Nucl. Phys. **B160** (1979) 253.

[45] A. Zee, *The Horizon Problem and the Broken Symmetric Theory of Gravity*, Phys. Rev. Lett. **44** (1980) 703.

[46] H.T. Nieh, *A spontaneously broken conformal gauge theory of gravitation*, Phys. Lett. **A88** (1982) 388.

[47] H. Terazawa, Y. Chikashige, K. Akama and T. Matsuki, *Simple Relation Between the Fine Structure and Gravitational Constants*, Phys. Rev. **D15** (1977) 1181.

[48] K. Akama, Y. Chikashige and T. Matsuki, *Unified Model of the Nambu–Jona-Lasinio Type for the Gravitational and Electromagnetic Forces*, Prog. Theor. Phys. **59** (1978) 653.

[49] K. Akama, Y. Chikashige, T. Matsuki and H. Terazawa, *Gravity and Electromagnetism as Collective Phenomena of Fermion-Antifermion Pairs*, Prog. Theor. Phys. **60** (1978) 868.

[50] S.L. Adler, *Order R Vacuum Action Functional in Scalar Free Unified Theories with Spontaneous Scale Breaking*, Phys. Rev. Lett. **44** (1980) 1567.

[51] S.L. Adler, *A Formula for the Induced Gravitational Constant*, Phys. Lett. **B95** (1980) 241.

[52] A. Zee, *Spontaneously Generated Gravity*, Phys. Rev. **D23** (1981) 858.

[53] S.L. Adler, *Einstein Gravity as a Symmetry-Breaking Effect in Quantum Field Theory*, Rev. Mod. Phys. **54** (1982) 729.

[54] P.D. Mannheim, *Making the Case for Conformal Gravity*, Found. Phys. **42** (2012) 388 [1101.2186].

[55] D.M. Ghilencea, *Spontaneous breaking of Weyl quadratic gravity to Einstein action and Higgs potential*, JHEP **03** (2019) 049 [1812.08613].

[56] I. Oda, *Planck and Electroweak Scales Emerging from Conformal Gravity*, *PoS* **CORFU2018** (2019) 057 [1903.09309].

[57] A. Barnaveli, S. Lucat and T. Prokopec, *Inflation as a spontaneous symmetry breaking of Weyl symmetry*, *JCAP* **01** (2019) 022 [1809.10586].

[58] K. Stelle, *Renormalization of Higher Derivative Quantum Gravity*, *Phys. Rev. D* **16** (1977) 953.

[59] G. 't Hooft, *A class of elementary particle models without any adjustable real parameters*, *Found. Phys.* **41** (2011) 1829 [1104.4543].

[60] PLANCK collaboration, *Planck 2018 results. VI. Cosmological parameters*, *Astron. Astrophys.* **641** (2020) A6 [1807.06209].

[61] A.A. Starobinsky, *A New Type of Isotropic Cosmological Models Without Singularity*, *Phys. Lett.* **B91** (1980) 99.

[62] D. Kazanas, *Dynamics of the Universe and Spontaneous Symmetry Breaking*, *Astrophys. J. Lett.* **241** (1980) L59.

[63] K. Sato, *First Order Phase Transition of a Vacuum and Expansion of the Universe*, *Mon. Not. Roy. Astron. Soc.* **195** (1981) 467.

[64] A.H. Guth, *The Inflationary Universe: A Possible Solution to the Horizon and Flatness Problems*, *Phys. Rev.* **D23** (1981) 347.

[65] A.D. Linde, *A New Inflationary Universe Scenario: A Possible Solution of the Horizon, Flatness, Homogeneity, Isotropy and Primordial Monopole Problems*, *Phys. Lett.* **108B** (1982) 389.

[66] A. Albrecht and P.J. Steinhardt, *Cosmology for Grand Unified Theories with Radiatively Induced Symmetry Breaking*, *Phys. Rev. Lett.* **48** (1982) 1220.

[67] S. Weinberg, *The quantum theory of fields. Vol. 2: Modern applications*, Cambridge University Press (8, 2013).

[68] R. Jackiw, *Functional evaluation of the effective potential*, *Phys. Rev. D* **9** (1974) 1686.

[69] M. Quiros, *Finite temperature field theory and phase transitions*, in *ICTP Summer School in High-Energy Physics and Cosmology*, pp. 187–259, 1, 1999 [hep-ph/9901312].

[70] F. Bezrukov, M.Y. Kalmykov, B.A. Kniehl and M. Shaposhnikov, *Higgs Boson Mass and New Physics*, *JHEP* **10** (2012) 140 [1205.2893].

[71] G. Degrassi, S. Di Vita, J. Elias-Miro, J.R. Espinosa, G.F. Giudice, G. Isidori et al., *Higgs mass and vacuum stability in the Standard Model at NNLO*, *JHEP* **08** (2012) 098 [1205.6497].

[72] C.T. Hill, *Is the Higgs Boson Associated with Coleman-Weinberg Dynamical Symmetry Breaking?*, *Phys. Rev. D* **89** (2014) 073003 [1401.4185].

[73] T. Hambye and M.H.G. Tytgat, *Electroweak symmetry breaking induced by dark matter*, *Phys. Lett. B* **659** (2008) 651 [0707.0633].

[74] S. Iso, N. Okada and Y. Orikasa, *Classically conformal B^-L extended Standard Model*, *Phys. Lett. B* **676** (2009) 81 [0902.4050].

[75] S. Iso, N. Okada and Y. Orikasa, *The minimal B-L model naturally realized at TeV scale*, *Phys. Rev. D* **80** (2009) 115007 [0909.0128].

[76] M. Holthausen, M. Lindner and M.A. Schmidt, *Radiative Symmetry Breaking of the Minimal Left-Right Symmetric Model*, *Phys. Rev. D* **82** (2010) 055002 [0911.0710].

[77] L. Alexander-Nunneley and A. Pilaftsis, *The Minimal Scale Invariant Extension of the Standard Model*, *JHEP* **09** (2010) 021 [1006.5916].

[78] A. Farzinnia, H.-J. He and J. Ren, *Natural Electroweak Symmetry Breaking from Scale Invariant Higgs Mechanism*, *Phys. Lett. B* **727** (2013) 141 [1308.0295].

[79] E. Gabrielli, M. Heikinheimo, K. Kannike, A. Racioppi, M. Raidal and C. Spethmann, *Towards Completing the Standard Model: Vacuum Stability, EWSB and Dark Matter*, *Phys. Rev. D* **89** (2014) 015017 [1309.6632].

[80] M. Lindner, S. Schmidt and J. Smirnov, *Neutrino Masses and Conformal Electro-Weak Symmetry Breaking*, *JHEP* **10** (2014) 177 [1405.6204].

[81] W. Altmannshofer, W.A. Bardeen, M. Bauer, M. Carena and J.D. Lykken, *Light Dark Matter, Naturalness, and the Radiative Origin of the Electroweak Scale*, *JHEP* **01** (2015) 032 [1408.3429].

[82] P. Humbert, M. Lindner and J. Smirnov, *The Inverse Seesaw in Conformal Electro-Weak Symmetry Breaking and Phenomenological Consequences*, *JHEP* **06** (2015) 035 [1503.03066].

[83] P. Humbert, M. Lindner, S. Patra and J. Smirnov, *Lepton Number Violation within the Conformal Inverse Seesaw*, *JHEP* **09** (2015) 064 [1505.07453].

[84] A. Ahriche, K.L. McDonald and S. Nasri, *The Scale-Invariant Scotogenic Model*, *JHEP* **06** (2016) 182 [1604.05569].

[85] A. Ahriche, A. Manning, K.L. McDonald and S. Nasri, *Scale-Invariant Models with One-Loop Neutrino Mass and Dark Matter Candidates*, *Phys. Rev. D* **94** (2016) 053005 [1604.05995].

[86] R. Jinno and M. Takimoto, *Probing a classically conformal B-L model with gravitational waves*, *Phys. Rev. D* **95** (2017) 015020 [1604.05035].

[87] C. Marzo, L. Marzola and V. Vaskonen, *Phase transition and vacuum stability in the classically conformal B–L model*, *Eur. Phys. J. C* **79** (2019) 601 [1811.11169].

[88] B. Barman and A. Ghoshal, *Probing pre-BBN era with scale invariant FIMP*, *JCAP* **10** (2022) 082 [2203.13269].

[89] T. Hambye and A. Strumia, *Dynamical generation of the weak and Dark Matter scale*, *Phys. Rev. D* **88** (2013) 055022 [1306.2329].

[90] I. Baldes and C. Garcia-Cely, *Strong gravitational radiation from a simple dark matter model*, *JHEP* **05** (2019) 190 [1809.01198].

[91] T. Prokopec, J. Rezacek and B. Świeżewska, *Gravitational waves from conformal symmetry breaking*, *JCAP* **02** (2019) 009 [1809.11129].

[92] C.D. Carone and R. Ramos, *Classical scale-invariance, the electroweak scale and vector dark matter*, *Phys. Rev. D* **88** (2013) 055020 [1307.8428].

[93] A. Karam and K. Tamvakis, *Dark matter and neutrino masses from a scale-invariant multi-Higgs portal*, *Phys. Rev. D* **92** (2015) 075010 [1508.03031].

[94] R. Foot, A. Kobakhidze, K.L. McDonald and R.R. Volkas, *Neutrino mass in radiatively-broken scale-invariant models*, *Phys. Rev. D* **76** (2007) 075014 [0706.1829].

[95] V. Brdar, A.J. Helmboldt and J. Kubo, *Gravitational Waves from First-Order Phase Transitions: LIGO as a Window to Unexplored Seesaw Scales*, *JCAP* **02** (2019) 021 [1810.12306].

[96] V. Brdar, Y. Emonds, A.J. Helmboldt and M. Lindner, *Conformal Realization of the Neutrino Option*, *Phys. Rev. D* **99** (2019) 055014 [1807.11490].

[97] V. Brdar, A.J. Helmboldt, S. Iwamoto and K. Schmitz, *Type-I Seesaw as the Common Origin of Neutrino Mass, Baryon Asymmetry, and the Electroweak Scale*, *Phys. Rev. D* **100** (2019) 075029 [1905.12634].

[98] J. Kubo and M. Yamada, *Scale genesis and gravitational wave in a classically scale invariant extension of the standard model*, *JCAP* **12** (2016) 001 [`1610.02241`].

[99] A. Lewandowski, K.A. Meissner and H. Nicolai, *Conformal Standard Model, Leptogenesis and Dark Matter*, *Phys. Rev. D* **97** (2018) 035024 [`1710.06149`].

[100] J. Kubo, K.S. Lim and M. Lindner, *Electroweak Symmetry Breaking via QCD*, *Phys. Rev. Lett.* **113** (2014) 091604 [`1403.4262`].

[101] T. Hur, D.-W. Jung, P. Ko and J.Y. Lee, *Electroweak symmetry breaking and cold dark matter from strongly interacting hidden sector*, *Phys. Lett. B* **696** (2011) 262 [`0709.1218`].

[102] T. Hur and P. Ko, *Scale invariant extension of the standard model with strongly interacting hidden sector*, *Phys. Rev. Lett.* **106** (2011) 141802 [`1103.2571`].

[103] M. Heikinheimo, A. Racioppi, M. Raidal, C. Spethmann and K. Tuominen, *Physical Naturalness and Dynamical Breaking of Classical Scale Invariance*, *Mod. Phys. Lett. A* **29** (2014) 1450077 [`1304.7006`].

[104] O. Antipin, M. Redi and A. Strumia, *Dynamical generation of the weak and Dark Matter scales from strong interactions*, *JHEP* **01** (2015) 157 [`1410.1817`].

[105] N. Haba, H. Ishida, N. Kitazawa and Y. Yamaguchi, *A new dynamics of electroweak symmetry breaking with classically scale invariance*, *Phys. Lett. B* **755** (2016) 439 [`1512.05061`].

[106] H. Hatanaka, D.-W. Jung and P. Ko, *AdS/QCD approach to the scale-invariant extension of the standard model with a strongly interacting hidden sector*, *JHEP* **08** (2016) 094 [`1606.02969`].

[107] E. Gildener and S. Weinberg, *Symmetry Breaking and Scalar Bosons*, *Phys. Rev. D* **13** (1976) 3333.

[108] T. Cohen, *As Scales Become Separated: Lectures on Effective Field Theory*, *PoS* **TASI2018** (2019) 011 [`1903.03622`].

[109] J.C. Collins, A. Duncan and S.D. Joglekar, *Trace and Dilatation Anomalies in Gauge Theories*, *Phys. Rev. D* **16** (1977) 438.

[110] K. Fujikawa and H. Suzuki, *Path integrals and quantum anomalies*, Oxford University Press (2004), 10.1093/acprof:oso/9780198529132.001.0001.

[111] M. Shaposhnikov and D. Zenhausern, *Quantum scale invariance, cosmological constant and hierarchy problem*, Phys. Lett. B **671** (2009) 162 [`0809.3406`].

[112] C.G. Callan, Jr., S.R. Coleman and R. Jackiw, *A New improved energy - momentum tensor*, Annals Phys. **59** (1970) 42.

[113] D.M. Capper and M.J. Duff, *Trace anomalies in dimensional regularization*, Nuovo Cim. **A23** (1974) 173.

[114] M.J. Duff, *Twenty years of the Weyl anomaly*, Class. Quant. Grav. **11** (1994) 1387 [`hep-th/9308075`].

[115] Y. Nakayama, *Scale invariance vs conformal invariance*, Phys. Rept. **569** (2015) 1 [`1302.0884`].

[116] H. Osborn, *Weyl consistency conditions and a local renormalization group equation for general renormalizable field theories*, Nucl. Phys. B **363** (1991) 486.

[117] M. Holthausen, K.S. Lim and M. Lindner, *Planck scale Boundary Conditions and the Higgs Mass*, JHEP **02** (2012) 037 [`1112.2415`].

[118] D.J. Gross and J. Wess, *Scale invariance, conformal invariance, and the high-energy behavior of scattering amplitudes*, Phys. Rev. D **2** (1970) 753.

[119] K. Farnsworth, M.A. Luty and V. Prilepina, *Weyl versus Conformal Invariance in Quantum Field Theory*, JHEP **10** (2017) 170 [`1702.07079`].

[120] G.K. Karananas and A. Monin, *Weyl vs. Conformal*, Phys. Lett. B **757** (2016) 257 [`1510.08042`].

[121] G.K. Karananas, *Poincaré, Scale and Conformal Symmetries Gauge Perspective and Cosmological Ramifications*, Ph.D. thesis, Ecole Polytechnique, Lausanne, 2016. `1608.08451`. 10.5075/epfl-thesis-7173.

[122] D. Baumann, *Inflation*, in *Theoretical Advanced Study Institute in Elementary Particle Physics: Physics of the Large and the Small*, 2011, DOI [`0907.5424`].

[123] D. Baumann, *Primordial Cosmology*, PoS **TASI2017** (2018) 009 [`1807.03098`].

[124] S. Weinberg, *Cosmology*, OUP Oxford (2008).

[125] V. Mukhanov, *Physical Foundations of Cosmology*, Cambridge University Press (2005), 10.1017/CBO9780511790553.

[126] S. Dodelson, *Modern Cosmology*, Academic Press, Amsterdam (2003).

[127] A.R. Liddle and D.H. Lyth, *Cosmological inflation and large scale structure*, Cambridge University Press (2000).

[128] J.M. Bardeen, *Gauge Invariant Cosmological Perturbations*, Phys. Rev. D **22** (1980) 1882.

[129] S. Weinberg, *Adiabatic modes in cosmology*, Phys. Rev. D **67** (2003) 123504 [`astro-ph/0302326`].

[130] D. Wands, K.A. Malik, D.H. Lyth and A.R. Liddle, *A New approach to the evolution of cosmological perturbations on large scales*, Phys. Rev. D **62** (2000) 043527 [`astro-ph/0003278`].

[131] PLANCK collaboration, *Planck 2018 results. X. Constraints on inflation*, Astron. Astrophys. **641** (2020) A10 [`1807.06211`].

[132] V.F. Mukhanov, H.A. Feldman and R.H. Brandenberger, *Theory of cosmological perturbations. Part 1. Classical perturbations. Part 2. Quantum theory of perturbations. Part 3. Extensions*, Phys. Rept. **215** (1992) 203.

[133] T.S. Bunch and P.C.W. Davies, *Quantum Field Theory in de Sitter Space: Renormalization by Point Splitting*, Proc. Roy. Soc. Lond. A **360** (1978) 117.

[134] J.M. Maldacena, *Non-Gaussian features of primordial fluctuations in single field inflationary models*, JHEP **05** (2003) 013 [`astro-ph/0210603`].

[135] PLANCK collaboration, *Planck 2018 results. IX. Constraints on primordial non-Gaussianity*, Astron. Astrophys. **641** (2020) A9 [`1905.05697`].

[136] R.K. Sachs and A.M. Wolfe, *Perturbations of a cosmological model and angular variations of the microwave background*, Astrophys. J. **147** (1967) 73.

[137] M. Kamionkowski, A. Kosowsky and A. Stebbins, *Statistics of cosmic microwave background polarization*, Phys. Rev. D **55** (1997) 7368 [`astro-ph/9611125`].

[138] M. Zaldarriaga and U. Seljak, *An all sky analysis of polarization in the microwave background*, Phys. Rev. D **55** (1997) 1830 [`astro-ph/9609170`].

[139] M. Kamionkowski and E.D. Kovetz, *The Quest for B Modes from Inflationary Gravitational Waves*, Ann. Rev. Astron. Astrophys. **54** (2016) 227 [`1510.06042`].

[140] BICEP2, KECK ARRAY collaboration, *BICEP2 / Keck Array x: Constraints on Primordial Gravitational Waves using Planck, WMAP, and New BICEP2/Keck Observations through the 2015 Season*, Phys. Rev. Lett. **121** (2018) 221301 [`1810.05216`].

[141] S. Hannestad, *What is the lowest possible reheating temperature?*, Phys. Rev. D **70** (2004) 043506 [`astro-ph/0403291`].

[142] P. Minkowski, $\mu \to e\gamma$ *at a Rate of One Out of* 10^9 *Muon Decays?*, Phys. Lett. B **67** (1977) 421.

[143] R.N. Mohapatra and G. Senjanovic, *Neutrino Mass and Spontaneous Parity Nonconservation*, Phys. Rev. Lett. **44** (1980) 912.

[144] T. Yanagida, *Horizontal Symmetry and Masses of Neutrinos*, Conf. Proc. **C7902131** (1979) 95.

[145] M. Gell-Mann, P. Ramond and R. Slansky, *Complex Spinors and Unified Theories*, Conf. Proc. **C790927** (1979) 315 [`1306.4669`].

[146] S.L. Glashow, *The Future of Elementary Particle Physics*, NATO Sci. Ser. B **61** (1980) 687.

[147] B. Dasgupta and J. Kopp, *Sterile Neutrinos*, Phys. Rept. **928** (2021) 1 [`2106.05913`].

[148] PARTICLE DATA GROUP collaboration, *Review of Particle Physics*, PTEP **2022** (2022) 083C01.

[149] I. Brivio and M. Trott, *Radiatively Generating the Higgs Potential and Electroweak Scale via the Seesaw Mechanism*, Phys. Rev. Lett. **119** (2017) 141801 [`1703.10924`].

[150] F.L. Bezrukov and M. Shaposhnikov, *The Standard Model Higgs boson as the inflaton*, Phys. Lett. **B659** (2008) 703 [`0710.3755`].

[151] A. Gundhi and C.F. Steinwachs, *Scalaron-Higgs inflation*, Nucl. Phys. B **954** (2020) 114989 [`1810.10546`].

[152] Y. Ema, *Higgs Scalaron Mixed Inflation*, Phys. Lett. B **770** (2017) 403 [`1701.07665`].

[153] A. Farzinnia and S. Kouwn, *Classically scale invariant inflation, supermassive WIMPs, and adimensional gravity*, Phys. Rev. D **93** (2016) 063528 [`1512.05890`].

[154] J. Garcia-Bellido, J. Rubio, M. Shaposhnikov and D. Zenhausern, *Higgs-Dilaton Cosmology: From the Early to the Late Universe*, *Phys. Rev.* **D84** (2011) 123504 [1107.2163].

[155] M. Rinaldi, G. Cognola, L. Vanzo and S. Zerbini, *Inflation in scale-invariant theories of gravity*, *Phys. Rev.* **D91** (2015) 123527 [1410.0631].

[156] J. Kubo, M. Lindner, K. Schmitz and M. Yamada, *Planck mass and inflation as consequences of dynamically broken scale invariance*, *Phys. Rev. D* **100** (2019) 015037 [1811.05950].

[157] H. Ishida and S. Matsuzaki, *A Walking Dilaton Inflation*, *Phys. Lett. B* **804** (2020) 135390 [1912.09740].

[158] I.D. Gialamas, A. Karam and A. Racioppi, *Dynamically induced Planck scale and inflation in the Palatini formulation*, *JCAP* **11** (2020) 014 [2006.09124].

[159] I.D. Gialamas, A. Karam, T.D. Pappas and V.C. Spanos, *Scale-invariant quadratic gravity and inflation in the Palatini formalism*, *Phys. Rev. D* **104** (2021) 023521 [2104.04550].

[160] M. Aoki, V. Brdar and J. Kubo, *Heavy dark matter, neutrino masses, and Higgs naturalness from a strongly interacting hidden sector*, *Phys. Rev. D* **102** (2020) 035026 [2007.04367].

[161] L. Alvarez-Gaume, A. Kehagias, C. Kounnas, D. Lüst and A. Riotto, *Aspects of Quadratic Gravity*, *Fortsch. Phys.* **64** (2016) 176 [1505.07657].

[162] D. Kirzhnits and A.D. Linde, *Macroscopic Consequences of the Weinberg Model*, *Phys. Lett. B* **42** (1972) 471.

[163] L. Casarin, H. Godazgar and H. Nicolai, *Conformal Anomaly for Non-Conformal Scalar Fields*, *Phys. Lett.* **B787** (2018) 94 [1809.06681].

[164] C.F. Steinwachs and A.Y. Kamenshchik, *One-loop divergences for gravity non-minimally coupled to a multiplet of scalar fields: calculation in the Jordan frame. I. The main results*, *Phys. Rev. D* **84** (2011) 024026 [1101.5047].

[165] T. Markkanen, S. Nurmi, A. Rajantie and S. Stopyra, *The 1-loop effective potential for the Standard Model in curved spacetime*, *JHEP* **06** (2018) 040 [1804.02020].

[166] A.D. Linde, *Coleman-Weinberg Theory and a New Inflationary Universe Scenario*, *Phys. Lett.* **114B** (1982) 431.

[167] M. Rinaldi and L. Vanzo, *Inflation and reheating in theories with spontaneous scale invariance symmetry breaking, Phys. Rev. D* **94** (2016) 024009 [1512.07186].

[168] D. Benisty and E.I. Guendelman, *Two scalar fields inflation from scale-invariant gravity with modified measure, Class. Quant. Grav.* **36** (2019) 095001 [1809.09866].

[169] D. Ghilencea and H.M. Lee, *Weyl gauge symmetry and its spontaneous breaking in the standard model and inflation, Phys. Rev. D* **99** (2019) 115007 [1809.09174].

[170] K. Kannike, A. Racioppi and M. Raidal, *Embedding inflation into the Standard Model - more evidence for classical scale invariance, JHEP* **06** (2014) 154 [1405.3987].

[171] N.D. Barrie, A. Kobakhidze and S. Liang, *Natural Inflation with Hidden Scale Invariance, Phys. Lett. B* **756** (2016) 390 [1602.04901].

[172] A. Farzinnia and S. Kouwn, *Classically scale invariant inflation, supermassive WIMPs, and adimensional gravity, Phys. Rev. D* **93** (2016) 063528 [1512.05890].

[173] A. Karam, T. Pappas and K. Tamvakis, *Nonminimal Coleman–Weinberg Inflation with an R^2 term, JCAP* **1902** (2019) 006 [1810.12884].

[174] A. Karam, L. Marzola, T. Pappas, A. Racioppi and K. Tamvakis, *Constant-Roll (Quasi-)Linear Inflation, JCAP* **05** (2018) 011 [1711.09861].

[175] D. Burns, S. Karamitsos and A. Pilaftsis, *Frame-Covariant Formulation of Inflation in Scalar-Curvature Theories, Nucl. Phys. B* **907** (2016) 785 [1603.03730].

[176] L. Järv, K. Kannike, L. Marzola, A. Racioppi, M. Raidal, M. Rünkla et al., *Frame-Independent Classification of Single-Field Inflationary Models, Phys. Rev. Lett.* **118** (2017) 151302 [1612.06863].

[177] A.Y. Kamenshchik and C.F. Steinwachs, *Question of quantum equivalence between Jordan frame and Einstein frame, Phys. Rev. D* **91** (2015) 084033 [1408.5769].

[178] K. Falls and M. Herrero-Valea, *Frame (In)equivalence in Quantum Field Theory and Cosmology, Eur. Phys. J. C* **79** (2019) 595 [1812.08187].

[179] S. Kaneda and S.V. Ketov, *Starobinsky-like two-field inflation, Eur. Phys. J.* **C76** (2016) 26 [1510.03524].

[180] D.D. Canko, I.D. Gialamas and G.P. Kodaxis, *A simple $F(\mathcal{R}, \phi)$ deformation of Starobinsky inflationary model*, Eur. Phys. J. C **80** (2020) 458 [1901.06296].

[181] A. Gundhi, S.V. Ketov and C.F. Steinwachs, *Primordial black hole dark matter in dilaton-extended two-field Starobinsky inflation*, 2011.05999.

[182] A. Gundhi and C.F. Steinwachs, *Scalaron-Higgs inflation reloaded: Higgs-dependent scalaron mass and primordial black hole dark matter*, 2011.09485.

[183] D. Baumann, H. Lee and G.L. Pimentel, *High-Scale Inflation and the Tensor Tilt*, JHEP **01** (2016) 101 [1507.07250].

[184] A. Salvio, *Inflationary Perturbations in No-Scale Theories*, Eur. Phys. J. C **77** (2017) 267 [1703.08012].

[185] D. Anselmi, E. Bianchi and M. Piva, *Predictions of quantum gravity in inflationary cosmology: effects of the Weyl-squared term*, JHEP **2020** (2020) [2005.10293].

[186] J.D. Barrow and S. Cotsakis, *Inflation and the Conformal Structure of Higher Order Gravity Theories*, Phys. Lett. B **214** (1988) 515.

[187] K.-i. Maeda, *Towards the Einstein-Hilbert Action via Conformal Transformation*, Phys. Rev. D **39** (1989) 3159.

[188] D. Wands, *Multiple field inflation*, Lect. Notes Phys. **738** (2008) 275 [astro-ph/0702187].

[189] V.F. Mukhanov and G.V. Chibisov, *Quantum Fluctuations and a Nonsingular Universe*, JETP Lett. **33** (1981) 532.

[190] A.A. Starobinsky, *The Perturbation Spectrum Evolving from a Nonsingular Initially De-Sitter Cosmology and the Microwave Background Anisotropy*, Sov. Astron. Lett. **9** (1983) 302.

[191] A.D. Linde, *Chaotic Inflation*, Phys. Lett. **129B** (1983) 177.

[192] K. Kannike, A. Racioppi and M. Raidal, *Linear inflation from quartic potential*, JHEP **01** (2016) 035 [1509.05423].

[193] A. Racioppi, *New universal attractor in nonminimally coupled gravity: Linear inflation*, Phys. Rev. D **97** (2018) 123514 [1801.08810].

[194] I. Brivio and M. Trott, *Examining the neutrino option*, JHEP **02** (2019) 107 [1809.03450].

[195] H. Davoudiasl and I.M. Lewis, *Right-Handed Neutrinos as the Origin of the Electroweak Scale*, Phys. Rev. D **90** (2014) 033003 [1404.6260].

[196] J.A. Casas, V. Di Clemente and M. Quiros, *The Effective potential in the presence of several mass scales*, *Nucl. Phys. B* **553** (1999) 511 [`hep-ph/9809275`].

[197] J. Casas, V. Di Clemente, A. Ibarra and M. Quiros, *Massive neutrinos and the Higgs mass window*, *Phys. Rev. D* **62** (2000) 053005 [`hep-ph/9904295`].

[198] G. Bambhaniya, P. Bhupal Dev, S. Goswami, S. Khan and W. Rodejohann, *Naturalness, Vacuum Stability and Leptogenesis in the Minimal Seesaw Model*, *Phys. Rev. D* **95** (2017) 095016 [`1611.03827`].

[199] R. Foot, A. Kobakhidze, K.L. McDonald and R.R. Volkas, *Poincaré protection for a natural electroweak scale*, *Phys. Rev. D* **89** (2014) 115018 [`1310.0223`].

[200] M. Fukugita and T. Yanagida, *Baryogenesis Without Grand Unification*, *Phys. Lett. B* **174** (1986) 45.

[201] W. Buchmuller, P. Di Bari and M. Plumacher, *Leptogenesis for pedestrians*, *Annals Phys.* **315** (2005) 305 [`hep-ph/0401240`].

[202] I. Brivio, K. Moffat, S. Pascoli, S. Petcov and J. Turner, *Leptogenesis in the Neutrino Option*, *JHEP* **10** (2019) 059 [`1905.12642`].

[203] G. Giudice, A. Notari, M. Raidal, A. Riotto and A. Strumia, *Towards a complete theory of thermal leptogenesis in the SM and MSSM*, *Nucl. Phys. B* **685** (2004) 89 [`hep-ph/0310123`].

[204] J. Kubo, J. Kuntz, M. Lindner, J. Rezacek, P. Saake and A. Trautner, *Unified emergence of energy scales and cosmic inflation*, *JHEP* **08** (2021) 016 [`2012.09706`].

[205] E.W. Kolb and M.S. Turner, *The Early Universe*, Westview Press (1990).

[206] B.A. Bassett, S. Tsujikawa and D. Wands, *Inflation dynamics and reheating*, *Rev. Mod. Phys.* **78** (2006) 537 [`astro-ph/0507632`].

[207] A.R. Liddle and S.M. Leach, *How long before the end of inflation were observable perturbations produced?*, *Phys. Rev. D* **68** (2003) 103503 [`astro-ph/0305263`].

[208] J. Martin and C. Ringeval, *First CMB Constraints on the Inflationary Reheating Temperature*, *Phys. Rev. D* **82** (2010) 023511 [`1004.5525`].

[209] J. Martin, C. Ringeval and V. Vennin, *Encyclopaedia Inflationaris*, *Phys. Dark Univ.* **5-6** (2014) 75 [`1303.3787`].

[210] PLANCK collaboration, *Planck 2018 results. VI. Cosmological parameters*, *Astron. Astrophys.* **641** (2020) A6 [1807.06209].

[211] K.D. Lozanov and M.A. Amin, *Self-resonance after inflation: oscillons, transients and radiation domination*, *Phys. Rev. D* **97** (2018) 023533 [1710.06851].

[212] M.S. Turner, *Coherent Scalar Field Oscillations in an Expanding Universe*, *Phys. Rev. D* **28** (1983) 1243.

[213] L.J. Hall, K. Jedamzik, J. March-Russell and S.M. West, *Freeze-In Production of FIMP Dark Matter*, *JHEP* **03** (2010) 080 [0911.1120].

[214] D.J. Chung, E.W. Kolb and A. Riotto, *Production of massive particles during reheating*, *Phys. Rev. D* **60** (1999) 063504 [hep-ph/9809453].

[215] R. Allahverdi and M. Drees, *Production of massive stable particles in inflaton decay*, *Phys. Rev. Lett.* **89** (2002) 091302 [hep-ph/0203118].

[216] M.A. Garcia, K. Kaneta, Y. Mambrini and K.A. Olive, *Reheating and Post-inflationary Production of Dark Matter*, *Phys. Rev. D* **101** (2020) 123507 [2004.08404].

[217] C. de Rham, *Massive Gravity*, *Living Rev. Rel.* **17** (2014) 7 [1401.4173].

[218] H. Weyl, *Reine Infinitesimalgeometrie*, *Math. Z.* **2** (1918) 384.

[219] G. 't Hooft and M.J.G. Veltman, *One loop divergencies in the theory of gravitation*, *Ann. Inst. H. Poincare Phys. Theor. A* **20** (1974) 69.

[220] M. Ostrogradsky, *Mémoires sur les équations différentielles, relatives au problème des isopérimètres*, *Mem. Acad. St. Petersbourg* **6** (1850) 385.

[221] R.P. Woodard, *Ostrogradsky's theorem on Hamiltonian instability*, *Scholarpedia* **10** (2015) 32243 [1506.02210].

[222] J. Kubo and J. Kuntz, *Analysis of unitarity in conformal quantum gravity*, *Class. Quant. Grav.* **39** (2022) 175010 [2202.08298].

[223] J. Kubo and J. Kuntz, *Spontaneous conformal symmetry breaking and quantum quadratic gravity*, *Phys. Rev. D* **106** (2022) 126015 [2208.12832].

[224] D. Anselmi, *On the quantum field theory of the gravitational interactions*, *JHEP* **2017** (2017) [1704.07728].

[225] D. Anselmi, *Fakeons and Lee-Wick models*, *JHEP* **2018** (2018) 141 [1801.00915].

[226] A. Salvio and A. Strumia, *Quantum mechanics of 4-derivative theories*, *Eur. Phys. J. C* **76** (2016) 227 [`1512.01237`].

[227] A. Salvio, *Quadratic Gravity*, *Front. in Phys.* **6** (2018) 77 [`1804.09944`].

[228] C.M. Bender, *Making sense of non-Hermitian Hamiltonians*, *Rept. Prog. Phys.* **70** (2007) 947 [`hep-th/0703096`].

[229] C.M. Bender and P.D. Mannheim, *No-ghost theorem for the fourth-order derivative Pais-Uhlenbeck oscillator model*, *Phys. Rev. Lett.* **100** (2008) 110402 [`0706.0207`].

[230] J.F. Donoghue and G. Menezes, *Unitarity, stability and loops of unstable ghosts*, *Phys. Rev. D* **100** (2019) 105006 [`1908.02416`].

[231] J.F. Donoghue and G. Menezes, *Ostrogradsky instability can be overcome by quantum physics*, *Phys. Rev. D* **104** (2021) 045010 [`2105.00898`].

[232] T.D. Lee and G.C. Wick, *Negative metric and the unitarity of the S-matrix*, *Nucl. Phys. B* **9** (1969) 209.

[233] J.W. York, Jr., *Conformatlly invariant orthogonal decomposition of symmetric tensors on Riemannian manifolds and the initial value problem of general relativity*, *J. Math. Phys.* **14** (1973) 456.

[234] P. Van Nieuwenhuizen, *On ghost-free tensor lagrangians and linearized gravitation*, *Nucl. Phys. B* **60** (1973) 478.

[235] BICEP, KECK collaboration, *Improved Constraints on Primordial Gravitational Waves using Planck, WMAP, and BICEP/Keck Observations through the 2018 Observing Season*, *Phys. Rev. Lett.* **127** (2021) 151301 [`2110.00483`].

[236] A. Salvio, *Dimensional Transmutation in Gravity and Cosmology*, *Int. J. Mod. Phys. A* **36** (2021) 2130006 [`2012.11608`].

[237] T. Mori, K. Kohri and J. White, *Multi-field effects in a simple extension of R^2 inflation*, *JCAP* **10** (2017) 044 [`1705.05638`].

[238] N. Bartolo, E. Komatsu, S. Matarrese and A. Riotto, *Non-Gaussianity from inflation: Theory and observations*, *Phys. Rept.* **402** (2004) 103 [`astro-ph/0406398`].

[239] LITEBIRD collaboration, *Probing Cosmic Inflation with the LiteBIRD Cosmic Microwave Background Polarization Survey*, `2202.02773`.

[240] L. Amendola et al., *Cosmology and fundamental physics with the Euclid satellite*, *Living Rev. Rel.* **21** (2018) 2 [`1606.00180`].

[241] LSST SCIENCE, LSST PROJECT collaboration, *LSST Science Book, Version 2.0*, 0912.0201.

[242] M. Escher, *The Graphic Work*, Taschen GmbH (2008).

[243] J. Kubo, J. Kuntz, J. Rezacek and P. Saake, *Inflation with massive spin-2 ghosts*, *JCAP* **11** (2022) 049 [2207.14329].